053

LOW TEMPERATURE PROPERTIES OF MODELS FOR MIXED-VALENCE COMPOUNDS

A thesis submitted for the degree of Ph.D.
at the University of London, and for
the Diploma of Imperial College

by

Nicholas Read

Department of Mathematics
Imperial College
London SW7 2BZ

ABSTRACT

A functional integral formalism for the infinite-U Anderson impurity model of mixed-valence systems is described, based upon the form of the model introduced by Coleman. A mean field approximation yields a description of low temperature properties consistent with known results from renormalisation group and Fermi liquid theory. The results form the first term in an expansion in $1/N$, where $N = 2j + 1$ is the degeneracy of the spin orbit coupled f electron states. Expressions for magnetic susceptibility $X(T)$, specific heat $C_v(T)/T$, magnetisation $m(h)$ and valence $n_f(T)$ are given to order T^2 or h^2. The approach is extended to impurity models containing crystal field splittings and to models with more than one f electron in the allowed states, and a comparison with scaling theory for these cases is made. Fluctuations around the mean field theory are calculated for the infinite U Anderson model and give the $1/N$ corrections to the leading order results at low temperatures. Infrared divergences appear in the expression for the order parameter; it is argued that they sum up to a power law in the infrared cutoff, thus forcing the order parameter to vanish. The divergences cancel in physical quantities, so that the mean field theory is still meaningful. A "perfect screening" result for the elementary excitations is proved at the mean field level. Finally, the extension to the lattice model describing concentrated systems is made and studied in mean field theory. The infinite-U Hubbard model is examined in the same fashion.

ACKNOWLEDGEMENTS

It is a pleasure to thank my supervisor, Dr. D.M. Newns, for his constant guidance and patient encouragement during the course of this work. I have also enjoyed many useful discussions with Dr. A.C. Hewson and Dr. J.W. Rasul. I thank Professor E.P. Wohlfarth and the other members of the Mathematical Physics and Solid State Theory group at Imperial College, especially Drs. D.M. Edwards, N. Rivier, D. Sherrington, H-U. Desgranges and K. Dharamvir for their interest in this project. I am grateful to the SERC for providing a research studentship. The preparation of this thesis was greatly aided by the fast, efficient and accurate typing of Mrs. G.A. Place. Finally, I would like to thank my parents, who have supported me morally and at times financially during this work; I dedicate this thesis to them.

CONTENTS

Abstract 2

Acknowledgements 3

CHAPTER 1 : Introduction

§1 Experiment 10

a) Ionic Energy levels and Spectroscopy 10

b) Lattice Constants and Thermal Expansion 20

c) Susceptibility and Specific Heat 23

§2 Theory 28

a) Anderson Impurity model: Expansion in U 28

b) Anderson Impurity model: Expansion in V 33

c) Kondo model: Scaling and Renormalisation Group 47

d) Other theoretical approaches 54

§3 Outline of Thesis 57

References 59

CHAPTER 2 : Large-N limit of the Coqblin-Schrieffer and Anderson impurity models

§1 Description of Models 61

§2 Functional Integral Formulae and Symmetries of the Models 67

§3 1/N Expansion: the basic ideas 75

§4 The large-N limit at T = 0 80

§5 Discussion 100

§6 Mean Field Theory at Finite Temperatures and Fields 103

a) General Formulae 103

b) $\varepsilon_f(T)$, $\Delta(T)$ and $n_f(T)$ to order T^2 108

c) T^2 corrections to $\chi(T)$, $C_v(T)/T$ and h^2 corrections to $M(h)/h$ in the Kondo limit 110

d) High temperature behaviour in the Kondo limit 114

References 119

CHAPTER 3 : Application of Mean-Field Technique to some other models

§1 Spin-Orbit and Crystal Field Splittings 122

§2 Application of Scaling Theory 129

§3 Models with Both Configurations Magnetic 147

a) Introductory remarks 147

b) Models: LS versus jj Coupling Schemes 148

c) Mean field theory of $H_{SU(N)}$ 152

§4 Scaling Theory and Critique of Mean Field Theory 160

References 174

CHAPTER 4 : Corrections to Mean Field Theory 176

§1 Expansion of Effective Action to Second Order 176

§2 Corrections to Free Energy 184

§3 Corrections to χ and γ 192

§4 Role of Infrared Divergences 200

§5 Quantum Numbers of Elementary Excitations 206

§6 Proof that Expansion in Number of Boson Loops is a 1/N Expansion 214

a) Proof by induction 215

b) Discussion of fluctuations in λ 224

§7 Summary of Results of Chapter 4 224

References 228

CHAPTER 5 : Application of Mean Field Theory to Anderson Lattice and Hubbard Models

§1 The U = ∞ Anderson Lattice Model 231

a) SU(N) invariant model and mean field solution 232

b) Discussion 241

c) Insulating Case 244

d) RKKY interactions in the Kondo limit 247

§2 The U = ∞ Hubbard Model 248

a) Introductory remarks 248

b) Mean field theory 249

c) Discussion 255

References 259

FIGURES

Chapter 1

1. Energy levels and multiplet structure a) for an ordinary rare earth ion; b) for a mixed valence case — 12
2. Valence band XPS spectrum of SmB_6 — 14
3. Example of combined XPS and BIS spectrum, for Nd metal — 17
4. Lattice constants of $REAl_2$ compounds vs. ionic radii — 21
5. Magnetic susceptibility of YbCuAl — 24
6. Specific heat of YbCuAl — 26
7. Second order corrections to E_0 and E_1 — 35
8. a) Chain of self-energy diagrams; b) Another f^0 self energy of order V^6 — 38
9. a) Scattering vertex J ; b), c) Second order scattering processes — 49
10. a) Example of a reducible third-order process; b) Irreducible third order process; c) Second-order self-energy diagram — 49

Chapter 2

1. Examples of diagrams contributing to the free energy of Eq. (40) — 77
2. Diagrammatic form of leading order self consistent conditions (46) and (47) — 80
3. Anomalous propagator for σ — 80

3. Sketches of $\chi(T)$, $C_v(T)$ and $M(h)$, showing phase transition at $T_c \simeq T_k/\ell n\ N$ for large N 117

Chapter 3

1. Self energies of f^0 and f^1 states 131

2. Schematic plot of the F-spectral function 142

3. Self energies contributing to Haldane scaling 162

Chapter 4

1. Diagrams resulting from expansion of S_{eff} to second order in $\sigma(\omega)$, $\sigma^*(\omega)$ 179

2. Analytic structure and contour of Eq. (11) 182

3. RPA-like diagrams resulting from Gaussian functional integral over fluctuations in σ and σ^* 185

4. Diagrammatic representation of equations (19) and (20) 187

5. Diagrams contributing to matrix elements of Q to leading order in $1/N$ 209

Chapter 5

1. Hybridised bands of H_{qp} 234

2. Density of states corresponding to Fig. 5.1 237

3. Densities of states for insulating case 246

4. Proposed phase diagram of the Hubbard model 257

TABLES

Chapter 1

1. Valence states z and magnetic configurations in the mixed valence ions 19

Chapter 2

1. Mean field theory results for $\varepsilon_f(T,h)$, $\Delta(T,h)$, $\chi(T)$, $C_v(T)$ and $M(h)$ for low temperatures and fields, in the Kondo limit 113

CHAPTER 1. INTRODUCTION

§1. Experiment

The study of mixed valence is concerned with the properties of strongly interacting electrons in narrow f bands significantly hybridised with other bands. In the present section, we elaborate on this statement, supporting it with experimental data interpreted with the simplest possible model. In the following section, we give an overview of more sophisticated theoretical treatments, concentrating on those most relevant to this thesis. Finally, we describe the objectives and layout of the thesis.

a) Ionic Energy Levels and Spectroscopy

In discussing the rare earth metals and their compounds, it is usually assumed that, because the partly filled f shells lie within the valence electron core of the ion and have little overlap with neighbouring f shells or with conduction band states, one may as a first approximation take the energy levels of the f states to be those of the free ion. For the latter, by far the largest contribution is the sum of the one electron energies of the electrons in the 4f shell plus the (repulsive) electrostatic energy. We may write this in the form [1]

$$E(f^n) = E_f n + \tfrac{1}{2} U_{ff} n(n-1) \qquad (1)$$

where f^n denotes a state with n electrons in the f shell ($\ell = 3$, so with spin degeneracy $0 \leq n \leq 14$), E_f is the energy

of a single electron in the shell, and the repulsive interaction is U_{ff}. Each state f^n is then split into multiplets by the remaining interactions. The strongest remaining effects are electrostatic in origin, while the spin-orbit coupling is weaker. The *lowest* multiplet for each n is then given by Hund's rules [2]. Multiplet structures in free rare earth ions are shown in [3].

In most rare earth metals and compounds, only a single set of multiplets, say f^n, lies near the bottom of the parabola (1) (Fig. 1.1a). Addition or removal of an f electron to or from the Fermi level of the conduction band requires a large energy of several eV. In this situation only the f^n multiplets need be considered for thermodynamic purposes, and often the lowest multiplet is sufficient. The lowest multiplet usually has a magnetic moment, which couples to the conduction electrons by a direct exchange interaction, originating from the repulsion felt by a conduction electron when it overlaps an f electron, and which may be treated as a perturbation. The interaction couples together the moments on different sites through the RKKY interaction, leading to a magnetically ordered ground state in most cases. The non-spherical environment of each ion can induce additional crystal field splittings of the multiplets. Most features of the ordinary rare earth metals and compounds can be accounted for in terms of these effects.

The situation is different in the mixed valence compounds. As shown in Fig. 1.1b, two configurations, say f^n and f^{n+1}, differ in energy by an amount not much different from the Fermi energy ε_F:

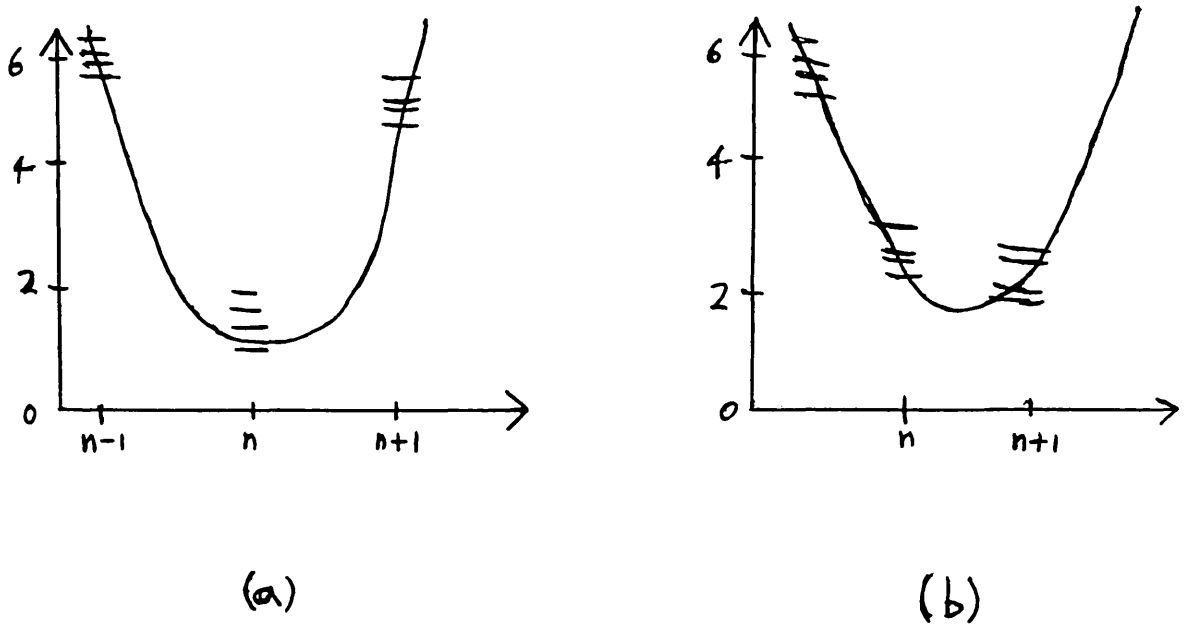


Fig. 1.1 Energy levels and multiplet structure a) for an ordinary rare earth ion; b) for a mixed valence case. Parabola is eq. (1).

$$E(f^{n+1}) - E(f^n) \simeq \varepsilon_F \qquad (2)$$

We specify later how accurately (2) must be satisfied. One expects the Hamiltonian to contain a hybridisation term transferring electrons to or from the band, and since the energy denominators for such processes in perturbation theory are small because of (2), such a term will be important. Then the ground state of the ion will be a quantum mechanical mixture of f^n and f^{n+1} states - a "mixed valence" state.

The large value of U_{ff} and the existence of two values of n in the ground state of mixed valence compounds may both be demonstrated by reference to photoemission experiments. In X-ray photoemission spectroscopy (XPS) and ultraviolet photoemission spectroscopy (UPS) an energetic incoming photon is absorbed by the f shell and causes it to emit a fast electron. The energy of the outcoming electron is measured and yields a continuous spectrum stretching up to an upper limit in energy which corresponds to removal of an electron from the Fermi level. If the sudden approximation is utilised, which states that the electron is removed instantaneously from the f shell, having no time to interact with the system during its passage from the solid, then the spectrum observed is the occupied part of the local f electron density of states, broadened by an instrumental resolution function.

Fig. 1.2 shows an XPS spectrum for SmB_6, taken from a recent, extensive review article [4]. The upper part of the Figure is the experimental data which clearly shows two main features, one just below ε_f, the other some 9 or 10 eV below. In the lower, theoretical curve, the structures are labelled Sm^{2+} and Sm^{3+},

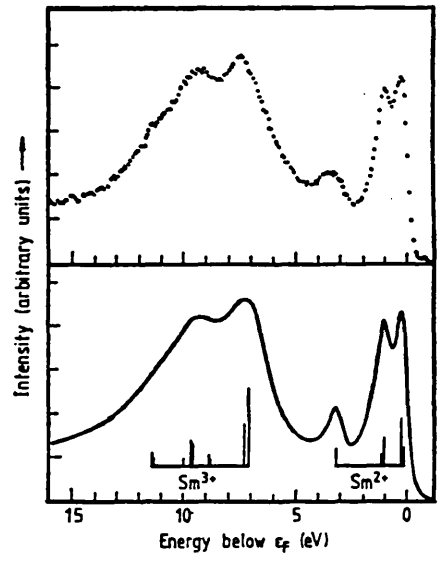


Fig. 1.2 Valence band XPS spectrum of SmB_6, taken from [4], Fig. 4. Upper part of Figure, experiment, lower part theory, showing identification of initial states, and final state multiplet structure.

which refer to the initial state of the ion. (We comment here that this notation refers to the electronic structure of the *core* states, including the f shell; thus Sm^{2+} is an f^6 state and Sm^{3+} is an f^5 state. The electrons removed from the neutral Sm atoms are of course to be found in the conduction band of the solid, or in the filled states of the B_6^{2-} clusters. The exponent (2+ or 3+) in this notation is termed the *valence*; thus for Sm the f^6 state is divalent and the f^5, trivalent.) Removal of an f electron from the f^6 state leaves the ion in a state in one of the multiplets of the f^5 configuration, whose energy lies close to that of f^6, as in condition (2). The Sm^{2+} peak thus shows the existence of mixed valence in the (initial) ground state of the ion. On the other hand, removal of an f electron from the f^5 state leaves the ion in an f^4 state of higher energy given by (1). The line of the Sm^{3+} peak of lowest binding energy therefore gives an estimate of U_{ff} of order 7 eV .

The bars shown inset in the theoretical spectrum correspond to multiplet structure in the final states. When an f electron is removed, the final state is in any one of the multiplets for that configuration, with weights calculated from overlaps with the initial state (assumed to be in the lowest multiplet of the initial configuration). Thus the bars shown (whose length indicates their weight) are calculated using the ionic picture already described, ignoring the effect of the environment. The final theoretical curve is obtained by convoluting with a realistic broadening. This procedure provides unambiguous identification of the final states.

In most rare earth systems, unlike SmB_6 , only a single structure appears in the XPS spectrum, corresponding to removal of an electron from a stable f^n state. The position of the centre of this structure (alternatively, of the lowest multiplet in the fitted spectrum) relative to the Fermi energy is, roughly,

$$\Delta_- = E(f^{n-1}) - E(f^n) + \varepsilon_F \qquad (3)$$

There is another spectroscopy, namely brehmstrahlung isochromat spectroscopy (BIS) , which is essentially the inverse of photo-emission. In BIS , an electron of known energy is captured by the system, emitting a photon whose energy is measured. The resulting spectrum represents the density of *unoccupied* states. Here peaks are seen in rare earth systems at an energy

$$\Delta_+ = E(f^{n+1}) - E(f^n) - \varepsilon_F \qquad (4)$$

relative to ε_F , corresponding to adding an electron to the f shell. The sum

$$\Delta_- + \Delta_+ = \left(E(f^{n-1}) - E(f^n)\right) + \left(E(f^{n+1}) - E(f^n)\right)$$

$$= U_{ff} \qquad (5)$$

according to (1). The combined XPS and BIS spectra therefore provide a direct measure of U_{ff} for the rare earth metals and compounds. An example is shown in Fig. 1.3. Values of U_{ff} of about 5 - 7 eV are found [5], confirming our picture of the importance of ionic energy levels (rather than f-band formation).

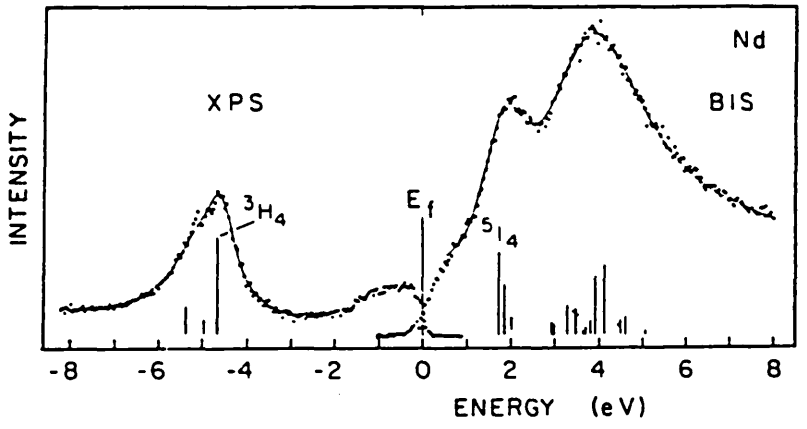


Fig. 1.3 Example combined XPS and BIS spectra, for Nd metal [5]. From (3) and (4), we estimate $\Delta_- \simeq 4.5$ eV , $\Delta_+ \simeq 2$ eV , so $U_{ff} \simeq 6$ eV .

This is found even in Ce metal [5], where the f orbitals are largest and close together, and the tendency to band formation might be thought to be greatest. Ce compounds, many of them mixed valent, have been extensively studied both theoretically and experimentally, by Gunnarsson and Schönhammer and their experimental colleagues [6]. The model used is essentially that described here and below, including hybridisation between f orbitals and the conduction band. Among other results, they confirm that U_{ff} is about 5 - 7 eV in these compounds.

We now identify those rare earth ions which are found to be mixed valent. In most rare earths, the configuration of lowest energy found in the metals and compounds is the trivalent one (R^{3+}, where R is the rare earth atom) with large values of $\Delta_{\pm}$. Common exceptions are Eu and Yb ions, which are often divalent (e.g. in the metals themselves) since by this means they form a half-closed or closed f-shell, gaining exchange energy. The mixed valence cases are found to lie near the ends or centre of the rare earth series; it is the extra energy available from full or half-full shells which makes two configurations (n , n + 1) close in energy, when the host environment is suitable chemically. Thus mixed valence is found in Ce metal and in compounds of Ce , Sm , Eu , Tm and Yb . The pairs of configurations, the characteristics of their lowest multiplets and their low-lying excited states, are set out in Table 1.1. Notice that all except Tm possess one non-magnetic (J = 0) and one magnetic (J = 5/2 or 7/2) configuration; it is these with which we are mostly concerned in this thesis, though the Tm-like case is treated briefly in Chapter 3. This emphasis reflects the fact that the vast majority of mixed valence compounds known do not involve Tm ions.

TABLE 1.1 Valence states z and magnetic configurations in the mixed valence ions (after [4]).

							Higher lying multiplets:	
Ion	z	f^n	S	L	J	g	J	E_J(K)
Ce	3+	f^1	1/2	3	5/2	6/7	7/2	3000
	4+	f^0	0	0	0	-	-	-
Sm	2+	f^6	3	3	0	-	1	410
	3+	f^5	5/2	5	5/2	2/7	7/2	1500
Eu	2+	f^7	7/2	0	7/2	2		
	3+	f^6	3	3	0	-	1	480
Tm	2+	f^{13}	1/2	3	7/2	8/7		
	3+	f^{12}	1	5	6	7/6		
Yb	2+	f^{14}	0	0	0	-		
	3+	f^{13}	1/2	3	7/2	8/7	5/2	15000

b) Lattice Constants and Thermal Expansion

A simple method for estimating the degree of mixing of f^n and f^{n+1} in rare earth compounds is provided by measurements of lattice constants. Compounds whose compositions differ only in the rare earth ion they contain in many cases have the same structure across the whole rare earth series, but with differing lattice constants. For, say, trivalent rare earth ions, the size of the ion decreases with increasing number of f electrons - the so-called *lanthanide contraction* - and so the lattice constants decrease monotically across the series. On the other hand, for a *given* ion, the radius *increases* with the number of f electrons. The lattice constant that a mixed-valence compound would have if the rare earth ion were trivalent can thus be found by extrapolation from the rest of the series, while a lattice constant for a hypothetical divalent ion must be estimated by another method, as we will see. Then, *assuming linear variation of* n *with lattice constant* (an assumption known as Végard's law), the valence can be estimated.

Figure 1.4 gives an example of the procedure, based on the $REAl_2$ series of compounds (RE = rare earth). The lattice constant is plotted against the radius of the trivalent ion. Two estimates of the lattice constant for $REAl_2$ containing Yb^{2+} are shown, one based on the ionic radius of Yb^{2+}, the other on the lattice constant of $CaAl_2$. These two estimates are very close. One then deduces that in $YbAl_2$, $z \simeq 2.5$.

An estimate such as that just given suffers from obvious drawbacks, such as the difficulty in obtaining the "divalent" (and in some cases also the "trivalent") reference point. Furthermore, the linear relationship of lattice constant and valence can be

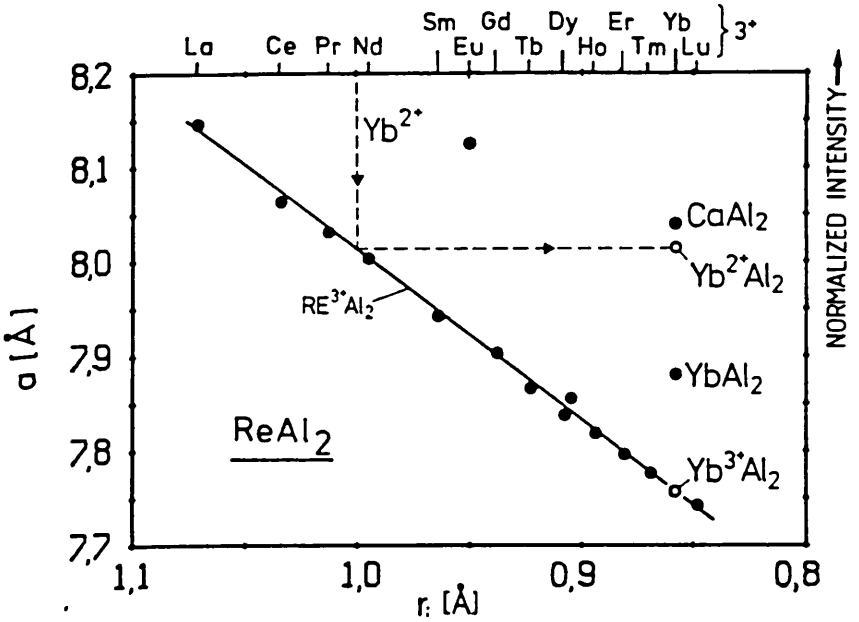


Fig. 1.4 Lattice constants of $REAl_2$ compounds vs. ionic radii (from [7]). Dashed line shows result of inputting ionic radius of divalent Yb .

questioned (see e.g. [7]). Nonetheless, the method demonstrates that mixed valence exists in many materials, and is easily applied to obtain a first estimate of the valence.

A related "anomaly" to that in the lattice constants appears in the thermal expansion. Most materials expand as T is increased. In the mixed valence compounds, the valence may also change with temperature, and as we have seen, this may in turn affect the lattice constants. Thus mixed valence compounds may have "anomalous thermal expansion", which is the remainder when the expansion of a suitable isostructural reference compound is subtracted off. Whether the anomaly is positive (increase in volume) or negative (decrease in volume) depends on whether n increases or decreases with temperature. Theoretical considerations predict (see for example Chapter 2, §6) that as T increases from zero, the valence shifts towards the configuration with the larger degeneracy $2J + 1$ (see Table 1.1). Therefore, the anomalous thermal expansion should be positive for Ce and negative for Yb. The former is confirmed in several Ce compounds [8], while a small negative anomalous expansion is seen in the compound YbCuAl [9]. If we are bold enough, we may try to extract values for $n(T)$ from these results, either by using reference compounds again, or by assuming that the anomalous expansion stops when the valence saturates at an integer value [8]. In the case of YbCuAl, we deduce that z is slightly less than 3. In fact, the valences of most Ce compounds, in particular, are nowadays given as 3 within a margin of 0.3 to 0.4 [10]; many Ce compounds formerly thought to be "tetravalent" are now believed to be in this category.

Finally in this subsection we comment on terminology. We are discussing *homogeneous* mixed valence, where each RE lattice site is equivalent, and has a genuinely non-integer average valence. Inhomogeneous examples are also known, in which the average valence is fractional because some sites have $z = 3$ and some $z = 2$. These do not constitute as interesting a many-body theory problem as those discussed here. We will use the term mixed valence to mean the homogeneous case; the terms intermediate valence and valence fluctuators will be used as synonyms also.

c) Susceptibility and Specific Heat

We now discuss briefly thermodynamic properties of mixed valence systems. We will see that they differ radically from normal "stable moment" rare earth compounds, especially at low temperatures, where instead of the usual magnetically ordered ground states, the majority of mixed valence materials possess "Fermi liquid" behaviour, characterized by very small effective Fermi temperatures.

Fig. 1.5 shows the magnetic susceptibility of YbCuAl. The main features are: a) Curie-Weiss behaviour at high temperatures ($T > 40K$) with effective moment and Curie-Weiss constant, defined by

$$\chi(T) = \frac{\frac{1}{3}\mu_{eff}^2}{k_B(T+\theta)} \qquad (6)$$

taking values [7] $\mu_{eff} = 4.33\ \mu_B$

$$\theta = 33K \quad ;$$

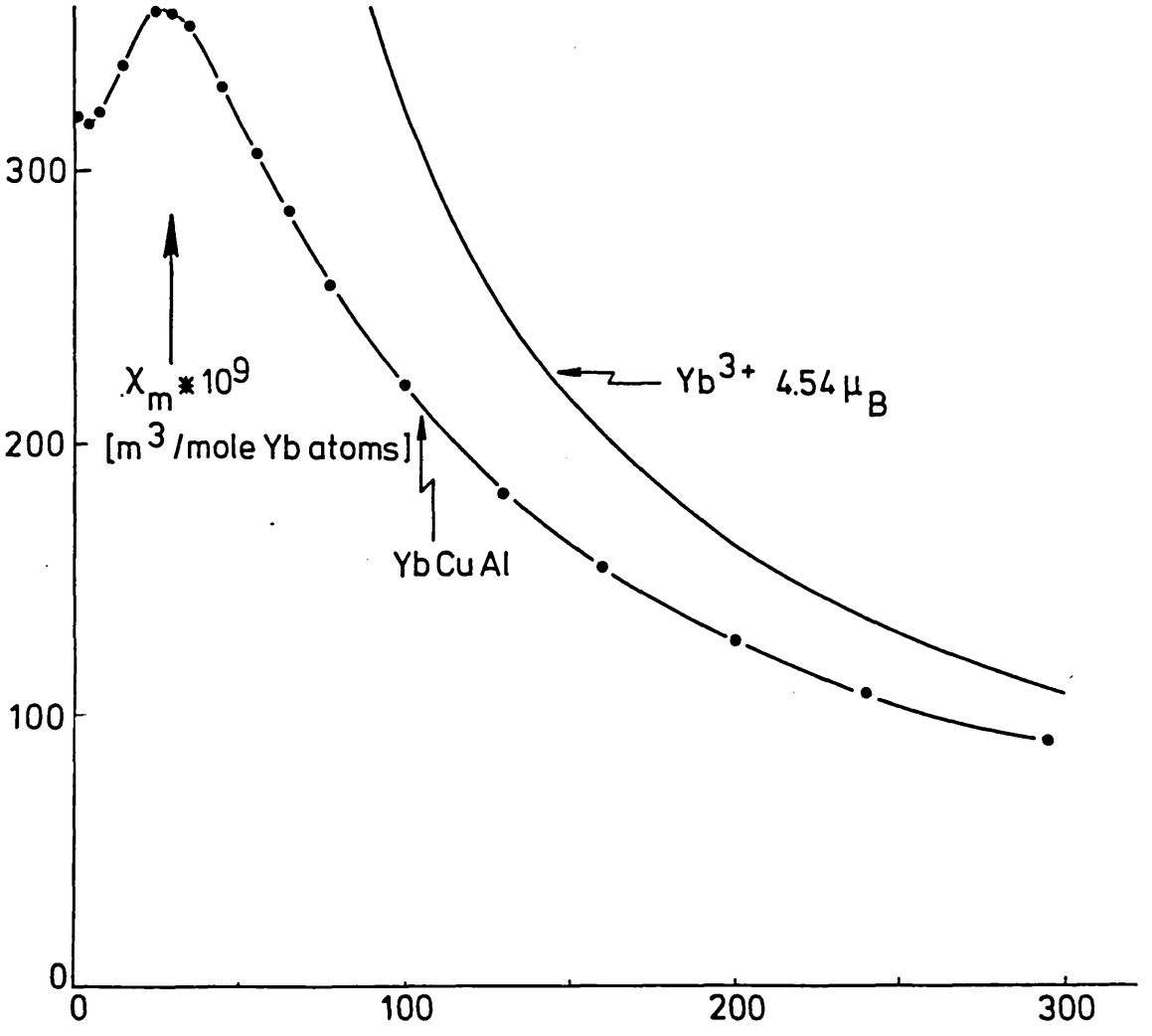


Fig. 1.5 Magnetic susceptibility of YbCuAl , after [9].

b) a maximum at around $T_{max} = 30K$;

c) $\chi(T)$ tends to a constant as $T \to 0$ (with corrections going like T^2) .

These features are typical of many mixed-valence systems [4,8], though the parameters μ_{eff} , θ , T_{max} of course vary from case to case. The high temperature moment is close to that of the magnetic configuration of the RE ion involved, as given in Table 1.1, with

$$\mu_{eff}^2 = g^2 J(J+1)\mu_B^2 \qquad (7)$$

At low temperatures, the susceptibility is presumably strongly influenced by the mixing of configurations. A simple view of the finite susceptibility at $T = 0$ is simply that the moment has only a finite lifetime, due to hybridisation. We return to this question in much more detail in the rest of this thesis. For now, we simply note the similarity to the (almost constant) Pauli susceptibility of a Fermi gas well below its Fermi temperature.

The electronic specific heat C_V of mixed valence systems is, as usual, more difficult to obtain because of the contribution of phonons. However for YbCuAl , and some other cases, the structures in C_V occur at low enough temperatures, and are large enough in magnitude that they can be distinguished fairly easily, after subtracting the (mainly phonon) specific heat of a reference material, such as in this case LuCuAl . Data are shown in Fig. 1.6.

One sees that the specific heat would apparently be small at high T , as expected for the moment discussed for the susceptibility. Below a temperature of 30K , where a maximum occurs as in $\chi(T)$,

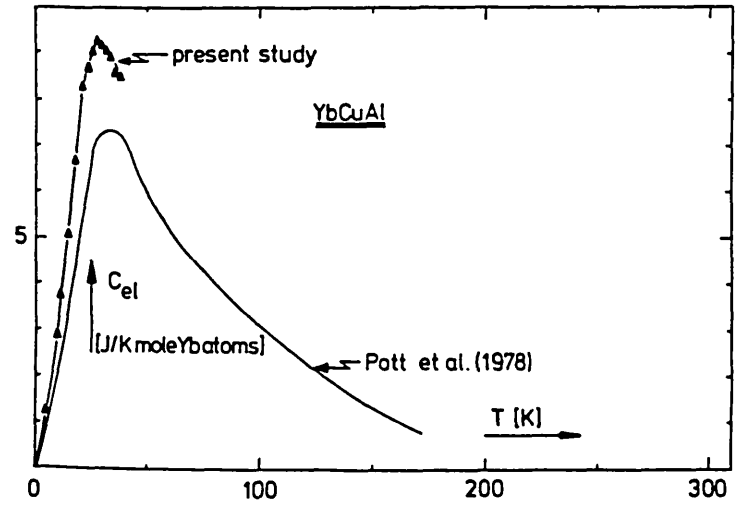


Fig. 1.6 Specific heat of YbCuAl , after subtraction of phonons [9].

the behaviour resembles the Sommerfeld formula for a Fermi liquid, with the form

$$C_v(T) = \gamma T + \beta T^3 + \ldots \qquad (8)$$

It is noteworthy that not only is γ non-zero (and large, $\gamma = 260$ mJ mol^{-1} K^{-1}) but also that β is measurable and found to be positive [9].

Finally we note that it has been shown by Newns and Hewson [8] that for a large number of intermetallic mixed valence compounds, the ratio of magnetic susceptibility at $T = 0$, $\chi(0)$, and linear coefficient of specific heat γ lies close to the value

$$\frac{\chi(0)}{\gamma} = \frac{\mu_{eff}^2}{\pi^2 k_B^2} \qquad (9)$$

(where (7) is used) to within 10-20%. This ratio would be 1 in a Fermi gas, neglecting correlations. Thus (9) is evidence that the quasiparticles responsible for the Fermi liquid behaviour of χ and C_v, while having a large density of states, have rather small many-body correlations. In addition, the appearance of μ_{eff}^2, which in Table 1.1 arose from the spin-orbit coupling and *local* conservation of $\underline{J}$, within a single f shell, suggests that intersite effects among the RE ions are negligible. The effects discussed in this subsection demand further theoretical explanation, as do the many other low temperature data (transport properties, photoemission spectroscopy, neutron scattering) not discussed here.

§2. Theory

a) Anderson Impurity model: Expansion in U

The approach discussed in §1, where ionic correlations (U) and other splittings are treated first, and mixing of configurations via hybridisation with the conduction band is treated last, as a perturbation, is known as the Hirst model [11]. Here we discuss a model which may be regarded as containing the bare essentials of Hirst's approach. Throughout this theoretical discussion we treat only the problem of a single mixed valent RE ion in a metal, as have most of the advanced discussions in the literature. The justification for applying the results of such a calculation to the concentrated experimental systems is still controversial; we comment further on this question in Chapter 5. Restricting ourselves, then, to models of a "single impurity" (a single RE ion interacting with the electronic states) we consider the Anderson Hamiltonian [12]:

$$H = \sum_{k\sigma} \varepsilon_k \, c^+_{k\sigma} c_{k\sigma} + \sum_{k\sigma} \left(V(k) f^+_\sigma c_{k\sigma} + h.c. \right) + E_f \sum_\sigma f^+_\sigma f_\sigma + U f^+_{\frac{1}{2}} f^+_{-\frac{1}{2}} f_{-\frac{1}{2}} f_{\frac{1}{2}} \qquad (10)$$

The model contains: (i) a spectrum of conduction electron states with energies ε_k and density of states, $\rho(\varepsilon)$, having a characteristic half-width D. Only s-wave states couple to the impurity in this model, so they alone are represented by the operators $c_{k\sigma}$, $c^+_{k\sigma}$, other states being omitted. The chemical potential μ is taken to be at the centre of the band, and set

equal to zero; thus electronic energies are measured relative to μ ; (ii) States created by f_σ^+ ($\sigma = \pm\frac{1}{2}$ for both f and conduction electrons) which hybridise with the conduction electrons through the term in V(k) , which is independent of spin. V(k) is often made independent of k ; (iii) The f electrons have energy E_f and a correlation energy U , giving back eq. (1) when V is neglected:

$$E(f^{n_f}) = E_f n_f + \frac{1}{2} U n_f(n_f - 1) \qquad (11)$$

where, from now on, n_f = no. of f electrons = $\sum_\sigma f_\sigma^+ f_\sigma = 0$, 1 or 2 . It will be noted that the orbital angular momentum of the f electrons has been dropped, so they are really s electrons.

While, as explained in §1, we are really interested in taking U large and treating V as a perturbation, much has been learned by instead using perturbation theory in U , with the one-body term V treated exactly in each order in U . The expansion can be carried out with infinite bandwidth, and a constant density of states, using ordinary many-body (Feynman-Matsubara) perturbation theory [13]. The most useful results are exact relations proved to all orders in U . One such result is the Friedel sum rule, which was first proved to hold for the Anderson model by Langreth [14]. The sum rule states that the occupation at t = 0 of the f states, n_f , is related to the phase shift seen by conduction electrons scattering off the impurity:

$$n_f = \sum_\sigma \frac{\delta_\sigma}{\pi} \qquad (12)$$

where δ_σ is the s-wave phase shift for spin σ. The phase shifts are related to the f Green's function [15]

$$G_f(\tau)_\sigma = -\langle T f_\sigma(\tau) f_\sigma^+(0)\rangle$$

by

$$\delta_\sigma = \tan^{-1}\left(\frac{\mathrm{Im}(\tilde{G}_f(i\eta)_\sigma^{-1})}{-\mathrm{Re}(\tilde{G}_f(i\eta)_\sigma^{-1})}\right) \qquad (13)$$

where $\tilde{G}_f(i\omega)$ is the Fourier transform of $G_f(\tau)$, η is an infinitesimal positive quantity, and the $\tan^{-1}$ obeys

$$0 \leqslant \tan^{-1} x \leqslant \pi$$

Noting that for the Anderson model $\tilde{G}_f$ can be written as

$$\tilde{G}_f(i\omega)_\sigma = \left(i\omega - \Sigma_f(i\omega) - V^2 \sum_k \frac{1}{i\omega - \varepsilon_k}\right)^{-1}$$

and that the self energy Σ_f is real at $\omega = 0$ when $T = 0$, Langreth also deduced that the f density of states at $\varepsilon = 0$ can be written

$$\left(\rho_f(\varepsilon) = -\frac{1}{\pi}\,\mathrm{Im}\,\tilde{G}_f(\varepsilon + i\eta)_\sigma\right)$$

$$\rho_f(0) = \frac{\sin^2\delta_\sigma}{\pi\Delta_o} \qquad (14)$$

where the conduction band propagator

$$\sum_k \frac{1}{i\omega - \varepsilon_k}$$

is approximated as $-i\pi\rho \operatorname{sgn}\omega$ for large bandwidth, and

$$\Delta_o = \pi\rho V^2 \tag{15}$$

Another important result was proved by Yamada [13] and generalized by Yoshimori [16]. First note that the expansion in U is an ordinary perturbation expansion about a non-interacting Fermi gas and as such can be expected to behave like a Fermi liquid to all orders in U (no phase transition occurs). The results are conveniently expressed in terms of the difference in the thermodynamic potential for the interacting and free case; we refer to this as the "free energy of the impurity" F, which is a function of the temperature and magnetic field. The latter is introduced by adding to the Hamiltonian (10) the terms

$$-g\mu_B h\left(\sum_\sigma \sigma f_\sigma^+ f_\sigma + \sum_{k\sigma} \sigma c_{k\sigma}^+ c_{k\sigma}\right)$$

where g is the Landé factor, here assumed equal for the two types of electrons. Note that this free energy for the impurity is *not* proportional to the size of the system, but to the number of impurities (here 1). The Fermi liquid behaviour to each order in U means that there is a non-vanishing linear coefficient of specific heat γ (see eq. (8)), a finite magnetic susceptibility at $T = 0$, defined by

$$\chi(0) = -\frac{\partial^2 F}{\partial h^2}\Big|_{T=0}$$

and also an "f charge susceptibility" defined by

$$\chi_c(0) = -\frac{dn_f}{dE_f}\Big|_{T=0}$$

Yamada proved that these quantities satisfy, to all orders in U, the relation

$$\gamma = \frac{\pi^2}{3} k_B^2 \left(\frac{1}{2}\chi_c(0) + \frac{\chi(0)}{2\cdot\frac{1}{3}\mu_{eff}^2}\right) \qquad (16)$$

where $\mu_{eff}^2 = s(s+1)(g\mu_B)^2$ with $s = \frac{1}{2}$. This relation holds for all E_f, U and Δ_0. The terms "symmetric Anderson model" and "asymmetric Anderson model" are sometimes applied respectively to the cases

$$E_f = -\tfrac{1}{2}U$$

and

$$U >> -2E_f \quad .$$

The asymmetric case is most relevant to mixed valence. When also $|E_f| >> \Delta_0$, one expects that $n_f \simeq 1$ in the ground state, and $\chi_c(0)$ is small, compared with γ and $\chi(0)$. Then one finds

$$\frac{\chi(0)}{\gamma} = \frac{2\mu_{eff}^2}{\pi^2 k_B^2} \qquad (17)$$

that is, *twice* the value for non-interacting electrons (c.f. eq. (9)). This result was also found by Wilson [37] in his numerical renormalization group study of the Kondo problem, which as we will see corresponds to this limit.

The proofs of these results, and some other exact relations, rely on Ward identities similar to those in Fermi liquid theory for homogeneous systems. The Ward identities result from conservation of particle number and spin, which still holds when interactions are included.

b) Anderson Impurity model: Expansion in V

We now turn to the expansion in powers of V for finite U. An early calculation was that of Scalapino [17]. Keiter and Kimball [18] developed a formalism that was widely used [19] despite questionable aspects which were later avoided [20]. Haldane [21] used a quite different formalism and provides the clearest discussion as well as the most accurate results to low order in V at high temperatures. Our discussion will avoid formal questions by using mainly Schrödinger perturbation theory. The point of all these methods is that one is perturbing around an *interacting* system ($U \neq 0$) so that the usual Feynman diagram methods, based on Wick's theorem, cannot be used (in contrast to the expansion in powers of U). Therefore we return to more fundamental perturbation techniques.

Returning to Hamiltonian (10), let us introduce the notation E_0 for the energy of the filled Fermi sea with the impurity unoccupied ($n_f = 0$) and E_1 for the Fermi sea with impurity state $n_f = 1$, $\sigma = \pm\frac{1}{2}$, with

$$E_f = E_1 - E_0 \tag{18}$$

in agreement with previous usage. It is convenient to neglect the contributions of states with $n_f = 2$ in the extreme asymmetric limit $U >> |E_f|$; for this to be strictly correct we need in fact $U >> D$, however the results we obtain can be readily extended to $U < D$ as we will indicate.

The advantage of the E_0 , E_1 notation is that we can calculate corrections to these energies in perturbation theory in V . At first order in V , these corrections are obviously zero. At second order, the corrections arise from intermediate states represented diagrammatically in Fig. 1.7. In these diagrams, "time" runs up the page, so upward arrows represent particles (including both f^0 and f^1 states) while downward arrows appear only as hole states in the conduction band. In Fig. 1.7(a), the intermediate state contains the f^1 state of the impurity, with a single hole created in the band; there is a summation over the (equal) spins of the f electron and conduction hole. Using (10) and the usual rules for Schrödinger perturbation theory [22], we have for $\tilde{E}_0$, the f^0 energy perturbed to order V^2 ,

$$\tilde{E}_0 = E_0 + \sum_{-D<\varepsilon_k<0,\ \sigma} \frac{V^2}{E_0 - E_1 + \varepsilon_k}$$

$$= E_0 + \frac{2\Delta_0}{\pi} \ln \frac{|E_f|}{D} \tag{19}$$

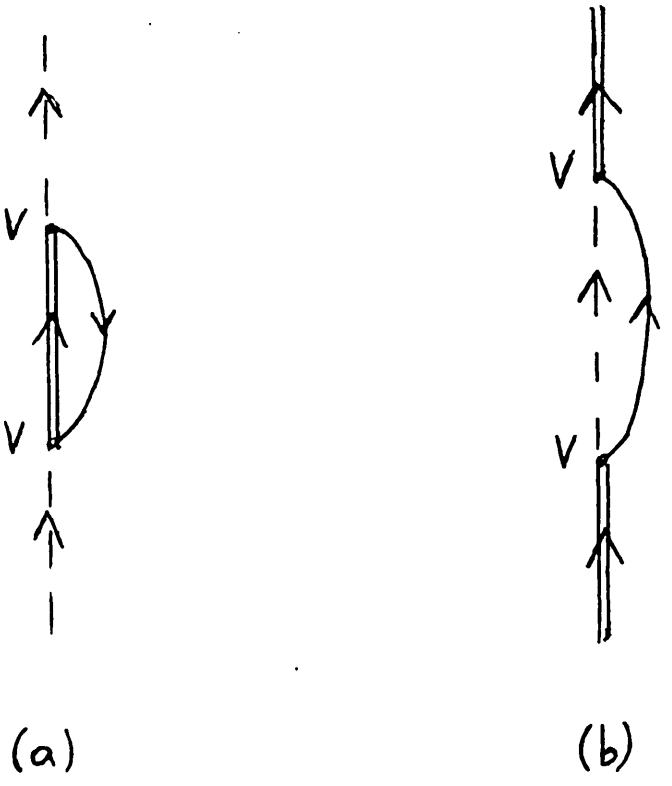


Fig. 1.7 Second order corrections to (a) E_0 , (b) E_1 . Double line: f^1 state; dashed line: f^0 state; ascending curved line: conduction electron; descending curved line: conduction hole. Diagram (a) involves a sum over spin; (b) does not.

Here we used (18), took $D >> |E_f|$ and ignored the possibility that the denominator in (19) might be zero for some E_f and ε_k. The latter problem is dealt with in more formal treatments [18,20, 21]. Similarly, for diagram (b), we find

$$\tilde{E}_1 = E_1 + \sum_{\substack{k \\ D>\varepsilon_k>0}} \frac{V^2}{E_1 - E_0 - \varepsilon_k}$$

$$= E_1 + \frac{\Delta_0}{\pi} \ln \frac{|E_f|}{D} \qquad (20)$$

The "small" perturbative correction is infinite when E_f passes through zero, and when $E_f \neq 0$, either (19) or (20) involves integrating across a $1/X$ singularity. In early work on mixed-valence [23,24] the singularities of the perturbation theory due to the degeneracy when $E_f \simeq 0$ ("mixed-valence regime") were a major preoccupation. Equally important is the logarithmic dependence on the bandwidth D in (19) and (20). Both of these aspects have been essentially solved by the work summarized in this chapter.

At this stage we note that if we had had $|E_f| << U << D$ then an extra term of order

$$\frac{\Delta_0}{\pi} \ln \frac{U}{D} \qquad (21)$$

would have appeared in (20) and the f^2 energy would have been shifted by a term like that in (19) but with U replacing E_f. All three energies contain a dependence on D

$$-\frac{2\Delta_0}{\pi}\ln D \qquad (22)$$

which can be absorbed into a shift of the zero of energy in the Hamiltonian, after which all remaining terms in perturbation theory contain U in place of D as the effective cutoff [21]. Physically, this occurs because electrons of energy much larger than U do not feel the interaction; the logarithmic shift (22) of all energies arises purely from hybridisation [21] as in the non-interacting case.

In an effort to improve on (19) and (20) we may try making them self-consistent, by substituting the renormalised energy $\tilde{E}_0$ for E_0 in the order V^2 self-energy. Then

$$\tilde{E}_0^{BW} = E_0 + \frac{2\Delta_0}{\pi}\ln\frac{|E_1 - \tilde{E}_0^{BW}|}{D} \qquad (23)$$

We call this $\tilde{E}_0^{BW}$ because such a substitution is made in Brillouin-Wigner perturbation theory, and is derived formally (and extended to finite temperature) in [18-20]. On physical grounds we take the lowest solution to the transcendental equation (23); it is found always to lie below E_0 and E_1, thus self-consistently avoiding the energy denominator problem mentioned after eq. (19). In effect, (23) sums up a chain of processes of the type of Fig. 1.7(a), as shown in Fig. 1.8(a).

Eq. (23) is also found in the variational approach of Varma and Yafet, whose variational wavefunction is a linear combination of (i) the unperturbed f^0 state and (ii) the f^1 state with a conduction hole of the same spin, labelled by its momentum k. On repeated application of the Hamiltonian, the two parts (i) and

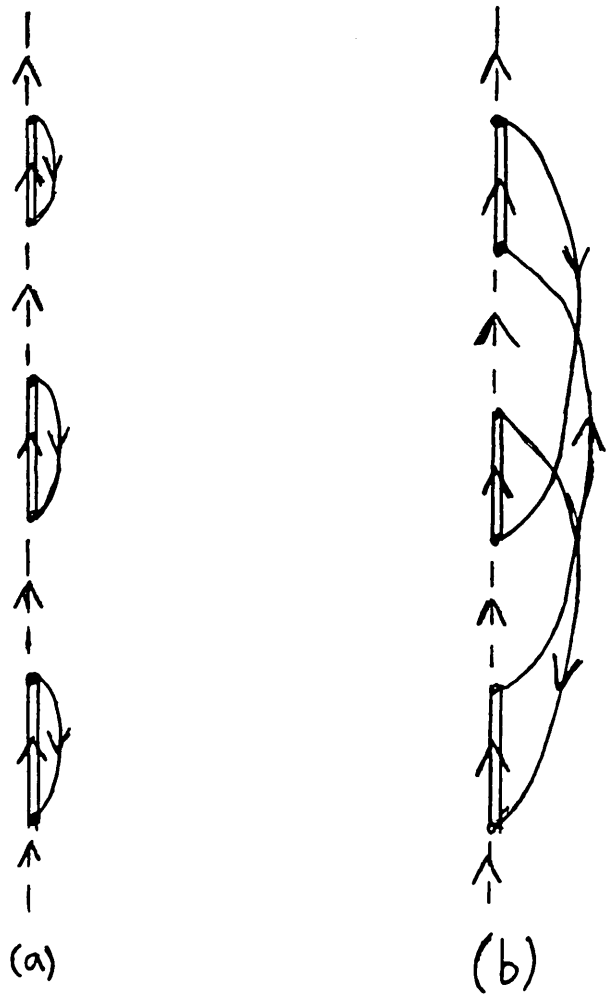


Fig. 1.8 (a) Chain of self-energy diagrams; (b) Another f^0 self-energy diagram of order V^6 .

(ii) are interchanged, as in Fig. 1.8(a), making evident the similarity of these approaches.

If (20) is also made self-consistent, then

$$\tilde{E}_1^{BW} = E_1 + \frac{\Delta_0}{\pi} \ln \frac{|\tilde{E}_1^{BW} - E_0|}{D} \tag{24}$$

Comparing $\tilde{E}_0^{BW}$ and $\tilde{E}_1^{BW}$, one finds that for $E_f >> \Delta_0$, $\tilde{E}_0^{BW}$ is the lower, while for $-E_f >> \Delta_0$, $\tilde{E}_1^{BW}$ is the lower. As may be apparent already from the experimental and theoretical results so far, the physically desirable result is that the ground state is a singlet, i.e. like $\tilde{E}_0^{BW}$, not like $\tilde{E}_1^{BW}$ which would give an infinite magnetic susceptibility at $T = 0$, for example. Thus the approach so far is not good as $n_f \to 1$ and we require a deeper understanding to see why (23) is (in fact) physically (if not always quantitatively) correct, while (24) is not. In the remainder of this and in the following subsection, we attempt to provide such an understanding.

Returning to the direct perturbation theory in powers of V, one finds more logarithms appearing in higher orders. Calculating at finite temperature [21] with $T >> |E_f|$, Δ_0, one finds that the temperature cuts off the logarithmic, low-energy ("infrared") divergences of the type discussed after eq. (20), instead of $|E_f|$. Furthermore, the logarithms appear always in the combination

$$E_f^*(T) = E_f - \frac{\Delta_0}{\pi} \ln \frac{T}{D} \tag{25}$$

when one calculates thermodynamic quantities in this regime [21]. This suggests that the dependence on D can be absorbed into a redefinition or "renormalisation" of E_f, so that all results depend only on the two quantities Δ_0 and the new E_f^*; in fact, one of these, say Δ_0, fixes the energy scale, and the ratio $\Delta_0/E_f^*(\Delta_0)$ is the only remaining parameter. We now show that this is so by describing Haldane's scaling approach [25].

Eq. (25), if true, implies that when D is varied (say by δD) E_f can also be changed such that physical results are invariant, up to terms which vanish for large D. It is convenient to show this by *reducing* D to $D - \delta D$. Since this process *removes* states involving excitations in this energy range, physical results can be left invariant if parameters in the Hamiltonian are changed to account for the perturbative effect of those excitations which are now missing (retardation of the effective interactions, that is, energy dependence, can be neglected, so the dynamics may still be described by a Hamiltonian). The differential "scaling equations" thus found may be integrated to give information about finite changes in D; in particular, by taking the lower limit value of D to be of order T, one obtains an effective Hamiltonian describing the system at that temperature. Thus reducing the bandwidth D in this way allows us to follow the evolution of the system as the temperature is reduced, and different temperature regimes can be identified. We note that while we are here concerned with static, thermodynamic quantities, similar considerations apply to dynamics (correlation functions) with frequency ω playing the role of T.

To carry out the calculation we return to the diagrams of Fig. 1.7 and eq. (19,20), but this time with the conduction electron energies constrained to lie in the range

$$D - \delta D < |\varepsilon_k| < D \tag{26}$$

with δD infinitesimal. Then with $|E_f| \ll D$, we obtain in place of (19) and (20),

$$\delta E_0 = -\frac{2\Delta_0}{\pi}\frac{\delta D}{D}$$

$$\delta E_1 = -\frac{\Delta_0}{\pi}\frac{\delta D}{D}$$

so that

$$\delta E_f = \delta E_1 - \delta E_0 = \frac{\Delta_0}{\pi}\frac{\delta D}{D} \tag{27}$$

Thus to this level of accuracy, results for the Hamiltonian with bandwidth D and f-level energy E_f are equivalent to those for bandwidth $D - \delta D$ and f-level energy $E_f + \delta E_f$. There is no change in Δ_0 [25], which is obtained by calculating the correction to the hopping vertex, and no wavefunction renormalisation, i.e. no rescaling of the states themselves, because the change in the norm of the states by the perturbation (26) vanishes as $D \to \infty$ [25].

While these results are correct to order V^2, it turns out that there are no higher order corrections, because higher order self energies, such as that shown in Fig. 1.8b are non-logarithmic

and their contribution to (27) vanishes as $D \to \infty$. It follows that the only divergences (with D) in self-energies are due to structures of the type of Fig. 1.7 (which may occur as sub-diagrams, inside other self-energies or even each other). Integrating (27) down to $D \simeq T$ confirms (25).

We now examine the different regimes of temperature and the breakdown of perturbation theory. Let us write

$$E_f(D) = E_f(D_0) - \frac{\Delta_0}{\pi} \ln \frac{D}{D_0} \qquad (28)$$

where D_0 is the *initial* bandwidth, previously called D, and $E_f(D_0)$ is the initial value of E_f. Clearly as we repeatedly perform the operation (26), it is $E_f(D)$ which determines the validity of the perturbation theory. Furthermore, when D is of the order of Δ_0, the perturbation expansion breaks down. We examine the possibilities in turn.

The first possibility is that the condition $D \gg E_f(D)$ is violated, but with $E_f(D) \gg \Delta_0$. This occurs when $D = T^*$ where

$$T^* = E_f(T^*)$$

$$= E_f(D_0) + \frac{\Delta_0}{\pi} \ln \frac{D_0}{T^*} \qquad (29)$$

At energies well below T^*, the excited f^1 state must also be eliminated, as it is thermally inaccessible (when $T \ll T^*$). The impurity therefore has $n_f \simeq 0$ and the remaining effect of the impurity on the system is due to residual interactions which arise

from virtual excitation of the f^1 state. There is therefore a phase shift of order Δ_0/T^*, giving for n_f,

$$n_f = \frac{2\Delta_0}{\pi T^*} + O\left(\left(\frac{\Delta_0}{T^*}\right)^2\right)$$

and the effective f density of states due to this resonant scattering gives (at low temperature)

$$\chi(0), \gamma \propto \frac{2\Delta_0}{\pi T^{*2}}$$

the factors being the usual magnetic or thermal factors. The full f density of states is expected to show a Lorentzian resonance at $\varepsilon \simeq T^*$, of width Δ_0, with logarithmic corrections at large ε. Note that in (29), terms vanishing as $D \to \infty$ are neglected, but a constant inside the logarithm could survive in this limit and is a universal number which can be obtained by comparing perturbation expansions above and below the cross-over at $D \simeq T^*$ [21].

In summary, this case shows the properties of a Fermi liquid, with the $\chi(0)/\gamma$ ratio taking the value of a non-interacting system (cf. (9), (17)). (29) is similar to (23), but with a different coefficient, which arises from the "folding-in" of the renormalisation of the f^1 state with the f^0 state, which was not included in (23). Note that the scaling means that even systems with initial or "bare" value of $E_f \simeq 0$ or < 0 may scale into this $n_f \simeq 0$ case, if D_0 (or Δ_0) is large enough. Thus we have begun to answer the "small denominator" problem of (19,20).

The next possibility, as $E_f(D_0)$ is reduced, is that we may avoid $D \simeq |E_f(D)|$ until we reach

$$D \simeq \Delta_0 \gtrsim |E_f(D)| \tag{30}$$

This is an intermediate case where we can say little, except by suggesting the study of a Hamiltonian with $D \ll \Delta_0$, in which one treats D (the hopping in a tight-binding model of the conduction band) as a perturbation on the rest of the Hamiltonian which one first solves exactly. This approach [26] again shows that the behaviour is that of a Fermi liquid, with now

$$\chi(0), \gamma \propto 1/\Delta_0$$

The final possibility (in our scheme of different qualitative or asymptotic behaviours) is that the first crossover that spoils the scaling is when

$$D \simeq -E_f(D)$$

This occurs when $D = \tilde{T}$ with

$$-\tilde{T} = E_f(D_0) + \frac{\Delta_0}{\pi} \ln \frac{D_0}{\tilde{T}} \tag{31}$$

(again, a constant can be introduced inside the logarithm and determined perturbatively [21]). This time, it is the f^0 state which must be eliminated at energies below $\tilde{T}$, and the impurity

has $n_f \simeq 1$ and is in one of the two degenerate spin states. Because of this degeneracy, the remaining Hamiltonian, with residual interactions induced by virtual fluctuations to the f^0 state, is not as simple to understand as the previous ($n_f \simeq 0$) case.

If we assume, then, that $D \ll \tilde{T}$, we may obtain the effective Hamiltonian perturbatively, neglecting the dependence of the new terms on the energies ε_k of the conduction electrons which are scattered from the impurity. This transformation, which was first applied to the case where the bare f level E_f lies *outside* the original bandwidth D_0, is known as the Schrieffer-Wolff transformation [27].

Since the initial and final states of the impurity are both f^1, the lowest order terms are $O(V^2)$. To this order the only possible scattering process is that where the f electron hops off the impurity to create the outgoing electron (or to destroy a hole) and another electron subsequently hops onto the impurity. This generates a term of order

$$\frac{V^2}{\tilde{T}} \sum_{kk'\sigma\sigma'} f^+_\sigma f_{\sigma'} c^+_{k'\sigma'} c_{k\sigma} \tag{32}$$

in the Hamiltonian, using the assumption $|\varepsilon_k|, |\varepsilon_{k'}| < D \ll \tilde{T}$. (A self-energy term of order $\rho V^2 D/\tilde{T}$ is merely a constant in the Hamiltonian, which we drop.) (32) can be written in the form

$$\frac{V^2}{2\tilde{T}} \sum_{\substack{kk' \\ \sigma_1\sigma_2 \\ \sigma_3\sigma_4 \\ i=1,2,3}} f^+_{\sigma_1} \tau^{(i)}_{\sigma_1\sigma_2} f_{\sigma_2} c^+_{k'\sigma_3} \tau^{(i)}_{\sigma_3\sigma_4} c_{k\sigma_4}$$

$$+ \frac{V^2}{2\tilde{T}} \sum_{\substack{kk' \\ \sigma\sigma'}} f^+_\sigma f_\sigma c^+_{k'\sigma'} c_{k\sigma'} \tag{33}$$

where the $\tau^{(i)}$ are the Pauli spin matrices, so that (33) contains a term of the form $\underline{S} \cdot \underline{s}$, where $\underline{S}$, ($\underline{s}$) are local spin (spin-density) operators for the f (conduction) electron states respectively, and the last term is simple potential scattering, similar to that in the $n_f \simeq 0$ case. It turns out to be unnecessary to go to higher order in V^2 in generating the effective Hamiltonian.

(33) defines the s - d or Kondo Hamiltonian with spin-flip coupling $J = -V^2/\tilde{T}$ and potential scattering $K = V^2/\tilde{T}$. The problem of solving this Hamiltonian was the long-standing and difficult "Kondo problem", which we review briefly from the scaling point of view in the next subsection. We can, however, make some final deductions in closing this subsection.

In analogy with the $n_f \simeq 0$ case, the deviation from $n_f = 1$ will be of order

$$n_f = 1 - \frac{\Delta_0}{\pi\tilde{T}} + O\left(\left(\frac{\Delta_0}{\tilde{T}}\right)^2\right)$$

and there will be a charge susceptibility:

$$\chi_c(0) = -\frac{dn_f}{dE_f(\Delta_0)} \simeq \frac{\Delta_0}{\pi\tilde{T}^2}$$

$\chi(0)$ and γ will contain terms of this order also, but will be dominated by the effects of the low-energy spin-fluctuations of the local moment (see next subsection), so that

$$\chi_c(0) \ll \chi(0), \gamma$$

as assumed in (17).

c) Kondo model: Scaling and Renormalisation Group

The basic spin-$\frac{1}{2}$ Kondo Hamiltonian that we consider is of the same form as (33):

$$H_k = \sum_{k\sigma} \varepsilon_k c^+_{k\sigma} c_{k\sigma} - J \sum_{\substack{kk' \\ \sigma\sigma'}} \underline{S} \cdot c^+_{k'\sigma'} \underline{\tau}_{\sigma'\sigma} c_{k\sigma} \qquad (34)$$

where $\underline{S}$ is the spin operator for the f states ($n_f = 1$) with $S = \frac{1}{2}$ and τ_x, τ_y, τ_z are the Pauli spin matrices. J is negative (antiferromagnetic) when H_k is derived from the Anderson model. A potential scattering term with coefficient K, as in (33), can be added but is not essential to understanding the properties of (34).

Kondo [28] discovered, when calculating resistivity, that logarithmic divergences as $T \to 0$ appear in perturbation theory in J. Similar divergences appear in thermodynamic properties such as susceptibility, specific heat, etc. It is possible [29] to sum the terms with the maximum number of logarithms in each order in J, i.e. $O(J^{n+1} \ell n^n \frac{T}{D})$ (the "leading logarithms"). Unlike the Anderson model, the result is a geometric series; thus

$$\chi(T) = \frac{\frac{1}{3}(g\mu_B)^2 S(S+1)}{k_B T} \left(1 - \frac{1}{\frac{-1}{2\rho J} + \ln \frac{k_B T}{D}} \right) \qquad (35)$$

When $J < 0$ the logarithmic term may be rewritten as

$$(\ln T/T_k)^{-1}$$

where

$$k_B T_k = D \exp\frac{1}{2\rho J} \ll D \qquad (36)$$

Thus when $J < 0$, the series becomes meaningless at around $T = T_k$. The problem is now how to calculate the low-temperature properties. (For a review of perturbative results, see [30].)

We first describe a scaling approach, similar to that used in the last section (in fact, this approach was first developed for the Kondo problem, by Anderson [31]). Again, the method is to calculate the effect of states within δD of the band edge perturbatively, modifying the Hamiltonian to account for the states lost as D is reduced. With the vertex J from Hamiltonian (34) as shown in Fig. 1.9(a), with $c^+_{k'\sigma'}$ represented by the outward pointing single line, and $c_{k\sigma}$ represented by the inward pointing single line, processes contributing to δJ to order J^3 are shown in Figs. 1.9 and 10. At order J^2, calculation is straightforward, and the terms are found to have the same $\underline{S} \cdot \underline{s}$ form as (34). At order J^3, diagrams such as Fig. 1.10(a), a reducible diagram since it arises by substitution of Fig. 1.9(c) in place of the lower vertex in (b), are found to cancel one another. The remaining contribution comes from the irreducible diagram, Fig. 1.10(b). However, the second order self-energy 1.10(c) diverges *linearly* with D, and its derivative with respect to energy E (the eigenvalue of (34), assumed small) gives a logarithmically divergent contribution to the normalisation of the states themselves which, on inclusion in (34) in the scaling approach, further contributes to J at order J^3, [31-34]. The result to order J^3 is

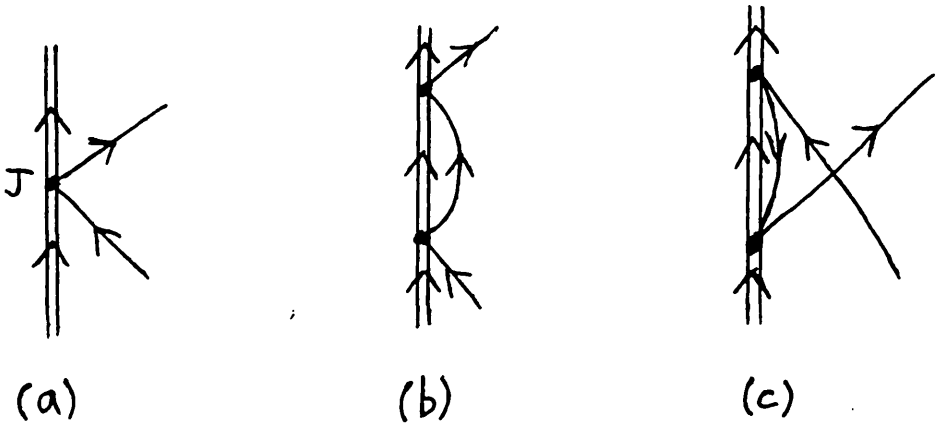


Fig. 1.9 (a) Scattering vertex J ; (b),(c) Second order scattering processes

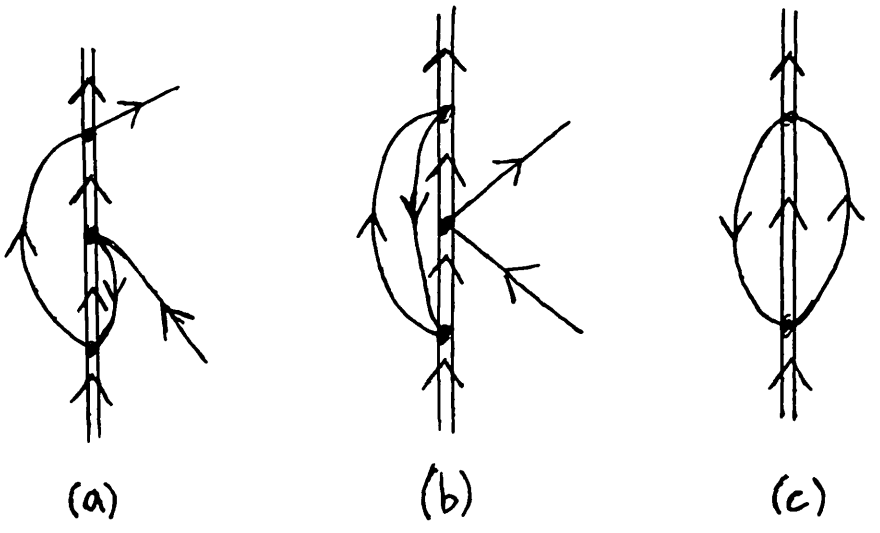


Fig. 1.10 (a) Example of a reducible third-order process; (b) Irreducible third-order process; (c) Second-order self-energy diagram

$$\rho\,\delta J = \left[-2(\rho J)^2 - 2(\rho J)^3\right]\frac{\delta D}{D} \qquad (37)$$

or in differential form, since δD reduces D,

$$\frac{d(\rho J)}{d\ln D} = 2(\rho J)^2 + 2(\rho J)^3 . \qquad (38)$$

Note that ρJ is the dimensionless combination that appears naturally. Other couplings, with multiple scattering, or k-dependence in (34), are found not to be logarithmic as $D \to \infty$ (i.e. higher order in $1/D$ in scaling) with the exception of the potential scattering K as in (33), which though in principle logarithmic, turns out to be invariant ($dK/d\,\ell n\, D = 0$) in each order, and does not contribute to (38). Its only effect is to modify the density of states in the band, an effect that may be included once and for all at the initial bandwidth, so we do not consider it further [35].

While (34) contains no energy scales, since ρJ is a dimensionless coupling, and D itself is too large to dominate low energy phenomena, a scale may be generated by scaling. First, in the case $J > 0$, note that from (38), $J \to 0$ as $D \to \infty$. In this case, perturbation theory holds good down to $T = 0$, and the magnetic behaviour as $T \to 0$ is that of a Curie law with (calculable) logarithmic corrections. In the physically more relevant case $J < 0$, $J \to 0$ as $D \to \infty$ (the phenomenon of "asymptotic freedom") and conversely $J \to O(1)$ as D decreases, so that scaling theory breaks down as D decreases. It is in this case that a new energy scale arises, as the scale at which the expansion fails. Since it must be an invariant of the scaling equations, it satisfies

$$\frac{d\,T_K(\rho J, D)}{d\ln D} = \frac{\partial T_K}{\partial \ln D} + \frac{\partial(\rho J)}{\partial \ln D}\frac{\partial T_K}{\partial(\rho J)} = 0$$

which is readily integrated using (38) to give

$$T_K = D\,|\rho J|^{1/2} \exp \frac{1}{2\rho J} \qquad (39)$$

Of course, T_k is only defined up to a constant multiplier. Higher order corrections to (38) are superfluous as they only multiply (39) by a series in ρJ which can be neglected for $\rho J \to 0$. (39) is thus a precise result, representing the sum of leading and next-to-leading logarithms in ordinary perturbation theory. Since (39) is the *only* quantity with dimensions of energy that can be constructed, all quantities (e.g. $\chi(T)$) are functions of T/T_k for $T \ll D$, and not of D or ρJ separately ("universality").

When J becomes large as D decreases, we can again use strong coupling ideas to understand the low energy properties, following Nozières [36]. If J is larger than D in (34), we neglect the kinetic energy whereupon the conduction band states appear only in the combination $\Sigma_k c_{k\sigma}$, i.e. a single state of each spin. The ground state in this subspace (which decouples from the other states in the band) is the singlet formed from singly-occupying this state in the band, with spin opposite to that of the impurity. Thermodynamic properties due to the impurity appear at higher order in D (coupling the band to the bound state) and are of order $1/J$, because they involve virtual excitation of the bound state. In the real (initially weak coupling) situation, there is thus an effective

density of states, determining $\chi(0)$ and γ, of order $1/T_k$, since T_k is the only energy scale in the problem. In addition, the strong coupling picture shows that there is a single Fermi liquid interaction parameter between the quasiparticles in the Fermi liquid, namely a repulsion between opposite spins when they are at the impurity site. Its value is fixed, relative to the impurity density of states, by the requirement that the f charge n_f not be changed by a shift of Fermi level. This corresponds to the vanishing of $\chi_c(0)$ discussed in §2(a), and again leads to the $\chi(0)/\gamma$ value as in (17), which is twice the non-interacting electron gas value.

This completes our description of the properties of the Anderson model also, since we now see that as n_f increases to 1, $\chi(0)$ and γ increase smoothly to order $1/T_k$, while $\chi_c(0)$ decreases to $1/\tilde{T}$. The ground state is always a singlet with Fermi liquid properties, including a resonant density of states at the Fermi level, and a $\chi(0)/\gamma$ value varying from 1 to 2 as n_f goes from zero to one.

The description of the Kondo and Anderson models needs further confirmation, however, since when strong coupling is approached, terms omitted from the Hamiltonian grow in strength and it might be thought that they alter the picture. That this does not occur is beautifully shown by Wilson's numerical renormalisation group approach to the Kondo model [37], and its extension to the Anderson model (with U finite) by Krishnamurthy *et al.* [38]. Wilson's procedure is similar in spirit to the scaling method above, since it involves gradual removal of the high energy degrees of freedom, while modifying the Hamiltonian. The conduction band is logarithmically discretised, and at each stage only the lowest few hundred

states are kept. The Hamiltonian is then a large matrix, so that all possible interaction terms, truncated to this basis, are kept, not only J, making it possible to continue renormalisation all the way from J small to the small D, strong coupling regime. Wilson produced a universal curve for $X(T)$ which depends only on T/T_k, confirming the universality of the model's properties for J small and $T \ll D$ discussed above.

In closing this subsection, we discuss the criterion for mixed valence, as promised above. First, let us consider how the Anderson model may be extended to include orbital degeneracy. One simply allows electrons of orbital angular momentum $(\ell, \ell_z = m)$ to hop into corresponding angular momentum states in the band (partial waves) conserving their angular momentum [39], and for simplicity, take U independent of m and σ :

$$H = \sum_{k\sigma m} \varepsilon_k c^{+}_{km\sigma} c_{km\sigma} + E_f \sum_{m\sigma} f^{+}_{m\sigma} f_{m\sigma}$$

$$+ V \sum_{km\sigma} \left(c^{+}_{km\sigma} f_{m\sigma} + h.c. \right)$$

$$+ \tfrac{1}{2} U \sum_{m\sigma \neq m'\sigma'} f^{+}_{m\sigma} f_{m\sigma} f^{+}_{m'\sigma'} f_{m'\sigma'} \qquad (40)$$

The effect of this is simply to replace the spin degeneracy of 2 by a degeneracy $N = 2(2\ell+1)$, and the arguments above for the properties of the $U = \infty$ model and the Kondo limit are essentially unchanged, the J term having the form

$$-J \sum_{\substack{kk' \\ \sigma\sigma' \\ mm'}} f^{+}_{m\sigma} f_{m'\sigma'} c^{+}_{k'm'\sigma'} c_{km\sigma} \qquad (41)$$

which is *not* simply $\underline{S} \cdot \underline{s}$. We have seen that the mixed-valence and Kondo effects appear when $V^2/|E_f|$ is not too small. On the other hand, conventional direct exchange will usually induce a term not of the form (41), but of the form $-J_x \underline{S} \cdot \underline{s}$, where $\underline{S}$ is the total spin of the impurity (RE) site in a given valence state, and $\underline{s}$ the local conduction spin density, with J_x positive. This conventional exchange will most likely produce magnetic order, if it is not overpowered by the mixed-valence effects. Thus our criterion is that

$$J_x < \frac{V^2}{|E_f|} \qquad (42)$$

Note that these different couplings J_x and J cannot be added since they have different symmetry. In the Kondo scaling equations, they will interfere with each other, but this effect has not so far been studied. In the Kondo regime, a condition

$$J_x < T_k$$

might be more appropriate than (42).

d) Other theoretical approaches

Finally, we mention briefly other more recent approaches to the impurity problem, restricting ourselves to those with which we compare some of our later results. First we describe the Bethe

Ansatz solutions (for reviews, see [40]) which have solved the Kondo and Coqblin-Schrieffer models, the Anderson spin-$\frac{1}{2}$ model for finite U, and the degenerate model for infinite U. The starting point is to regard the constant density of states at the Fermi level as arising from electrons moving past the impurity on a line in one direction, to the right, say, with a velocity independent of their energy; note that this spectrum is unbounded below. For small numbers of particles this model can be solved and possesses the remarkable property that the eigenstates are essentially plane waves with a set of momenta $(k_1 \ldots k_n)$ (for n particles) which are not scattered into different momenta by the impurity. This generalises to an arbitrary number of electrons, and a Fermi sea filled up to a Fermi energy is then constructed. The ground state properties (with a magnetic field) and finite temperature thermodynamic properties can be calculated, but the method does not extend to dynamical correlation functions (even at $T = 0$) nor to finite-temperature transport properties.

The other approach that we mention here is the so-called $1/N$ expansion, where N is the degeneracy in some form of degenerate Anderson model, as in the last section. This forms a major theme in this thesis; here we mention approaches to the expansion which have been developed by other authors during the time that the work in this thesis was being done.

The main alternative to our own functional integral method has been a resummation of the thermodynamic perturbation theory to which we have already referred [18-20,41,42]. The basic idea can be understood by returning to Schrödinger perturbation theory for the ground state (§2(b)). Referring to Fig. 1.7, we see that if V is taken to be of order $1/\sqrt{N}$, then Fig. 1.7(a) is now of order

1 , because of the summation over spin and angular momentum in the intermediate states, while (b), having no summation, is of order $1/N$. Furthermore, higher order self-energies such as Fig. 1.8(b) are of order $N(1/N)^3 = 1/N^2$. This then justifies using (23) as the ground state energy, E_G in the $N \to \infty$ limit, which now takes the form

$$\tilde{E}_o^{BW} = E_o + \frac{N\Delta_o}{\pi} \ln \frac{|E_1 - \tilde{E}_o^{BW}|}{D} \tag{43}$$

$$E_G = E_o - \tilde{E}_o^{BW} .$$

To leading order in $1/N$, E_1 is unchanged [20], thus resolving the problem of the old Brillouin-Wigner method [18,19,41] as $n_f \to 1$. The susceptibility $\chi(0)$ is found to be of order $(E_1 - \tilde{E}_0^{BW})^{-1}$. We delay a fuller discussion of the results of the expansion to our own Chapters 2 and 4. For completeness we give finally the Haldane scaling equation for the degenerate model, generalising (28)

$$E_f(D) = E_f(D_o) + (N-1)\frac{\Delta_o}{\pi} \ln \frac{D_o}{D} \tag{44}$$

and the Kondo temperature of the resulting Kondo (Coqblin-Schrieffer) model

$$T_K = D(N\rho|J|)^{1/N} \exp \frac{1}{N\rho J} . \tag{45}$$

§3. Outline of Thesis

In the last section we have seen, on the one hand, the problems obstructing the use of perturbation theory to reach the low temperature region, especially as the Kondo regime is reached, and on the other that techniques (numerical renormalisation group and Bethe Ansatz) do exist which allow calculation of only certain properties. It would be most useful to have some sort of method, based essentially on resummation of perturbation theory, capable of reaching the low-temperature (strong coupling) regime and general enough that it could be applied to calculation of all properties, including dynamics, of the impurity, and also the lattice models. In this thesis we develop such a method, making use of functional integral techniques. The diagrams involved are Feynman diagrams, unlike those in §2. The method seems to work best at low temperatures and magnetic fields, thus complementing perturbation theory and scaling theory. The use of the method to calculate static and dynamic properties of the impurity and the lattice represents a great deal of work, and we have chosen to concentrate on basic results which can be compared with existing exact results in order to confirm and understand the method. Basic steps in the extensions to models other than the $U = \infty$ Anderson impurity, including the lattice model, are made also.

The detailed outline of the thesis is as follows. Chapter 2 describes the impurity model studied, and sets up the formalism. The $1/N$ expansion and the difficulty in using it in the present case is briefly discussed, and the leading order results are derived as a mean field approximation to a functional integral. We also obtain results for $\chi(T)$, $C_v(T)$ and magnetisation $m(h)$

up to order T^2 and h^2 in this approximation. Chapter 3 extends the mean field approach to two other models: first a generalisation that includes non-zero crystal field or spin-orbit splittings, and second a model of a thulium-like impurity in which the allowed occupations are f^1 and f^2. For each model, we compare the results with a Haldane-like scaling theory; the mean field approach works well in the first case, not so well in the second. Chapter 4 returns to the model of Chapter 2, and considers the effects of fluctuations around the mean field theory. The free energy at low temperature and field, $\chi(0)$ and γ and n_f are obtained to order $1/N$ and found to be in good agreement with known exact results. The role of infrared divergences appearing in certain unobservable quantities, and the interpretation of the mean field theory, is discussed carefully. A "perfect screening" result for the quasiparticles is proved in leading order and ties in with the proposed interpretation. A scheme for a proof that the expansion is good to all orders in $1/N$ is outlined. Finally, Chapter 5 applies mean field theory to the Anderson lattice model and to an infinite-U Hubbard model, giving physically reasonable results in each case.

References

1. J. Hubbard, Proc. R. Soc. A*276* (1963) 238.
2. See e.g. C. Kittel "Introduction to Solid State Physics", Wiley, 1976.
3. R.J. Elliott, "Rare Earth Metals", Plenum Press, 1972, p. 7.
4. J.M. Lawrence, P.M. Riseborough and R.D. Parks, Rep. Prog. Phys. *44* (1981) 1.
5. Y. Baer in "Moment Formation in Solids", ed. W.J.L. Buyers, Plenum, 1984.
6. O. Gunnarsson and K. Schönhammer, Phys. Rev. B*28* (1983) 4315, and references therein.
7. D. Wohlleben, in Ref. 5.
8. D.M. Newns and A.C. Hewson, J. Phys. F*10* (1980) 2429.
9. W. Mattens, Thesis, University of Amsterdam, 1980.
10. O. Gunnarsson and K. Schönhammer, ref. 6.
11. L.L. Hirst, Z. Phys. *244* (1971) 230.
12. P.W. Anderson, Phys. Rev. *124* (1961) 41.
13. K. Yamada, Prog. Theor. Phys. *54* (1975) 316 and references therein.
14. D. Langreth, Phys. Rev. *150* (1966) 712.
15. A.L. Fetter and J.D. Walecka, "Quantum Theory of Many Particle Systems", McGraw-Hill, 1971.
16. A. Yoshimori, Prog. Theor. Phys. *55* (1976) 67.
17. D.J. Scalapino, Phys. Rev. Lett. *16* (1966) 937.
18. H. Keiter and J.C. Kimball, Int. J. Magn. *1* (1971) 233.
19. A. Bringer and H. Lustfeld, Z. Phys. B*28* (1977) 213.
20. J.W. Rasul and A.C. Hewson, J. Phys. C *16* (1983) L933; C *17* (1984) 2555, 3337.

21. F.D.M. Haldane, J. Phys. C *11* (1978) 5015.

22. See e.g. L. Schiff, "Quantum Mechanics", 3rd Edition McGraw-Hill.

23. A.C. Hewson, J. Phys. C *10* (1977) 4973.

24. C.M. Varma, Rev. Mod. Phys. *48* (1976) 219.

25. F.D.M. Haldane, Phys. Rev. Lett. *40* (1978) 416.

26. H.R. Krishnamurthy, J.W. Wilkins and K.G. Wilson, Phys. Rev. B *21* (1980) 1003, 1044.

27. J.R. Schrieffer and P.A. Wolff, Phys. Rev. *149* (1966) 491.

28. J. Kondo, Prog. Theor. Phys. *44* (1964) 39.

29. A.A. Abrikosov, Physics *1* (1965) 5.

30. H.R. Krishnamurthy, Thesis, Cornell University, 1976.

31. P.W. Anderson, J. Phys. C *3* (1970) 2346.

32. M. Fowler and A. Zawadowski, Solid State Comm. *9* (1971) 471.

33. J. Solyom and A. Zawadowski, J. Phys. F *4* (1974) 80.

34. A.C. Hewson, J. Phys. C *14* (1981) 2747.

35. D. Cragg and P. Lloyd, J. Phys. C *12* (1979) 3301.

36. P. Nozières, J. Physique *39* (1978) 1117.

37. K.G. Wilson, Rev. Mod. Phys. *47* (1975) 773.

38. Krishnamurthy *et al.*, Ref. 26.

39. B. Coqblin and J.R. Schrieffer, Phys. Rev. *185* (1969) 847.

40. N. Andrei, K. Furuya and J.H. Lowenstein, Rev. Mod. Phys. *55* (1983) 331; P.B. Wiegmann and A.M. Tsvelick, Adv. Phys. *32* (1983) 453.

41. T.V. Ramakrishnan and K. Sur, Phys. Rev. B *26* (1982) 1798.

42. F.C. Zhang and T.K. Lee, Phys. Rev. B *28* (1983) 33.

CHAPTER 2. LARGE-N LIMIT OF THE COQBLIN-SCHRIEFFER AND ANDERSON IMPURITY MODELS

§1. Description of Models

The Anderson impurity [1,2] model has already been described in Chapter 1. In the infinite-U limit it can be written

$$H = E_c \sum_m f_m^+ f_m + \sum_{km} \varepsilon_k c_{km}^+ c_{km} + V \sum_{km} \left(f_m^+ c_{km} + c_{km}^+ f_m \right) P_m \qquad (1)$$

The f , f^+ operators are standard fermion operators, destroying or creating 4f-electrons. The suffix m runs from $-j$ to j and denotes z-component of total angular momentum. As in Ref. 2, we treat the case of infinite spin-orbit splitting, that is only the lowest spin-orbit multiplet is retained ($j = 5/2$, Ce f^1 ; $j = 7/2$, Yb f^{13}) . The c_{km}^+ operators create electrons of radial quantum number k in partial wave states in the conduction band [2], which we take to have a rectangular density of states ρ , width $2D$, with the Fermi level at the centre. Electronic energies are measured relative to the chemical potential, so $\mu = 0$. For an impurity model, the localized perturbation due to the impurity cannot affect the bulk of electrons at distances far from the impurity (represented in the partial wave basis by the other values of j , decoupled from the impurity) and so the chemical potential never departs from its value in the system without the impurity. The f electron energy E_0 we call the position of the

f-level, and the real hybridisation matrix element V leads to a quantity

$$\Delta_0 = \pi \rho V^2 \tag{2}$$

which we call the hybridisation width.

We have left to last the definition of the all-important projection operator

$$P_m = \prod_{m' \neq m} \left(1 - f^+_{m'} f_{m'}\right) \quad , \tag{3}$$

whose effect is to disallow hybridisation if the initial or final f occupation

$$n_f = \sum_m f^+_m f_m \tag{4}$$

is not equal to 0 or 1. The parts of Hilbert space with $n_f > 1$ are therefore trivial and we disregard them here. Thus from the point of view of stakes with $n_f = 0$ or 1, the model is equivalent to an Anderson model with $U \to \infty$. It is this restriction on the allowed states which makes the hybridisation of f and conduction band states a difficult many-body problem (some simplification is gained over the situation of U finite, however). Attempts to treat this restriction in perturbation theory have led either to expansions with a generalised Wick's theorem [3] or to Goldstone diagram expansions [4]. While the latter have very recently [5], been quite successful, many diagrams have to be summed to achieve quite simple results, since each time ordering of operators is expressed in a separate diagram. A central theme of this thesis is a different way of introducing the occupation

restriction, leading to simpler calculations and simpler physical pictures, at least at low temperatures and magnetic fields. Before we can present this technique, however, we need to introduce another representation of the $U = \infty$ Anderson model, and one for the Coqblin-Schrieffer model.

Following Coleman [6] (and earlier, similar ideas by Barnes [7]) we replace the hybridisation term in (1) by

$$V \sum_{km} \left(c_{km}^{+} f_m b^{+} + f_m^{+} c_{km} b \right) . \tag{5}$$

The operators b , b^{+} are canonical boson operators;

$$[b, b^{+}] = 1 \tag{6}$$

and other commutators involving b , b^{+} vanish. We see immediately that

$$Q = n_f + b^{+} b \tag{7}$$

commutes with the Hamiltonian and so is conserved. Therefore the Hilbert space splits into sectors of different Q which evolve independently in time. In particular, if we fix initially $Q = 1$, this condition is maintained for all time. In other words, we always have either 1 f-electron (and no boson) or 1 boson and no f-electron. Identifying the latter as the $n_f = 0$, (unoccupied) state, we see that, *in the subspace* $Q = 1$, our new Hamiltonian is equivalent to (1). The advantage of Coleman's idea is that the Hamiltonian is represented in terms of canonical operators, and the restriction on occupation is imposed on the states, not through operators; furthermore, the

restriction involves a quantity conserved by the Hamiltonian (we will see that this introduces a new symmetry into the problem).

In order to apply Coleman's ansatz to correlation functions we notice the correspondence [6], within the $Q = 1$ subspace,

$$\begin{aligned} f_m^+ b &\leftrightarrow |m\rangle\langle c| = X_{mo} \\ f_m^+ f_{m'} &\leftrightarrow |m\rangle\langle m'| = X_{mm'} \\ b^+ b &\leftrightarrow |0\rangle\langle 0| = X_{oo} \end{aligned} \tag{8}$$

where $|0\rangle$ is the $n_f = 0$ state of the ion, and $|m\rangle$ is the $n_f = 1$ state with $J_z = m$. The X operators defined in (8) are the Hubbard "standard basis" operators [3]. In terms of the finite-U Anderson Hamiltonian, [1,8]

$$\begin{aligned} H = E_o \sum_m F_m^+ F_m + \sum_{km} \varepsilon_k c_{km}^+ c_{km} \\ + V \sum_{km} \left(c_{km}^+ F_m + F_m^+ c_{km} \right) \\ + \tfrac{1}{2} U \sum_{mm'} F_m^+ F_{m'}^+ F_{m'} F_m \end{aligned} \tag{9}$$

(where U is large and F_m, F_m^+ are fermion operators) we may also write,

$$\begin{aligned} X_{mo} &\leftrightarrow F_m^+ \\ X_{mm'} &\leftrightarrow F_m^+ F_{m'} \\ X_{oo} &\leftrightarrow 1 - \sum_m F_m^+ F_m \end{aligned} \tag{10}$$

Then the spectral function [9] of the true f electrons, which is the spectral function of the F's , can be written in terms of

$$\langle T F_m(\tau) F_m(0)\rangle = \langle T X_{om}(\tau) X_{mo}(0)\rangle$$

$$= \langle T b^+(\tau) f_m(\tau) f_m^+(0) b(0)\rangle \tag{11}$$

We call the corresponding spectral function the F-spectral function from now on; it must not be confused with the spectral function for the f's alone.

For dynamical spin or charge susceptibilities we have for example

$$\sum_{mm'} \langle T F_m^+(\tau) F_m(\tau) F_{m'}^+(0) F_{m'}(0)\rangle$$

$$= \sum_{mm'} \langle T f_m^+(\tau) f_m(\tau) f_{m'}^+(0) f_{m'}(0)\rangle \tag{12}$$

which does not involve the b's .

As a special case of the correspondences (8), (10), we note that

$$n_f = \sum_m F_m^+ F_m = n_F \tag{13}$$

which will have special importance later.

Leaving the question of how the constraint $Q = 1$ is to be imposed to the next section, we now discuss an important limiting case of the model (1). When E_0 is large and negative ($-E_0 >> N\Delta_0$, where $N = 2j + 1$) we expect that $\langle n_f\rangle \simeq 1$ and fluctuations into the

$n_f = 0$ state can be treated as virtual, giving rise to transitions between states m , m' of the $n_f = 1$ state, accompanied by scattering of conduction electrons. We derive an expression for these effective interactions in second order perturbation theory, using Coleman's formalism.

The energy of the ion can be rewritten

$$E_o \sum_m f_m^+ f_m = E_o - E_o b^+ b \tag{14}$$

so the boson has a large positive energy, $-E_0$. To second order in V we obtain the effective interaction,

$$\frac{V^2}{E_o} \sum_{\substack{mm' \\ kk'}} \left(f_m^+ c_{km} \right) \left(c_{k'm'}^+ f_{m'} \right) \tag{15}$$

in which we have neglected the energies ε_k , $\varepsilon_{k'}$ relative to $-E_0$. This means that (15) can be used for all states k only when $-E_0 >> D$. The form (15) is also valid when $-E_0 < D$ for states sufficiently close to the Fermi energy, since it is possible to gradually reduce D , at the same time renormalising E_0 until the transformation to a form (15) is valid, provided the renormalised E_0 is larger than $N\Delta_0$ [10].

We rewrite (15) as

$$- J \sum_{\substack{kk' \\ mm'}} f_m^+ f_{m'} c_{k'm'}^+ c_{km} + J n_f 2\rho D$$

with $$J = V^2/E_0 \tag{16}$$

which was first obtained by Coqblin and Schrieffer [2]. The constraint

$n_f = 1$ applies to the states of the model. Notice that the Anderson model gives rise to an antiferromagnetic J $(J < 0)$. A separation

$$-J \sum_{\substack{kk' \\ mm'}} c^+_{k'm'} c_{km} \left(f^+_m f_{m'} - \frac{1}{N} \delta_{mm'} n_f \right)$$

$$- \frac{J}{N} \sum_{\substack{kk' \\ m}} c^+_{k'm} c_{km} n_f \qquad (17)$$

is sometimes made, the last term being referred to as potential scattering, while the first term represents purely spin-flip scattering. When $j = \frac{1}{2}$ $(N = 2)$, the first term reduces to the usual Kondo Hamiltonian. The coefficient of potential scattering may be taken different from J, and can be included exactly as a modification of the conduction band density of states via a phase shift [11]. We will be interested in J small, in which case these effects are negligible.

§2. Functional Integral Formulae and Symmetries of the Models

In this section we obtain exact expressions for the partition functions of the models of §1, including the constraint $Q = 1$, and study their symmetries.

Coleman [6] includes the constraint through a variant of Abrikosov's trick [12], adding to the Hamiltonian a term λQ. The partition function is differentiated with respect to λ and then the limit $\lambda \to \infty$ is taken. The differentiation brings down a factor Q, so that $Q = 0$ is suppressed, and $\lambda \to \infty$ makes all states with $Q > 1$ high in energy, thus only $Q = 1$ states contribute

to the partition function. Coleman shows that with this prescription the partition function is given by the sum of those Feynman diagrams in which the f and b lines form only one loop (recall that Q is conserved, so lines carrying units of Q, namely f and b, must form distinct closed loops in unlinked diagrams). No simple expression for the free energy emerges; instead one is led back to the expressions of the Goldstone diagram approach [5] (though the derivation may be shorter).

Our starting point is to write the partition function as

$$\mathcal{Z} = \operatorname*{Tr}_{\{Q=1\}} e^{-\beta H} \tag{18}$$

where H is that of eq^{ns}. (1) and (5) and the trace is over states of the Fermi sea and states of the ion with Q = 1. The latter restriction can be removed as follows. In a basis of states of definite Q we can write

$$\begin{aligned}
\mathcal{Z} &= \operatorname{Tr} e^{-\beta H} \delta_{Q,1} \\
&= \int_{-\pi/\beta}^{\pi/\beta} \frac{\beta\, d\lambda}{2\pi} \operatorname{Tr} e^{-\beta H} e^{-i\beta\lambda(Q-1)} \\
&= \int_{-\pi/\beta}^{\pi/\beta} \frac{\beta\, d\lambda}{2\pi} \operatorname{Tr} e^{-\beta(H + i\lambda(Q-1))}
\end{aligned} \tag{19}$$

where the trace is now unrestricted, and we have used the fact that Q commutes with H in the last line. Factors of β multiplying λ

are introduced for later convenience. At this stage, our λ plays a role similar to that of Coleman; the usefulness of our choice will become apparent in our later treatment of λ as a fluctuating field.

The trace in (19) can be written as a functional integral over both boson and fermion fields. The latter involves Grassmann number integration which has been described by many authors [13]. Our expression for the partition function is then

$$Z = \int_{-\pi/\beta}^{\pi/\beta} \frac{\beta d\lambda}{2\pi} \int \mathcal{D}b\,\mathcal{D}b^{+}\,\mathcal{D}f\,\mathcal{D}f^{+}\,\mathcal{D}c\,\mathcal{D}c^{+}\, e^{-\int_0^\beta \mathcal{L}(\tau)d\tau} \tag{20}$$

where $\mathcal{D}f$ abbreviates $\prod_m \mathcal{D}f_m$, etc. and the Lagrangian $\mathcal{L}$ is

$$\mathcal{L} = b^{+}\frac{d}{d\tau}b + \sum_m f_m^{+}\left(\frac{d}{d\tau} + E_0\right)f_m + \sum_{km} c_{km}^{+}\left(\frac{d}{d\tau} + \varepsilon_k\right)c_{km}$$

$$+ V\sum_{km}\left(c_{km}^{+} f_m\, b^{+} + f_m^{+} c_{km}\, b\right)$$

$$+ i\lambda\left(n_f + b^{+}b - 1\right) \tag{21}$$

Here b, b^{+} are now c-number τ-dependent fields which are periodic with period β ($b(\tau+\beta) = b(\tau)$) while f_m, f_m^{+}, c_{km}, c_{km}^{+} are Grassmann number fields (which anticommute at all times) with the antiperiodicity $f_m(\tau+\beta) = -f_m(\tau)$.

We now use expressions (20) and (21) to discuss the symmetries of the model. The most basic symmetry is obtained by considering the f_m's and c_{km}'s as forming N-component vectors

$$\underline{f} = \begin{pmatrix} f_{-j} \\ \vdots \\ f_j \end{pmatrix} \quad , \quad \underline{c}_k = \begin{pmatrix} c_{k-j} \\ \vdots \\ c_{kj} \end{pmatrix} \tag{22}$$

Then (21) and the measure in (20) are invariant under unitary transformations

$$\underline{f} \to \underline{\underline{U}}\,\underline{f} \quad , \quad \underline{c}_k \to \underline{\underline{U}}\,\underline{c}_k \tag{23}$$

(and their conjugates), where $\underline{\underline{U}}$ is an $N \times N$ unitary matrix, and so is a member of the group $U(N)$. A special case of these transformations is the $U(1)$ subgroup, where

$$\underline{\underline{U}} = e^{i\phi}\,\underline{\underline{1}} \tag{24}$$

where $\underline{\underline{1}}$ is the $N \times N$ identity matrix. This $U(1)$ subgroup just corresponds to conservation of fermion number. The group generated by the remaining generators of $U(N)$ is $SU(N)$; it is the existence of this symmetry group which forms the basis for the $1/N$ expansion.

The other obvious symmetry corresponds to the conservation of Q, noted above, and can be described by the phase transformation,

$$\begin{aligned} &\underline{f} \to e^{i\phi}\underline{f} \quad , \quad b \to e^{i\phi} b \\ &\underline{c}_k \to \underline{c}_k \, . \end{aligned} \tag{25}$$

So far our transformations have been independent of τ ; however, the symmetry (25) can be extended to make ϕ τ-dependent, so the symmetry is a gauge symmetry. As it stands, the Lagrangian (21) is not gauge invariant, but this is simply because we have already implicitly made a choice of gauge. If we write (20) as

$$\mathcal{Z} = \int \mathcal{D}\lambda \mathcal{D}f \mathcal{D}f^{+} \mathcal{D}b \mathcal{D}b^{+} \mathcal{D}c \mathcal{D}c^{+} \left(\prod_{\tau} \delta(\dot{\lambda}) \right) e^{-\int_0^\beta \mathcal{L}(\tau) d\tau} \tag{26}$$

(where $\mathcal{L}$ is as in (21) with λ now τ-dependent, and we drop factors multiplying Z from now on) we see that $\mathcal{L}$ is invariant under (25) when supplemented by

$$\lambda \rightarrow \lambda + \dot{\phi} \tag{27}$$

but that a gauge is fixed by the delta functions in (26) [14]. The delta functions remove the redundancy (multiple counting of gauge-related field configurations) introduced by the symmetry (25,27). More general gauge-fixing conditions can be introduced, such as the form

$$(\det M) \prod_{\tau} \delta(F(\lambda)) \tag{28}$$

where F is a local, differential operator acting on λ , such as

$$F(\lambda) = \dot{\lambda} \tag{29}$$

above, and

$$\mathfrak{M} = \frac{\delta \tilde{F}}{\delta \alpha} \tag{30}$$

is the linear response of $\tilde{F}$ to a small gauge transformation α. $\mathfrak{M}$ is included to normalise the delta functions, so that the desired gauge is picked out with weight 1 [14].

Another choice that is sometimes useful is to consider b as

$$b = re^{i\theta} \tag{31}$$

and use

$$\prod_{\tau} r(\tau)\, \delta(\theta(\tau)) \tag{32}$$

Due to the singularity of polar co-ordinates at $r = 0$, this will be sensible only when expanding about a non-zero value of r, as appears later (§4; Ch. 4). Evidently

$$\prod_{\tau} r(\tau) \tag{33}$$

is just the Jacobian for the change of variable, but it may also be considered as having the same role as $\mathfrak{M}$ in (30). In this gauge (the "unitarity" gauge) θ disappears from the functional integral and there are 2 bose fields, $r(\tau)$ and $\lambda(\tau)$.

In closing this section we show that the Coqblin-Schrieffer model partition function can be brought into a form similar to (20). For the Coqblin-Schrieffer Hamiltonian (15)

$$Z = \int_{-\pi/\beta}^{\pi/\beta} \frac{\beta d\lambda}{2\pi} \int \mathcal{D}f \mathcal{D}f^{+} \mathcal{D}c \mathcal{D}c^{+} e^{-\int_0^\beta \mathcal{L}(\tau) d\tau} \tag{34}$$

with

$$\begin{aligned} \mathcal{L} &= \sum_m f_m^{+} \frac{d}{d\tau} f_m + \sum_{km} c_{km}^{+} \left(\frac{d}{d\tau} + \varepsilon_k \right) c_{km} \\ &+ J \sum_{\substack{mm' \\ kk'}} \left(f_m^{+} c_{km} \right) \left(c_{k'm'}^{+} f_{m'} \right) \\ &+ i\lambda \left(n_f - 1 \right) \end{aligned} \tag{35}$$

The four-field coupling in (35) can be replaced by a coupling to a Gaussian random field via a Stratonovich-Hubbard transformation [15] using the identity

$$\begin{aligned} &\int \mathcal{D}\sigma \mathcal{D}\sigma^{*} \exp\left(\frac{-1}{|J|} \int_0^\beta d\tau \left| \sigma^{*}(\tau) + |J| \sum_{km} f_m^{+} c_{km} \right|^2 \right) \\ &= \text{const.} \end{aligned} \tag{36}$$

The partition function becomes

$$\mathcal{Z} = \int_{-\pi/\beta}^{\pi/\beta} \frac{\beta d\lambda}{2\pi} \int \mathcal{D}\sigma \mathcal{D}\sigma^* \mathcal{D}f \mathcal{D}f^* \mathcal{D}c \mathcal{D}c^* e^{-\int_0^\beta \mathcal{L}(\tau)\, d\tau} \tag{37}$$

where

$$\begin{aligned} \mathcal{L}(\tau) = & \sum_m f_m^+ \frac{d}{d\tau} f_m + \sum_{km} c_{km}^+ \left(\frac{d}{d\tau} + \varepsilon_k \right) c_{km} \\ & + \sum_{km} \left(\sigma^* c_{km}^+ f_m + \sigma f_m^+ c_{km} \right) \\ & + \frac{1}{|J|} |\sigma|^2 + i\lambda (n_f - 1) \end{aligned} \tag{38}$$

But this now has the form of (20, 21), where we have dropped

$$b^+ \left(\frac{d}{d\tau} + i\lambda \right) b \tag{39}$$

and written $\sigma = Vb$. (Note that we use (14) to obtain the term

$$\left. - \frac{E_0}{V^2} |\sigma|^2 \; . \right)$$

In effect, the Stratonovich-Hubbard transformation has reversed the Schrieffer-Wolf transformation! The field σ , which cannot represent a true excitation, represents the *virtual* excitations to the singlet state $n_f = 0$.

The expression (37, 38) has the same symmetries as (20, 21), including the gauge properties.

§3. 1/N Expansion : The Basic Ideas

A readable, but unfortunately unpublished, account of the 1/N expansion in quantum field theory is given by S. Coleman [16]. A recent review describing the proliferation of modern approaches is given by Yaffe [17] which includes also references to the older diagrammatic method we shall use. Our approach is closest to that of Gross and Neveu [18]. Applications in statistical mechanics can be found in [19].

In applying the 1/N expansion to our models problems are encountered due to the constraint $Q = 1$. To outline the idea of the expansion free of these problems, we apply it to a related model for which they do not occur. This model is similar to (38) with

$$\begin{aligned} \mathcal{L} = & \sum_m f_m^+ \frac{d}{d\tau} f_m + \sum_{km} c_{km}^+ \left(\frac{d}{d\tau} + \varepsilon_k \right) c_{km} \\ & + \sum_{km} \left(\sigma^* c_{km}^+ f_m + \sigma f_m^+ c_{km} \right) \\ & + \frac{1}{|J|} |\sigma|^2 + i\lambda \left(n_f - \frac{N}{2} \right) \end{aligned} \tag{40}$$

The difference from (38) lies in the constraint

$$n_f = \frac{1}{2} N \tag{41}$$

hence (40) is a "half-filled" version of the Coqblin-Schrieffer model.

The partition function of (40) is similar to (37); we now consider a diagrammatic expansion for the free energy, which as usual is a sum of linked diagrams (i.e. diagrams in which all the parts are linked by some path along the lines of the diagram, with no external legs). We do not specify the precise rules for the expansion, as we work out our physically-relevant case in full below, nor at first do we specify what is included in the unperturbed fermion Hamiltonian, to give the expression for the fermion propagators (Green's functions). We will, however, mention that the time independent λ variable is treated like an ordinary (time-dependent) field, except that when diagrams are to be evaluated by summing over frequencies running round closed loops, the additional restriction is introduced that the frequency in any λ line must be zero.

Consider then the examples of diagrams for the free energy shown in Fig. 2.1. First note that any fermion loop gives a free sum over m labels and so a factor of N. We now introduce a crucial assumption concerning the large-N limit: the limit is taken with

$$N|J| = \text{constant} = J_0 \tag{42}$$

as $N \to \infty$. Now the dashed lines in the figure, representing σ fluctuations, are given by the inverse of the coefficient of the $|\sigma|^2$ term in (40) and so are of order $1/N$. The fermion lines are taken to be of order 1, an assumption we will verify shortly. Then the powers of $1/N$ associated with each diagram in Fig. 2.1 are found by simple counting. In fact, by a simple topological argument [16,18,19] one finds that if the number of *independent boson* loops in a diagram (i.e. regard the fermion loops merely as

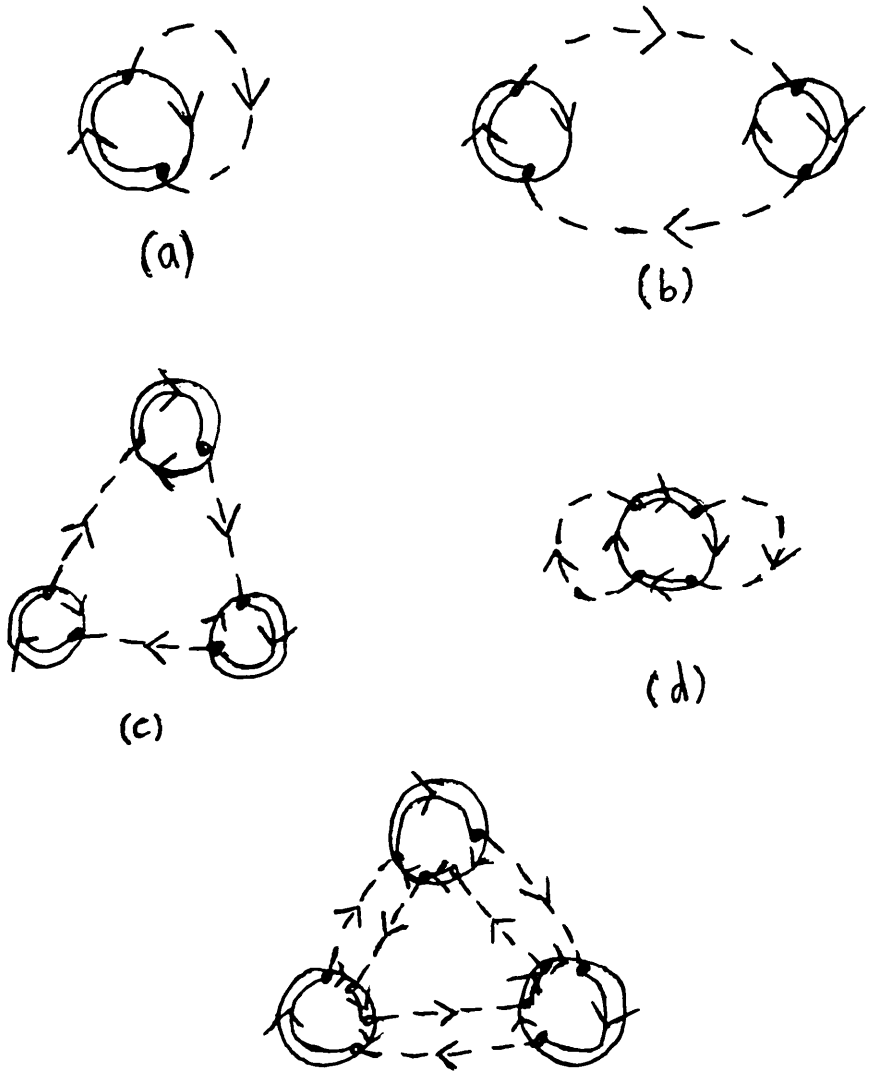


Figure 2.1 Examples of diagrams contributing to the free energy of (40). Solid line, propagator for conduction electrons, double line, propagator for f electrons, dashed line, propagator for σ field. Orders of the diagrams, as explained in text, are: (a), (b), (c), all of order 1 ; (d) order $1/N$; (e) order $1/N^3$.

multi-boson vertices and count the number of independent loops remaining) is L, then the power of N associated with it is

$$N^{1-L} . \tag{43}$$

The same counting applies to diagrams containing λ lines, though we have not yet explained how to obtain a λ propagator, as no term quadratic in λ appears in (40).

From (43) we learn that *fluctuations* in σ and λ (giving rise to loops) vanish in the large-N limit by comparison with the leading order term $(L = 0)$. The expectation values of these fields may still be considered, however, as may diagrams involving λ or σ lines but without closed boson loops (tree diagrams). In fact, these two points are related; inclusion of tree diagrams is equivalent to allowing expectation values of σ and λ.

With these facts in mind we may specify precisely how the expansion is developed. We first integrate out the fermion fields (equivalently, perform the trace over fermion states) in the presence of the σ and λ fields to obtain a formal expression (details in next section):

$$\mathcal{Z} = \int_{-\pi/\beta}^{\pi/\beta} \frac{\beta d\lambda}{2\pi} \int \mathcal{D}\sigma \mathcal{D}\sigma^* \exp\left\{ - S_{eff}[\sigma, \sigma^*, \lambda] \right\} \tag{44}$$

The effective action S_{eff} is represented by a sum of fermion loops, for which the propagators are evaluated in the presence of the time-dependent background fields σ, σ^* and λ. As each loop has a

factor of N , S_{eff} is proportional to N :

$$S_{eff} = N \Sigma (\text{fermion loops}) + \int_0^\beta d\tau \left(\frac{N}{J_0} |\sigma|^2 - i\lambda \frac{N}{2} \right)$$

(45)

suggesting the use of a steepest descent type of calculation to obtain an expansion in $1/N$. The first term is then obtained by maximising the integrand at fixed values of $\sigma(\tau)$, $\sigma^*(\tau)$ and λ ; as the problem is time-independent, these may all be taken independent of τ . The values of these parameters are chosen to maximise (45) at each T and magnetic field h . Since varying each parameter gives the expectation of the operator multiplying it in (40), these conditions are Hartree-like conditions e.g.

$$\langle n_f \rangle = \frac{1}{2} N \qquad (46)$$

is obtained by varying λ (actually it is always found that the value of $i\lambda$ is real, as it now plays the role of a simple Lagrange multiplier) and

$$\left\langle \sum_{km} c_{km}^+ f_m \right\rangle = \frac{N\sigma_0}{J_0} \qquad (47)$$

where σ_0 is the expectation value of σ . Fig. 2.2 gives a diagrammatic form of these equations.

Evaluating corrections to these leading order terms brings in diagrams like those in Fig. 2.1, the corrections in the steepest descent approach have orders in $1/N$ given by the same formula (43).

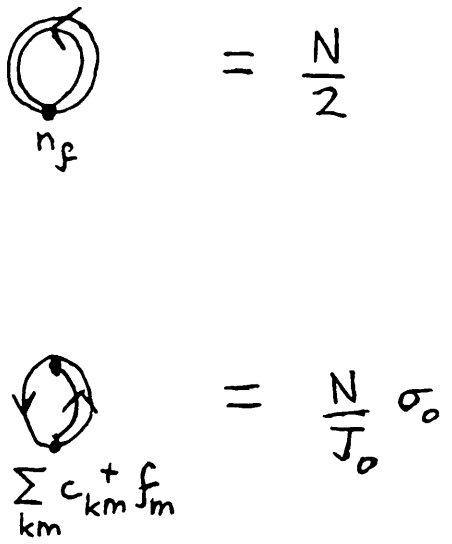


Figure 2.2 Diagrammatic form of leading order self consistent conditions (46) and (47).

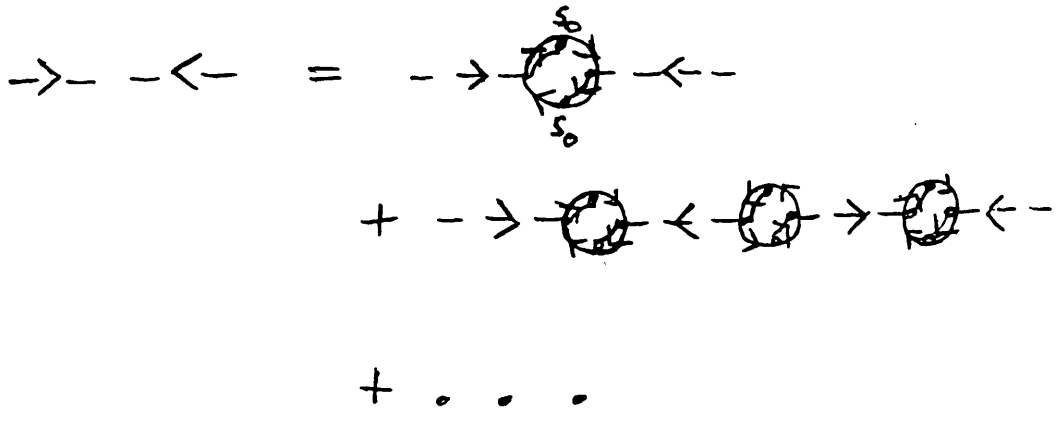


Figure 2.3 Anomalous propagator for σ .

Note that the presence of expectation values of σ , σ^* allows for "anomalous" propagators for σ , as in the theory of superfluidity (Fig. 2.3). Note also that when S_{eff} is expanded to second order in the fluctuations of σ and σ^* about their expectation values, terms from the fermion loops are the same order as from the $N|\sigma|^2/J_0$ term, and are included in evaluating Gaussian functional integrals over σ , σ^* .

Fluctuations in λ are included by expanding (45) to second (or higher) order in λ . The terms quadratic in λ , like those quadratic in σ , provide the gaussian weight factors for integration over λ , and hence are the inverse of the λ propagator. There are also terms proportional to $\lambda\sigma$ or $\lambda\sigma^*$ which mix the fields. Note that in performing Gaussian integrals over λ , we replace the finite limits on the integration by infinity. One expects this to be good at low temperatures, but at high temperatures thermal excitation might make the limits important.

Now we compare with our physical case (21) or (38). The occupation n_f , or Q , is now of order 1 instead of N , so that not all terms in S_{eff} are of order N , spoiling the expansion. As we will see in the next section, in this case it is found that the free energy at low T is of order 1 , and so one might think that the fluctuations are of the same order. That this is not the case is shown in Chapter 4, where we also show that the expansion still works in our case. For the time being, however, we regard it simply as a prescription for a mean field theory, leaving to later a proof that the mean field theory *is* the large N limit.

§4. The large-N Limit at T = 0

In this section we obtain a formal expression for the effective action and solve the mean field theory at $T = 0$, which contains the large N limit.

To integrate out the fermion fields, we first complete the square in the Lagrangian (21):

$$\begin{aligned} \mathcal{L} = {} & b^+ \frac{d}{d\tau} b + i\lambda (b^+ b - 1) \\ & + \sum_{km} \left[c_{km}^+ + V b f_m^+ \left(\frac{d}{d\tau} + \varepsilon_k \right)^{-1} \right] \left(\frac{d}{d\tau} + \varepsilon_k \right) \\ & \times \left[c_{km} + \left(\frac{d}{d\tau} + \varepsilon_k \right)^{-1} f_m b^+ V \right] \\ & + \sum_m f_m^+ \left[\frac{d}{d\tau} + E_0 + i\lambda - V^2 \sum_k b \left(\frac{d}{d\tau} + \varepsilon_k \right)^{-1} b^+ \right] f_m \end{aligned} \tag{48}$$

The c_{km} variables may be translated formally, whereupon the Grassmann gaussian integrals can be done trivially [13] to give

$$\mathcal{Z} = \mathcal{Z}_0 \int \mathcal{D}b \, \mathcal{D}b^+ \int_{-\pi/\beta}^{\pi/\beta} \frac{\beta d\lambda}{2\pi} \exp(-S_{eff}) \tag{49}$$

where

$$\mathcal{Z}_0 = \exp N \, \mathrm{Tr} \sum_k \ln \left(\frac{d}{d\tau} + \varepsilon_k \right) \tag{50}$$

results from the integration over the shifted c_{km} , c^{+}_{km} and is the partition function of the conduction band in the absence of the impurity, and

$$S_{eff} = -N\,Tr\,ln\left(\frac{d}{d\tau} + E_o + i\lambda - V^2 b \sum_k \left(\frac{d}{d\tau} + \varepsilon_k\right)^{-1} b^{+}\right)$$

$$+ \int_0^{\beta} d\tau \left[b^{+}\left(\frac{d}{d\tau} + i\lambda\right) b - i\lambda \right] \qquad (51)$$

The "Trℓn" expressions are defined as the trace over functions antiperiodic when $\tau \to \tau + \beta$ and are conveniently evaluated in frequency space, as we shall see below. Note that b , b^{+} are τ dependent, and attention must be paid to the order of these fields relative to the $\frac{d}{d\tau}$ operator. The effective action (51) is the free energy (over kT) of the fermion system subject to the τ-dependent background fields, b , b^{+} , and is represented diagrammatically by a single fermion loop; hence the minus in (51) which arises from the Fermi statistics [13].

It is, of course, very difficult to evaluate exactly the effective action (51). In this section we will evaluate it for τ-independent fields at $T = 0$, in §6 at $T \neq 0$ and in Chapter 4 we will start to expand it as a functional Taylor series about the stationary point.

Suppose then that λ , b are τ-independent. For convenience we write

$$V b = s e^{i\theta}$$
$$i\lambda = \varepsilon_f - E_o + i\tilde{\lambda} \tag{52}$$

where s , θ , ε_f , $\tilde{\lambda}$ are real. θ cancels out, because of the symmetry (25). The shift $\varepsilon_f - E_0$ in the contour of λ-integration makes no difference to the efficacy of the integral. As $\tilde{\lambda}$ turns out, at the stationary point, to be zero (modulo an integer multiple of $2\pi/\beta$) we will ignore it.

To carry out the trace we define the complete set of orthonormal, antiperiodic functions

$$u_n = \beta^{-1/2} e^{-i\omega_n \tau}$$
$$\omega_n = (2n+1)\pi/\beta \tag{53}$$

and introduce into the trace the delta function (decomposition of unity)

$$\delta(\tau - \tau') = \sum_{n=-\infty}^{\infty} u_n(\tau)\, u_n^*(\tau') \tag{54}$$

Then S_{eff} becomes

$$S_{eff} = -N \int_0^\beta d\tau \sum_{n=-\infty}^{\infty} u_n^*(\tau) \ln\left(\frac{d}{d\tau} + \varepsilon_f - s^2 \sum_k \left(\frac{d}{d\tau} + \varepsilon_k\right)^{-1}\right) u_n(\tau)$$
$$+ \beta(\varepsilon_f - E_o)\left(\frac{s^2}{V^2} - 1\right) \tag{55}$$

Bringing $u_n(\tau)$ through the $\frac{d}{d\tau}$'s and doing the τ integral gives

$$S_{eff} = -N \sum_{n=-\infty}^{\infty} \ln \left(-i\omega_n + \varepsilon_f + s^2 \sum_k \frac{1}{i\omega_n - \varepsilon_k} \right) + \beta(\varepsilon_f - E_0)\left(\frac{s^2}{V^2} - 1\right) \tag{56}$$

We evaluate the integral in the standard way [9], replacing the summation by an integral around a contour surrounding the poles of the Fermi function. The contour is then distorted to surround the real axis. We make use of the approximations

$$\sum_k \frac{1}{i\omega_n - \varepsilon_k} \simeq -i\pi\rho \operatorname{sgn} \omega_n$$

$$\sum_k \frac{1}{\varepsilon - \varepsilon_k + i\delta} \simeq \begin{cases} -i\pi\rho \operatorname{sgn} \delta, & |\varepsilon| < D \\ 0, & \text{otherwise} \end{cases} \tag{57}$$

for the local conduction electron propagator when ε and δ (or ω) are real, and neglect its real part. We define

$$\Delta = \pi\rho s^2 \tag{58}$$

Then the sum is

$$\sum_n \ln \left(-i\omega_n + \varepsilon_f - i\Delta \operatorname{sgn} \omega_n \right)$$

$$= -\frac{\beta}{2\pi i}\int_C d\varepsilon f(\varepsilon)\ln\left(-\varepsilon+\varepsilon_f - i\Delta\,\mathrm{sgn}(\mathrm{Im}\,\varepsilon)\right)$$

(59)

where $f(\varepsilon) = (e^{\beta\varepsilon}+1)^{-1}$ is the Fermi function, and the contour surrounds its poles (lying on the imaginary ε axis) in the positive direction. Bending the contour gives

$$-\frac{\beta}{2\pi i}\int_{\to} d\varepsilon\, f(\varepsilon)\left[\ln\left(-\varepsilon+\varepsilon_f - i\Delta\right) - \ln\left(-\varepsilon+\varepsilon_f + i\Delta\right)\right]$$

$$= \beta\int_{\to}\frac{d\varepsilon}{\pi} f(\varepsilon)\tan^{-1}\frac{\Delta}{\varepsilon_f-\varepsilon}$$

(60)

(where $0 \le \tan^{-1} x \le \pi$) and so

$$S_{\mathrm{eff}}(\varepsilon_f, s) = -N\beta\int_{\to}\frac{d\varepsilon}{\pi} f(\varepsilon)\tan^{-1}\frac{\Delta}{\varepsilon_f-\varepsilon} + \beta(\varepsilon_f - E_0)\left(\frac{s^2}{V^2}-1\right)$$

(61)

At $T = 0$, we set

$$S_{eff} = \beta U(\varepsilon_f, s) \tag{62}$$

U is the "effective potential" of the Bose fields [16], and we find

$$U(\varepsilon_f, s) = -\frac{N\Delta}{\pi} + \frac{N\varepsilon_f}{\pi}\tan^{-1}\frac{\Delta}{\varepsilon_f} + \frac{N\Delta}{2\pi}\ln\frac{\varepsilon_f^2+\Delta^2}{D^2} + (\varepsilon_f - E_0)\left(\frac{\Delta}{\Delta_0} - 1\right) \tag{63}$$

where $\Delta_0 = \pi\rho V^2$, and we have assumed $D >> \varepsilon_f$, Δ . We comment that the form (60) is the expected form for the free energy of a non-interacting resonance in terms of the phase shift.

Now we must minimise U with respect to variations in ε_f and Δ . These give, respectively,

$$\frac{N}{\pi}\tan^{-1}\frac{\Delta}{\varepsilon_f} = 1 - \frac{\Delta}{\Delta_0}$$

$$\frac{N\Delta_0}{\pi}\ln\frac{(\varepsilon_f^2 + \Delta^2)^{1/2}}{D} = E_0 - \varepsilon_f \tag{64}$$

The first equation originates directly from the constraint $Q = 1$, the left hand side being the expectation value of the f occupation (which we will call n_f) in terms of the phase shifts, given by the Friedel sum rule [20, 21]. As will become clear later, the ratio

$$Z_f = \Delta / \Delta_0 \tag{65}$$

is the (inverse of the) "mass-enhancement" (effective wave-function renormalisation factor) for the f quasiparticles, and so we have

$$Z_f = 1 - n_f \tag{66}$$

In the present "mean-field" approximation, the Hamiltonian is that of non-interacting quasiparticles with a Friedel-like Lorentzian resonance centred at ε_f, with (renormalised) width Δ, which is partly occupied [21]. The overall energy scale of the resonance is

$$k_B T_A = (\varepsilon_f^2 + \Delta^2)^{1/2} \tag{67}$$

Since (64a) implies that ε_f is positive, (64b) has a unique solution for all E_0 (negative ε_f allows two further solutions in the regime $E_0 \lesssim 0$, which was a problem in earlier treatments).

The limit

$$\begin{gathered} N \to \infty \\ N\Delta_0 \text{ , } E_0 \text{ fixed} \end{gathered} \tag{68}$$

as in §3, allows us to approximate

$$\Delta \simeq \frac{\pi \varepsilon_f n_f}{N} \tag{69}$$

and hence

$$n_f \simeq \frac{1}{1 + \frac{\pi \varepsilon_f}{N \Delta_0}} \tag{70}$$

where now $k_B T_A \simeq \varepsilon_f$ satisfies

$$0 < \varepsilon_f = E_0 - \frac{N \Delta_0}{\pi} \ln \frac{\varepsilon_f}{D} \tag{71}$$

This is the same as the Brillouin-Wigner equation obtained by earlier diagrammatic treatments [4], some of which, however, broke down in the regime $n_f \to 1$, unlike the present scheme.

Substituting into U gives

$$U(\varepsilon_f, s = s_0) = \frac{N}{\pi}\left(\varepsilon_f \tan^{-1}\frac{\Delta}{\varepsilon_f} - \Delta\right) + E_0 - \varepsilon_f \tag{72}$$

at the point (ε_f, s_0) satisfying (64), and at large N,

$$U = E_0 - \varepsilon_f \tag{73}$$

Thus (71) gives the ground state energy at large N, as in the Goldstone diagram large-N treatment [4,5].

When E_0 is large and positive, (71) implies that ε_f is the same as Haldane's T* [10] (generalized to large N) and is not far from E_0. Evidently in this limit n_f is small ($\lesssim \frac{1}{2}$) and the ground state is largely f^0. This is confirmed by the ground state energy as E_0 is mostly cancelled by ε_f, leaving U small and negative.

When E_0 is large and negative, ε_f is small:

$$\ln \frac{\varepsilon_f}{D} = \frac{\pi(E_0 - \varepsilon_f)}{N\Delta_0} \simeq \frac{\pi E_0}{N\Delta_0} \tag{74}$$

so

$$\varepsilon_f = D \exp \frac{\pi E_0}{N\Delta_0} = k_B T_K \tag{75}$$

which is the Kondo temperature of lowest-order renormalisation group treatments. This identification holds fairly trivially when E_0 lies outside the band, and the Schrieffer-Wolf transformation (16) is valid, giving [2]

$$k_B T_K = D \exp(1/N\rho J) \tag{76}$$

but it also holds (in leading order in $1/N$) when E_0 is inside the band [10] which is less trivial (see Chapter 3, §4 for an example where this does not occur). In this limit, n_f is close to 1 , and the ground state energy (in this approximate treatment) is the energy E_0 of f^1 , plus a small correction, $-k_B T_k$.

Note also that when $n_f \simeq 0$, $Z_f \simeq 1$ so $\Delta \simeq \Delta_0$ and there is little renormalisation of the f electron properties (see also below for χ , γ) but when $n_f \simeq 1$, $\Delta \simeq \pi T_k/N$ and Z_f is very small, so there is much renormalisation.

We now calculate the change in the linear coefficient of specific heat γ and $T = 0$ magnetic susceptibility χ_0 due to the addition of the impurity to the system (throughout this thesis we will refer to susceptibility and specific heat for the impurity, with the understanding that the contribution due to the non-interacting electron gas is subtracted out). The calculation of thermodynamic

properties at finite temperature T and magnetic field h in general means that the stationary point equations corresponding to (64) must be solved at finite T and h, giving ε_f and Δ as functions of T and h, which are substituted into the free energy before derivatives with respect to T or h can be taken. This is done in §6. For the calculation of χ_0 and γ however, this is simplified: they may be calculated with the neglect of the dependence of ε_f and Δ on T and h, using the expression for the free energy of the resonance characterised by the $T = h = 0$ values of ε_f and Δ (discussed above). This follows from the stationary point equations satisfied by ε_f and Δ and the fact that their leading T or h dependence is quadratic.

The calculation of χ_0 and γ is then effected through the partition function, in the present approximation,

$$Z = Z_0 \exp\{-S_{eff}(\varepsilon_f, \Delta)\} \qquad (77)$$

where ε_f, Δ take their $T = h = 0$ stationary point values, (64). We first calculate γ. Z_0 gives the partition function of the band without the impurity, which we said we would subtract off. The free energy is therefore given by

$$F = -N\int_{-D}^{D} \frac{d\varepsilon}{\pi} f(\varepsilon) \tan^{-1}\frac{\Delta}{\varepsilon_f - \varepsilon} + (\varepsilon_f - E_0)\left(\frac{\Delta}{\Delta_0} - 1\right) \qquad (78)$$

After the discussion above, the T dependence comes only from the Fermi factor. The Sommerfeld formula

$$\int_{-D}^{D} d\varepsilon\, f(\varepsilon) A(\varepsilon) = \int_{-D}^{0} d\varepsilon\, A(\varepsilon) + \frac{\pi^2}{6}(k_B T)^2 A'(0) + O(T^4) \tag{79}$$

gives the expansion

$$F(T) = F(0) - \frac{\pi^2}{6}(k_B T)^2 \frac{N\Delta/\pi}{\varepsilon_f^2 + \Delta^2} + O(T^4) \tag{80}$$

and as

$$\gamma = -\left.\frac{\partial^2 F}{\partial T^2}\right|_{T=0} \tag{81}$$

we find

$$\gamma = \frac{\pi^2}{3} k_B^2 \frac{N\Delta/\pi}{\varepsilon_f^2 + \Delta^2} \tag{82}$$

We identify the right hand side as the expected result for non-interacting electrons in an N-fold degenerate Lorentzian resonance, whose density of states is (per channel)

$$\rho_f(\varepsilon) = \frac{\Delta/\pi}{(\varepsilon - \varepsilon_f)^2 + \Delta^2} \,. \tag{83}$$

The relation to the density of states is the hallmark of a Fermi liquid; here we see that adding the impurity contributes only an f-density of states, and no change in the conduction electron density of states; the latter is a consequence of our assumption of a wide, flat conduction band.

The calculation of χ_0 can be done in a similar way, adding a term

$$-g\mu_B h \sum_m m f_m^+ f_m - g\mu_B h \sum_{km} m c_{km}^+ c_{km} \qquad (84)$$

to the Hamiltonian (g is the usual Landé factor). We remark here that the latter term is often dropped, as it only gives rise to the conduction band contribution. For a wide, flat band, the change in total number of electrons, and likewise (in our model with SU(N) symmetry) the occupation of each angular momentum state m, is given only by the occupation of the f-projected density of states (just as our result for γ was). This is Anderson's compensation theorem [1, 22]. It is therefore possible to couple the magnetic field only to the f-states.

We then have, in a field, neglecting the effect on Z_0,

$$F = -\sum_m \int_{-D}^{D} \frac{d\varepsilon}{\pi} f(\varepsilon) \tan^{-1} \frac{\Delta}{\varepsilon_f - g\mu_B h m - \varepsilon} + (\varepsilon_f - E_0)\left(\frac{\Delta}{\Delta_0} - 1\right) \qquad (85)$$

giving for

$$\chi_o = - \frac{\partial^2 F}{\partial h^2}\Big|_{T=h=0} \tag{86}$$

$$\chi_o = \frac{1}{3} j(j+1) N \rho_f(0) g^2 \mu_B^2 \tag{87}$$

We have used

$$\sum_{m=-j}^{j} m^2 = \frac{1}{3} j(j+1)(2j+1) \tag{88}$$

We see that χ_0 , like γ , is given by the density of states, as expected for a non-interacting Fermi liquid. Defining

$$R = \frac{\pi^2 k_B^2 \chi_0}{j(j+1) g^2 \mu_B^2 \gamma} \tag{89}$$

we have in our approximation,

$$R = 1 \tag{90}$$

independent of n_f . We compare this with the exact result (derived from Ward identities in the perturbation theory in U for the Anderson model [23])

$$1 < R < \frac{N}{N-1} \tag{91}$$

For the Coqblin-Schrieffer model [24]

$$R = \frac{N}{N-1} \tag{92}$$

and R should vary from 1 to N/(N-1) as n_f goes from 0 to 1. Our result is in any case correct to leading order in 1/N. (91) follows from the relation [23] between χ_0, γ and χ_c, the charge susceptibility,

$$\gamma = \frac{\pi^2 k_B^2}{3}\left[\frac{1}{N}\chi_c + \frac{N-1}{N}\frac{\chi_0}{\frac{1}{3}j(j+1)(g\mu_B)^2}\right] \tag{93}$$

on assuming positivity.

Our result for χ_0 or γ can be rewritten for large N as

$$\chi_0 \simeq \frac{1}{3}j(j+1)(g\mu_B)^2 \frac{n_f}{T_A} \tag{94}$$

or as

$$\chi_0 = \frac{1}{3}j(j+1)(g\mu_B)^2 \frac{N \sin^2(\pi n_f/N)}{\pi Z_f \Delta_0}$$

$$\simeq \frac{1}{3}j(j+1)(g\mu_B)^2 \frac{\pi n_f^2}{N\Delta_0 Z_f} \tag{95}$$

This shows that χ_0 diverges as $n_f \to 1$ (where $\chi_0 \propto 1/T_k$) and that

$$Z_f = 1 - n_f \tag{96}$$

is enhancing the susceptibility (or γ) by comparison with a similar resonance of the same occupation and width Δ_0, in the same manner that mass enhancement Z_f^{-1} appears in χ_0 or γ for conventional (translationally invariant) Fermi liquids [25].

We complete these results with the static, $T = 0$ charge susceptibility. While, as may be seen using the power-counting argument of §3, the general dynamic charge susceptibility requires some consideration of fluctuations even in leading order (unlike the dynamic magnetic susceptibility, since the former is a singlet fluctuation) the $\omega = 0$ (static) charge susceptibility can be calculated from

$$\chi_c = -\frac{dn_f}{dE_0} \tag{97}$$

with n_f determined as above. Unlike χ_0 and γ, the calculation of χ_c requires us to evaluate the change in ε_f, Δ with E_0, since the leading dependence on E_0 is linear, not quadratic.

In fact, as the stationarity equations (64) give n_f, we use then to obtain χ_c. We write them as

$$n_f = 1 - \frac{T_A}{\Delta_0} \sin \frac{\pi n_f}{N} \tag{98}$$

$$\frac{N\Delta_0}{\pi} \ln \frac{T_A}{D} = E_0 - T_A \cos \frac{\pi n_f}{N}$$

Then

$$\frac{dn_f}{dE_o} = -\frac{\sin\frac{\pi n_f}{N}}{\Delta_o}\frac{dT_A}{dE_o} - \frac{\pi T_A}{N\Delta_o}\cos\frac{\pi n_f}{N}\frac{dn_f}{dE_o}$$

$$\frac{N\Delta_o}{\pi T_A}\frac{dT_A}{dE_o} = 1 - \frac{dT_A}{dE_o}\cos\frac{\pi n_f}{N} + \frac{\pi T_A}{N}\sin\frac{\pi n_f}{N}\frac{dn_f}{dE_o}$$

Hence on rearranging and using (98a)

$$\chi_c = \frac{\pi}{N\Delta_o(1-n_f)}\left(\frac{\pi^2}{N^2} + \left(\frac{1}{1-n_f} + \frac{\pi}{N}\cot\frac{\pi n_f}{N}\right)^2\right)^{-1} \tag{99}$$

and for large N ,

$$\chi_c = \frac{\pi}{N\Delta_o} n_f^2(1-n_f) \tag{100}$$

which can also be obtained more directly from (70, 71). χ_c at large N resembles χ_0 , multiplied by $(1-n_f)^2$. We interpret this as meaning that the f quasiparticles at the Fermi energy carry a reduced f charge of magnitude Z_f , giving a factor Z_f^2 in χ_c , relative to the quasiparticle density of states. Physically, χ_c is small when $n_f \to 0$, or when $n_f \to 1$, because $|E_0|$ is large compared with $N\Delta_0$, and so changing E_0 should not change n_f by much. We will later learn, however, that both n_f and χ_c are given incorrectly by mean field theory when $n_f \to 1$, since the leading order in $1/N$ terms behave as $T_k/N\Delta_0$, while the $1/N$ corrections, though of higher order in $1/N$, behave as power laws

as $n_f \to 1$, and so dominate the leading, exponential behaviour. The corrections then give behaviour in close accord with the physical argument just given, and can also be derived from simple perturbation theory (supplemented by scaling theory).

As a last application of this mean field theory, we consider the F-spectral function (see §1). In the present approximation the correlation function is

$$\langle T\, b^+ f_m(\tau) f_m^+ b(0)\rangle = |\langle b\rangle|^2 \langle T\, f_m(\tau) f_m^+(0)\rangle \tag{101}$$

the F-spectral function is then

$$\rho_F(\varepsilon) = \frac{Z_f \Delta/\pi}{(\varepsilon-\varepsilon_f)^2+\Delta^2} \tag{102}$$

Here Z_f plays its conventional role of reducing the weight in the quasiparticle peak, in this case to $(1-n_f)$ per channel.

A sum role for the total F weight (summed over m) is available [26], it is

$$\sum_m \int_{-\infty}^{\infty} d\varepsilon\, \rho_F(\varepsilon) = N(1-n_f) + n_f \tag{103}$$

The sum rule is easily understood; the last term is the weight below the Fermi energy, which must equal the occupation. The first term is the weight above the Fermi energy, which has a factor N as there are N ways of adding an electron to the f shell, each with weight $(1-n_f)$. The sum rule is easily proved using the X operators of eqn. (8); the proof simply formalises our argument.

In the large-N limit, the sum rule simplifies to $N(1-n_f)$, this is exactly what our result (103) gives, at any N and n_f .

We can also check the density of states at the Fermi energy. Langreth [20] showed in perturbation theory in U, that at $T = 0$ the F self energy is real at the Fermi energy, and that the Friedel sum rule is obeyed. Therefore the imaginary part of the inverse F Green's function is Δ_0. Then we have

$$\rho_F(0) = \frac{\sin^2 \pi n_f/N}{\pi \Delta_0} \tag{104}$$

Since $Z_f = \Delta/\Delta_0$, this agrees with our result. Another way of stating Langreth's result is that, if Δ is *defined* as the width at $\epsilon = 0$ in the quasiparticle propagator, then

$$Z_f = \Delta/\Delta_0 \tag{105}$$

is exact. The large-N result $\frac{\Delta}{\Delta_0} = 1 - n_f$ then follows (assuming a quasiparticle resonance of weight 1) simply from the sum rule (103) alone, without the details of the large N theory.

§5. Discussion

In this section we comment on the mean field results of the previous section, with particular reference to the large-N limit.

We have already mentioned that the large-N limit of our mean field results for n_f and ground state energy, eqns. (70), (71) and (73) coincides with the Brillouin-Wigner formulae of earlier diagrammatic treatments [4] and variational methods [27]. Our results for χ_0 , γ and χ_c (eqns. (94),(100)) have also been obtained this way. Recent work [5] in which a $1/N$ expansion is developed from the Goldstone diagram perturbation expansion, together with a careful comparison with Bethe Ansatz results at $T = 0$, has confirmed that our results are indeed exact when $N \to \infty$, as we had hoped they would be. Furthermore, we found that the Friedel-Langreth sum rule (104) was satisfied exactly by our F-spectral function, and the sum rule for the total weight, (103), was satisfied at large-N . This is evidence that our basic picture of the physics of the problem, that it is governed by a Lorentzian quasiparticle resonance without interactions, is correct at large N .

However, if we examine our result for the F-spectral function at arbitrary frequency, (102) we see that for large N the density of states becomes a delta function. This may be compared with the results of Gunnarsson and Schönhammer [27] , who studied the F-spectral function (and others) using a variational formulation of the $1/N$ expansion, and found that in the infinite N limit, the weight in ρ_F should not be concentrated in a delta function at T_A (eq. 71) but instead is spread into a continuum over all frequencies larger than T_A . In the region $|\varepsilon| < T_A$, our Lorentzian (102), which now gives a density of states of order $1/N$ per channel, is consistent with their results (see their analysis in [27b] , sections 6, 7). In the

region $\varepsilon < -T_A$, they find an extra continuum contribution of the same order in $1/N$ as the Lorentzian term (102). We conclude that the result (102) can be trusted only in the region $|\varepsilon| \lesssim T_A$. We may also note the important point, already implicit in (103), that different parts of the F-spectral density are of different orders in $1/N$; namely, for $\varepsilon < T_A$, the F-spectral density is of order $1/N$ per channel, and for $\varepsilon > T_A$, of order 1. This will eventually be shown (in Chapter 4, §6) to be connected with the reason for the existence of a $1/N$ expansion despite the restriction $Q = 1$. In our formulation, high and low frequency response (and high and low temperatures, etc.) require separate treatment, and our approach based on mean field theory is most appropriate to *low* energy features.

Another feature of the mean field theory worth emphasizing is that it breaks the symmetry (25), since the expectation value of b is non-zero;

$$\langle b \rangle \neq 0 \tag{106}$$

as is also the fermion propagator

$$\langle T c_{km}(\tau) f_m^+(0) \rangle \tag{107}$$

which also breaks the symmetry. In other words, Q is not conserved in the ground state of the mean field theory, which is a mixture of states of different Q (and so includes states with $n_f > 1$) even though the expectation value of Q is fixed at 1 by (64). Even so, the theory works well, despite this apparently undesirable feature; in particular, the low value of X_c as $n_f \to 1$ shows that fluctuations into states with $n_f > 1$ are not contributing greatly,

contrary to the naive expectation for a quasiparticle resonance (if we ignored the self-consistent condition (64a) we would have had $\chi_c \sim \chi_0$). Note that physical observables are always operators that commute with Q, and so do not take the system between subspaces with different values of Q, e.g.

$$n_f = \sum_m f_m^+ f_m$$

or

$$\sum_m m f_m^+ f_m \qquad \text{etc.}$$

The true ground state must have $Q \equiv 1$ and variational ground-states satisfying this condition were constructed some years ago [27]. As we have seen, our results coincide with those for $Q = 1$ states in the large N limit. The fact that our symmetry-breaking parameter is

$$s_0 = V\langle b\rangle \propto N^{-1/2} \tag{108}$$

as $N \to \infty$, is perhaps significant here. Our mean field results e.g. (64) can be expanded in powers of Δ with Δ vanishing as $N \to \infty$ at which point they coincide with the variational results as we have said. At finite N, the extra terms are due to the symmetry breaking parameter (108) and physically represent the fully-Lorentzian form of our resonance, rather than its large-N limit,

$$\frac{\Delta/\pi}{(\epsilon - \epsilon_f)^2}$$

An analogy with the theory of superconductivity is also evident, [28] where the BCS variational state contains a mixture of states of different particle numbers, so that the Cooper pair density is non-vanishing, breaking the phase symmetry, in analogy with (106). As in the case of BCS theory, there seem to be advantages of simplicity in allowing states of indefinite Q as our ground state, rather than building in the constraint $Q \equiv 1$ exactly throughout. However, in the BCS case, the average occupation of the state is proportional to the size of the system, and the fluctuations in particle number are small. In our case, $\langle Q \rangle = 1$ and we will have to justify the mean field theory another way (through the 1/N expansion), for which (108) is the key. We return to this in Chapter 4.

§6. Mean Field Theory at Finite Temperatures and Fields

a) General formulae

We start from (85) which gives the free energy in mean field theory, at any temperature and magnetic field:

$$F(T,h) = -\sum_m \int_{-\Lambda}^{\Lambda} \frac{d\varepsilon}{\pi} f(\varepsilon) \tan^{-1} \frac{\Delta}{\varepsilon_f - g\mu_B h m - \varepsilon} + (\varepsilon_f - E_0)\left(\frac{\Delta}{\Delta_0} - 1\right) \tag{109}$$

where ε_f and Δ depend on h and T ; requiring that they minimise F at each T and h we find

$$\sum_m \int_{-D}^{D} \frac{d\varepsilon}{\pi} \left(-\frac{df(\varepsilon)}{d\varepsilon}\right) \tan^{-1} \frac{\Delta}{\varepsilon_f - g\mu_B h m - \varepsilon} = 1 - \frac{\Delta}{\Delta_o}$$

$$\sum_m \int_{-D}^{D} \frac{d\varepsilon}{2\pi} \left(-\frac{df(\varepsilon)}{d\varepsilon}\right) \ln \frac{(\varepsilon_f - g\mu_B h m - \varepsilon)^2 + \Delta^2}{D^2} = \frac{E_o - \varepsilon_f}{\Delta_o} \quad (110)$$

Once ε_f and Δ are known, we can obtain magnetisation M(h)

$$M(h) = -\frac{\partial F}{\partial h} = \sum_m g\mu_B m \int_{-D}^{D} d\varepsilon \frac{f(\varepsilon)\,\Delta/\pi}{(\varepsilon_f - g\mu_B h m - \varepsilon)^2 + \Delta^2} \quad (111)$$

(where we have used conditions (110) to eliminate terms coming from the dependence of ε_f and Δ on h) and entropy S

$$S = -\frac{\partial F}{\partial T} = -\sum_m \frac{1}{(k_B T)^2} \int_{-D}^{D} \frac{d\varepsilon}{\pi} \frac{\varepsilon e^{\beta\varepsilon}}{(e^{\beta\varepsilon}+1)^2} \tan^{-1} \frac{\Delta}{\varepsilon_f - g\mu_B h m - \varepsilon}$$

(112)

where again (110) has been used. In the case of

$$\chi(T) = \frac{\partial M}{\partial h}\bigg|_{h=0}$$

we can take a further derivative with respect to h , ignoring the dependence of ε_f and Δ in (111) on h because they can be expanded in even powers of h for small h , and so

$$\chi(T) = -\sum_m (g\mu_B)^2 m^2 \int_{-D}^{D} \frac{d\varepsilon}{\pi} \frac{f(\varepsilon)\, 2\Delta(\varepsilon-\varepsilon_f)}{[(\varepsilon-\varepsilon_f)^2+\Delta^2]^2}$$

$$= \frac{1}{3} j(j+1)(g\mu_B)^2 N \int_{-D}^{D} d\varepsilon \left(-\frac{df(\varepsilon)}{d\varepsilon}\right) \frac{\Delta/\pi}{(\varepsilon-\varepsilon_f)^2+\Delta^2} \tag{113}$$

These expressions can be written in closed form in terms of the digamma function and its derivatives (and the log of Euler's gamma function in the case of the free energy (109)). For later use, we give the self consistent equations (110) in this form.

The digamma function $\psi(z)$ is defined by

$$\psi(z) = \frac{d}{dz} \ln \Gamma(z) \tag{114}$$

where Γ is Euler's gamma function. Many properties of ψ can be found in the standard references [29]. Here we use the fact that, for any complex ε,

$$f(\varepsilon) = \frac{1}{2} + \frac{1}{2\pi i}\left(\psi\left(\frac{1}{2} + \frac{\beta\varepsilon}{2\pi i}\right) - \psi\left(\frac{1}{2} - \frac{\beta\varepsilon}{2\pi i}\right)\right) \tag{115}$$

We use the forms of (110) integrated by parts; then (110a) becomes

$$\sum_m \int_{\to}^{D} d\varepsilon f(\varepsilon) \frac{\Delta/\pi}{(\varepsilon-\varepsilon_f+g\mu_B h m)^2+\Delta^2}$$

$$= \sum_m \int_{\to D} \frac{d\varepsilon}{2\pi i}\left[\frac{1}{\varepsilon-\varepsilon_f+g\mu_B h m-i\Delta} - \frac{1}{\varepsilon-\varepsilon_f+g\mu_B h m+i\Delta}\right]$$

$$\times\left(\frac{1}{2}+\frac{1}{2\pi i}\left(\psi\left(\frac{1}{2}+\frac{\beta\varepsilon}{2\pi i}\right)-\psi\left(\frac{1}{2}-\frac{\beta\varepsilon}{2\pi i}\right)\right)\right) \tag{116}$$

The term with the $\frac{1}{2}$ integrates up to $\frac{1}{2}N$. The poles of $\psi(\frac{1}{2}+\frac{\beta\varepsilon}{2\pi i})$ lie on the negative imaginary ε axis, and $\psi(z)$ behaves as $\ell n\ z$ for large $|z|$ with $\mathrm{Re}\ z > 0$; therefore in this term the contour lying along the real ε axis can be distorted into a semicircular contour at $|\varepsilon|$ large, $\mathrm{Im}\ \varepsilon > 0$. The term from the contour vanishes and only the pole of the integrand at

$$\varepsilon - \varepsilon_f + g\mu_B h m = i\Delta$$

contributes, giving

$$\sum_m \frac{1}{2\pi i}\psi\left(\frac{1}{2}+\frac{\beta}{2\pi i}(\varepsilon_f - g\mu_B h m + i\Delta)\right).$$

The other term is treated similarly, taking the contour into the $\mathrm{Im}\ \varepsilon < 0$ half plane. Then (110a) becomes

$$\frac{N}{2} + \frac{1}{\pi}\sum_m \mathrm{Im}\,\psi\left(\frac{1}{2} + \frac{\beta}{2\pi i}\left(\varepsilon_f - g\mu_B h m + i\Delta\right)\right)$$

$$= n_f(T) = 1 - \frac{\Delta}{\Delta_0} \qquad (117)$$

(117) correctly reproduces the $T = h = 0$ limit.

To treat (110b) we must be careful about the band-edge cutoff. The easiest analytic treatment is obtained by replacing our rectangular band by a Lorentzian one,

$$\rho(\varepsilon) = \pi\rho D \cdot \frac{D/\pi}{\varepsilon^2 + D^2} \qquad (118)$$

whose density of states at the Fermi energy is the same as the previous one. The left hand side of (110) becomes

$$\sum_m \int_{-\infty}^{\infty} \frac{d\varepsilon}{2\pi i}\frac{\pi D}{2}\left(\frac{1}{\varepsilon - iD} - \frac{1}{\varepsilon + iD}\right)\left(\frac{1}{\varepsilon - \varepsilon_f + g\mu_B h m + i\Delta} + \frac{1}{\varepsilon - \varepsilon_f + g\mu_B h m - i\Delta}\right)$$

$$\times\left(\frac{1}{2} + \frac{1}{2\pi i}\left(\psi\left(\frac{1}{2} + \frac{\beta\varepsilon}{2\pi i}\right) - \psi\left(\frac{1}{2} - \frac{\beta\varepsilon}{2\pi i}\right)\right)\right) \qquad (119)$$

and we may use the same tricks to do the integral. The $\frac{1}{2}$ in the Fermi function gives a term which vanishes for $D \gg \varepsilon_f$, Δ, h.

The other terms give finally, for T, h, ε_f, $\Delta \ll D$,

$$\frac{1}{\pi}\sum_m \mathrm{Re}\,\psi\left(\frac{1}{2} + \frac{\beta}{2\pi i}\left(\varepsilon_f - g\mu_B h m + i\Delta\right)\right) - \frac{N}{\pi}\ln\frac{\beta D}{2\pi}$$

$$= \frac{E_0 - \varepsilon_f}{\Delta_0} \qquad (120)$$

Again, this reproduces the $T = h = 0$ limit, with the same cutoff D as before.

b) $\varepsilon_f(T)$, $\Delta(T)$ and $n_f(T)$ to order T^2

We introduce

$$z(T,h) = \varepsilon_f(T,h) + i\Delta(T,h) \tag{121}$$

and combine eqns. (110) into a single expression,

$$\frac{\Delta_0}{\pi} \sum_m \int_{-\infty}^{\infty} d\varepsilon \left(-\frac{df(\varepsilon)}{d\varepsilon}\right) \ln \frac{z - g\mu_B h m - \varepsilon}{D}$$

$$= (E_0 + i\Delta_0) - z \tag{122}$$

Now with $h = 0$, write

$$z(T) = z_0 + z_2 (k_B T)^2 + O(T^4) \tag{123}$$

and expand (122) to $O(T^2)$ using (79) or

$$\int d\varepsilon\, \varepsilon^2 \left(-\frac{df}{d\varepsilon}\right) = \frac{\pi^2}{3} (k_B T)^2 \tag{124}$$

to obtain

$$\frac{N\Delta_0}{\pi} \left(\ln \frac{z_0}{D} + \frac{z_2}{z_0} (k_B T)^2 - \frac{\pi^2}{6} \left(\frac{k_B T}{z_0}\right)^2 \right)$$

$$= E_0 + i\Delta_0 - z_0 - z_2 (k_B T)^2 \tag{125}$$

Hence on equating coefficients of T^2 ,

$$z_2 = \frac{\pi^2}{6 z_0}\left(1 + \frac{\pi z_0}{N\Delta_0}\right)^{-1} \tag{126}$$

Now $|z_0| = T_A$, so

$$z_0 = T_A\, e^{\pi i n_f(0)/N}$$

and expressions for the T^2 corrections to ε_f , Δ can be read off from (126). For large N , they become

$$\varepsilon_f(T) = \varepsilon_f(0)\left(1 + \frac{\pi^2}{6}\left(\frac{k_B T}{T_A}\right)^2 \frac{1}{1 + \frac{\pi T_A}{N\Delta_0}} + O(T^4)\right)$$

$$\Delta(T) = \Delta(0)\left(1 - \frac{\pi^2}{6}\left(\frac{k_B T}{T_A}\right)^2 \frac{\left(1 + \frac{2\pi T_A}{N\Delta_0}\right)}{\left(1 + \frac{\pi T_A}{N\Delta_0}\right)^2} + O(T^4)\right) \tag{127}$$

From this we obtain the corrections to n_f , for large N ,

$$n_f(T) = 1 - \frac{\Delta(T)}{\Delta_0} = n_f(0)$$

$$+ \left(1 - n_f(0)\right)\frac{\pi^2}{6}\left(\frac{k_B T}{T_A}\right)^2 \frac{\left(1 + \frac{2\pi T_A}{N\Delta_0}\right)}{\left(1 + \frac{\pi T_A}{N\Delta_0}\right)^2} + O(T^4) \tag{128}$$

In the Kondo limit $n_f \to 1$, where $T_A \ll N\Delta_0$, we see that

$$n_f(T) \simeq n_f(0) + (1 - n_f(0))\frac{\pi^2}{6}\left(\frac{k_B T}{T_k}\right)^2 + O(T^4) \tag{129}$$

here the increase in n_f with T is small, even though it is measured over a temperature on the scale of T_k. The fact that n_f increases with T, at least at low temperatures, is typical of mixed valence, due to the partly filled resonance, whose occupation tends to increase due to thermal excitation of quasiparticles in the density of states which curves upwards as energy is increased, provided N is large or n_f is small (or both). In the limit $n_f \to 0$, $\Delta \simeq \Delta_0$ and we find

$$n_f(T) = n_f(0)\left(1 + \frac{\pi^2}{3}\left(\frac{k_B T}{T_k}\right)^2 + O(T^4)\right) \tag{130}$$

which is hardly affected by the infinite-U that restricts the build-up in the number of f-electrons, i.e. it is the result for a non-interacting, temperature-independent resonance.

c) T^2 corrections to $\chi(T)$, $C_v(T)/T$, and h^2 corrections to $M(h)/h$ in the Kondo limit

We now consider corrections to the remaining thermodynamic quantities $\chi(T)$, $C_v(T)$ (at $h = 0$) and $M(h)$ (at $T = 0$) for low temperatures and fields. While the expressions for general values of n_f are straightforward to obtain, we will concentrate on the Kondo limit, as there some novel features appear.

In the Kondo limit,

$$T_A \ll \frac{N\Delta_0}{\pi}$$

and (126) leads to

$$\varepsilon_f(T) = \varepsilon_f(0)\left(1 + \frac{\pi^2}{6}\left(\frac{k_B T}{T_K}\right)^2 + O(T^4)\right)$$

$$\Delta(T) = \Delta(0)\left(1 - \frac{\pi^2}{6}\left(\frac{k_B T}{T_K}\right)^2 + O(T^4)\right) \tag{131}$$

which we emphasize are correct for *any* value of N, unlike (127).

$\chi(T)$ and $C_v(T)$,

$$C_v(T) = T\frac{\partial S}{\partial T} \tag{132}$$

both calculated at $h = 0$, and $M(h)$, calculated at $T = 0$ are found from (111), (112) and (113) by expanding in powers of T (or h), including the dependence of ε_f, Δ on T (or h). To second order in h, (131) is

$$\varepsilon_f(h) = \varepsilon_f(0)\left(1 + \frac{1}{2}\left(\frac{g\mu_B h}{T_K}\right)^2 \alpha_2 + O(h^2)\right)$$

$$\Delta(h) = \Delta(0)\left(1 - \frac{1}{2}\left(\frac{g\mu_B h}{T_K}\right)^2 \alpha_2 + O(h^2)\right) \tag{133}$$

where we define

$$\alpha_{2r} = \frac{1}{N}\sum_{m=-j}^{j} m^{2r} \tag{134}$$

so

$$\alpha_2 = \frac{1}{3} j(j+1)$$

$$\alpha_4 = \frac{1}{15} j(j+1)(3j^2+3j-1)$$

All the results for the Kondo limit are collected in Table 2.1.

A notable feature in Table 2.1 is that the h^2 and T^2 coefficients in the thermodynamic quantities all vanish when $N = 3$ and are positive when $N > 3$, and negative when $N < 3$, with the sole exception of $M(h)$ for $N = 2$, where it so happens that

$$\frac{1}{3}\alpha_4 - \frac{1}{2}\alpha_2^2 < 0 \qquad (135)$$

making the h^3 coefficient positive. The reason for the changes in sign is essentially the curvature of the Lorentzian density of states at the Fermi energy, which is positive for $N > 4$, and negative for $N = 2, 3$ (for $N = 2$ the Fermi level is at the maximum in the resonance). The precise position of the change of sign in the coefficients is $N = 3$ rather than $N = 4$ as a result of the self-consistency conditions (110) and hence (131), (133). One expects that when $N = 2, 3$, the signs become positive again as n_f moves away from 1. This is verified by explicit calculation with the mean field theory for the Anderson model.

The signs of the coefficients, negative for $N = 2$, zero at $N = 3$, and positive for $N > 3$ are found also in the results from Bethe Ansatz solution of the Coqblin-Schrieffer model [30,31]. For $N > 3$ this of course implies the existence of a maximum in $\chi(T)$, even in the Kondo limit, which is a characteristic feature observed in mixed-valent materials. In the case of YbCuAl, the upward curvature of $C_v(T)$ with increasing T can also be discerned, as

TABLE 2.1 Mean field theory results for $\varepsilon_f(T,h)$, $\Delta(T,h)$, $\chi(T)$, $C_v(T)$ and $M(h)$ for low temperatures and fields, in the Kondo limit

$$\varepsilon_f(T,h) = \cos\frac{\pi}{N}\cdot T_K\left(1 + \frac{\pi^2}{6}\left(\frac{k_B T}{T_K}\right)^2 + \frac{1}{2}\alpha_2\left(\frac{g\mu_B h}{T_K}\right)^2\right)$$

$$\Delta(T,h) = \sin\frac{\pi}{N}\cdot T_K\left(1 - \frac{\pi^2}{6}\left(\frac{k_B T}{T_K}\right)^2 - \frac{1}{2}\alpha_2\left(\frac{g\mu_B h}{T_K}\right)^2\right)$$

$$\chi(T) = \frac{1}{3}j(j+1)(g\mu_B)^2\frac{N}{\pi T_K}\left(\sin\frac{\pi}{N} + \sin\frac{3\pi}{N}\,\frac{\pi^2}{6}\left(\frac{k_B T}{T_K}\right)^2\right)$$

$$C_v(T) = \frac{\pi^2}{3}k_B^2\frac{T}{T_K}\frac{N}{\pi}\left(\sin\frac{\pi}{N} + \sin\frac{3\pi}{N}\cdot\frac{9\pi^2}{10}\left(\frac{k_B T}{T_K}\right)^2\right)$$

$$M(h) = (g\mu_B)^2\frac{N}{\pi}\frac{h}{T_K}\left(\alpha_2\sin\frac{\pi}{N} + \sin\frac{3\pi}{N}\left(\frac{g\mu_B h}{T_K}\right)^2\left(\frac{1}{3}\alpha_4 - \frac{1}{2}\alpha_2^2\right)\right)$$

$$\alpha_2 = \frac{1}{N}\sum_m m^2 = \frac{1}{3}j(j+1)$$

$$\alpha_4 = \frac{1}{N}\sum_m m^4 = \frac{1}{15}j(j+1)(3j^2+3j-1)$$

can upward curvature in the magnetization curve at low temperature. The latter has been well fitted by Bethe Ansatz results [30,32] providing strong evidence for the applicability of the Coqblin-Schrieffer impurity model to this compound.

The negative curvature of $\chi(T)$ at low T, in the $N = 2$ Kondo model, and positive curvature in the $N = 2$ valence-fluctuating Anderson model, were seen first in numerical renormalisation group calculations by Wilson [33] and Krishnamurthy [34].

It is evident that our success in obtaining the change in sign of the T^2 and h^2 coefficients is due to the fully-Lorentzian resonance appearing in our mean field theory, and would not be obtained by strict expansion in powers of $1/N$.

d) High temperature behaviour in the Kondo limit

Still in the Kondo limit, we consider the high temperature behaviour of (110) for the Coqblin-Schrieffer model in zero field. The decreasing trend in $\Delta(T)$, (131b) suggests that Δ might vanish at high temperatures. If $\Delta = 0$, (110a) is satisfied by

$$\varepsilon_f = k_B T \ln(N-1) \quad . \tag{136}$$

This does not satisfy (110b) in general (in which the term $-\varepsilon_f$ on the right hand side is dropped). However, (110b) was derived by taking $\partial F/\partial \Delta$. Strictly, we should take

$$\frac{\partial F}{\partial s_0}$$

which is equivalent to $\partial F/\partial \Delta$ only after dividing by $2\pi\rho s_0$. Thus if $s_0 \neq 0$, (110b) applies, but $s_0 = 0$ is always an alternative

stationary point. This is a result of symmetry: the free energy as a function of $\langle b \rangle$ has rotational symmetry, so $\langle b \rangle = 0$ is always either a maximum or minimum (and in fact, the free energy is smooth there).

When (136) is substituted into (120), the equation is satisfied at only a single temperature, T_c :

$$\mathrm{Re}\,\psi\left(\frac{1}{2} + \frac{\ln(N-1)}{2\pi i}\right) = \frac{\pi E_0}{N\Delta_0} + \ln\frac{D}{2\pi k_B T_c}$$

$$= \ln\frac{T_K}{2\pi k_B T_c} \qquad (137)$$

For large z , $\psi(z) \sim \ell n\, z$, so we find for large N ,

$$k_B T_c = \frac{T_K}{2\pi}\exp\left(-\mathrm{Re}\,\psi\left(\frac{1}{2} + \frac{\ln(N-1)}{2\pi i}\right)\right)$$

$$\to \frac{T_K}{\ln N} \qquad (138)$$

as $N \to \infty$. This is the temperature at which the non-zero solution of (110b) at s_0 coalesces with the origin, in a continuous transition. Note that the free energy of solution (136) is higher than that for the solution with $\Delta \neq 0$ at low temperatures.

In the thermodynamics, solution (136) behaves almost like a free spin. We find

$$\chi(T) = \tfrac{1}{3} j(j+1)(g\mu_B)^2 \frac{N-1}{N} \frac{1}{k_B T}$$

$$S(T) = \ln(N-1) - N \ln\left(1 - \frac{1}{N}\right) \qquad (140)$$

which as $N \to \infty$ give the correct Curie constant and entropy of a free spin.

Similar behaviour is found at high magnetic fields at $T = 0$, where $\Delta = 0$ and only a single channel is occupied.

At the transition temperature T_c itself, there is a discontinuity of slope in both $\chi(T)$ and $S(T)$; hence there is a discontinuity in $C_v(T)$, which jumps to zero in the high temperature region. This behaviour also holds for $M(h)$ at $T = 0$. These behaviours are shown schematically in Fig. 2.4.

The behaviour found is close to that expected for the Kondo impurity, at large N. At high temperatures or fields, it is found by perturbation expansion [35] that the logarithmic corrections are controlled by factors of $1/N$, e.g.

$$\chi(T) = \tfrac{1}{3} j(j+1)(g\mu_B)^2 \frac{1}{k_B T}\left[1 - \frac{2}{N \ln T/T_K} - \frac{2 \ln(\ln T/T_K)}{N^2 (\ln T/T_K)^2}\right]$$

$$(T \gtrsim T_K) \qquad (141)$$

Hence for large N, the high temperature behaviour is that of a free

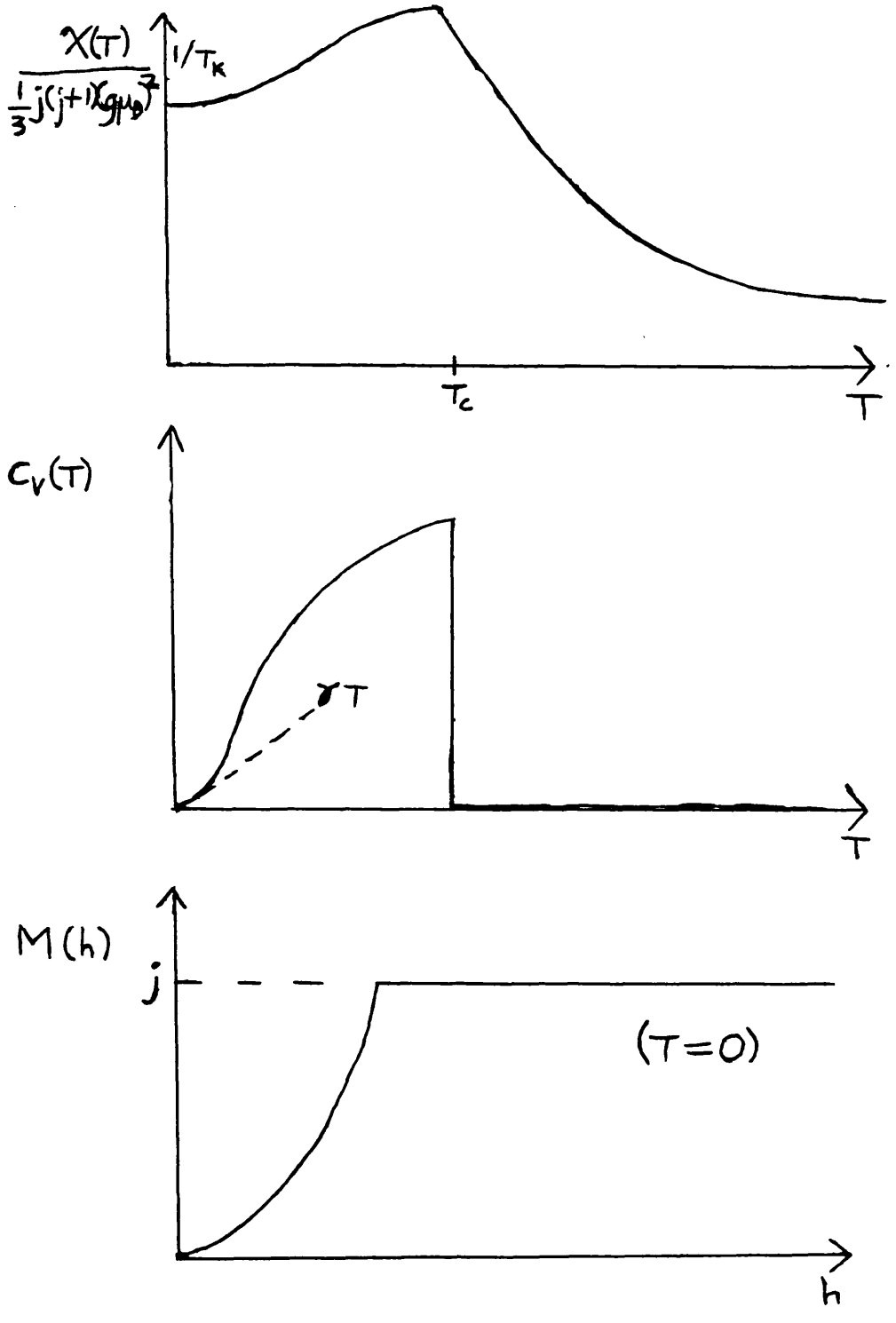


Fig. 2.4 Sketches of $\chi(T)$, $C_v(T)$ and $M(h)$, showing phase transition at $T_c \simeq T_k/\ell n\ N$ for large N .

spin. At low temperatures, we know that a Kondo singlet forms, with a binding energy of order T_k (at least as given by mean field theory). This suggests a competition between the entropy of the free spin and the energy lowering of the singlet ground state:

$$Z = e^{-\beta(-T_k)} + Ne^{0} \tag{142}$$

Hence a transition should occur at around

$$k_B T_c = T_k / \ln N$$

as found in mean field theory.

For the Anderson model, if Δ vanishes at high temperatures, then $n_f = 1$. This is consistent, since in the Anderson model, $n_f = N/(N+1) \simeq 1$ for sufficiently high temperatures ($T_c = T_A/\ell n\ N$ for large N, independent of the value of E_0). Other properties will be similar to those of Fig. 2.4 with T_A replacing T_k.

All in all, the mean field theory predicts high temperature behaviour for the Kondo case in remarkable agreement with expectations for the large N limit, even though at high temperatures there must be some contribution from $n_f > 1$; it appears that the contributions of the unwanted subspaces ($n_f > 1$) vanish as $N \to \infty$.

REFERENCES

1. P.W. Anderson, Phys. Rev. *124* (1961) 41.

2. B. Coqblin and J.R. Schrieffer, Phys. Rev. *185* (1969) 847.

3. A.C. Hewson, J. Phys. C. *10* (1977) 4973.

4. H. Keiter and J.C. Kimball, Int. J. Magn. *1* (1971) 233;
   A. Bringer and H. Lustfeld, Z. Phys. B *28* (1977) 213;
   T.V. Ramakrishnan and K. Sur, Phys. Rev. B *26* (1982) 1798;
   J.W. Rasul and A.C. Hewson, J. Phys. C. *16* (1983) L933.

5. J.W. Rasul and A.C. Hewson, Ref. 4 and J. Phys. C *17* (1984) 2555, 3337.

6. P. Coleman, Phys. Rev. B *29* (1984) 3035.

7. S. Barnes, J. Phys. F *6* (1976) 1375, F *7* (1977) 2637.

8. A. Yoshimori, Prog. Theor. Phys. (Kyoto) *55* (1976) 67.

9. A.L. Fetter and J.D. Walecka, "Quantum Theory of Many Particle Systems", McGraw-Hill, 1971.

10. F.D.M. Haldane, Phys. Rev. Lett. *40* (1978) 416.

11. D. Cragg and P. Lloyd, J. Phys. C *12* (1979) 3301.

12. A.A. Abrikosov, Physics *1* (1965) 5.

13. C. Itzykson and J.B. Zuber, "Quantum Field Theory", (McGraw-Hill) 1980.
    P. Ramond, "Field Theory - A Modern Primer", (Benjamin Cummings) 1981.
    D. Sherrington, J. Phys. C *4* (1971) 401.
    G.J. Papadopoulos, in "Path Integrals", ed. G.J. Papadopoulos and J.T. Devreese (Plenum) 1978, p.85.

14. Itzykson and Zuber, *op. cit.*, p.574.
    Ramond, *op. cit.*, p.280.

15. A. Yoshimori and A. Sakurai, Prog. Theor. Phys. Supp. *46* (1970) 162.

S. Chakravarty, 1981, unpublished.

16. S. Coleman, "1/N" SLAC preprint Pub-2484 (Erice lectures, 1979).

17. L. Yaffe, Rev. Mod. Phys. *54* (1982) 407.

18. D.J. Gross and A. Neveu, Phys. Rev. D *10* (1974) 3235.

19. D.J. Amit, "Field Theory, the Renormalization Group and Critical Phenomena" (New York: McGraw-Hill) 1978.

20. D. Langreth, Phys. Rev. *150* (1966) 712.

21. D.M. Newns and A.C. Hewson, J. Phys. F *10* (1980) 2429.

22. A. Yoshimori and F. Zawadowski, J. Phys. C *15* (1982) 5241.

23. K. Yamada, Prog. Theor. Phys. *54* (1975) 316.

A. Yoshimori, Prog. Theor. Phys. *55* (1976) 67.

P. Schlottmann, Phys. Lett. *100A* (1984) 509.

24. P. Nozières and A. Blandin, J. Physique *41* (1980) 193.

25. P. Nozières, "Interacting Fermi Systems" (Benjamin) 1964.

26. Y. Kuramoto, "Moment Formation in Solids", ed. W.J.L. Buyers, (Plenum) 1984, p.273.

27. C. Varma and Y. Yafet, Phys. Rev. B. *13* (1975) 2950.

O. Gunnarsson and K. Schönhammer, Phys. Rev. B *28* (1983) 4315, Phys. Rev. Lett. *50* (1983) 604.

28. e.g. J.R. Schrieffer, "Superconductivity" (Benjamin) 1964.

29. e.g. M. Abramovitch and I.A. Stegun, "Handbook of Mathematical Functions" (Dover, N.Y.) 1965, p.258.

30. A.C. Hewson and J.W. Rasul, J. Phys. C *16* (1983) 6799.

31. V.T. Rajan, Phys. Rev. Lett. *51* (1983) 308.

32. A.C. Hewson, D.M. Newns, J.W. Rasul and N. Read, Proc. 4th Int. Conf. on Valence Fluctuations (Cologne) 1984 to be published in J. Magn. Magn. Mat.

33. K.G. Wilson, Rev. Mod. Phys. *47* (1975) 773.

34. H.R. Krishnamurthy, J.W. Wilkins and K.G. Wilson, Phys. Rev. B *21* (1980) 1003, 1044.

35. A.C. Hewson and J.W. Rasul, Phys. Lett. *92A* (1982) 95.

CHAPTER 3. APPLICATION OF MEAN-FIELD TECHNIQUE TO SOME OTHER MODELS

§1. Spin-orbit and Crystal Field Splittings

In this chapter we apply the mean-field method of Chapter 2 to some other models of magnetic impurities in a metallic host. Our eventual aim is to understand realistic models of rare earth impurities, where each f-occupation may have a number of excited states, split by spin-orbit coupling, Hund's rule coupling, or crystal electric fields; these situations are not so far covered by the $U = \infty$ Anderson model used in Chapter 2. This ambitious programme will not be completed here; we will concentrate on what may be learned about the energy scales relevant to the low temperature behaviour from mean-field theory (supplemented by scaling theory) for intermediate values of the splittings in a few simple cases.

As a first concrete example consider a Ce^{3+} or Ce^{4+} impurity (in, say, a simple metal or intermetallic host). The Ce^{4+} state has no electrons in the f shell (we say it is f^0); there is therefore no degeneracy and no splitting, and nothing more to say about it. The Ce^{3+} configuration is f^1; the f electron has angular momentum $\ell = 3$ and spin $\frac{1}{2}$. Spin-orbit coupling splits this 14-fold degenerate manifold into a $j = 5/2$ (6-fold degenerate) multiplet and a $j = 7/2$ (8-fold degenerate) multiplet, with the $j = 7/2$ multiplet some 270 meV above the $j = 5/2$ when measured in vacuum [1]. In the framework of the Anderson model, other f

occupations are again assumed inaccessible in energy ($U = \infty$) and hybridisation with the band takes f^0 into f^1 and vice versa, while absorbing or emitting electrons into the band. As in [2] we again assume a spherically symmetric environment, so total angular momentum about the rare earth is conserved and f electrons in the $j = 5/2$ multiplet hybridise with $j = 5/2$ partial waves, while those in the $j = 7/2$ multiplet hybridise with $j = 7/2$ partial waves. Our model Hamiltonian is then

$$H = E_0 \sum_m f_m^{(5/2)+} f_m^{(5/2)} + (E_0+\delta E)\sum_m f_m^{(7/2)+} f_m^{(7/2)} + \sum_{km} \varepsilon_k \left(c_{km}^{(5/2)+} c_{km}^{(5/2)} + c_{km}^{(7/2)+} c_{km}^{(7/2)} \right) + V \sum_{km} \left(c_{km}^{(5/2)+} f_m^{(5/2)} b^+ + h.c. \right) + V \sum_{km} \left(c_{km}^{(7/2)+} f_m^{(7/2)} b^+ + h.c. \right) \tag{1}$$

with the constraint

$$\sum_m f_m^{(5/2)+} f_m^{(5/2)} + \sum_m f_m^{(7/2)+} f_m^{(7/2)} + b^+ b = 1 \tag{2}$$

Note that m runs from $-5/2$ to $5/2$ in the $j = 5/2$ multiplet, and $-7/2$ to $7/2$ in the $7/2$ multiplet, and that V is the same for both multiplets. δE is the splitting and could be set equal to 270 meV for Ce . To keep the model general, call the degeneracy of the lower multiplet N_1 , and of the higher multiplet N_2 , and $N = N_1 + N_2$.

The same considerations apply to Yb^{2+} , Yb^{3+} impurities when we consider the states of the *holes* in the f shell (Yb^{2+} is f^{14} , so no holes; Yb^{3+} is f^{13} , so one hole) only here the $j = 7/2$ multiplet is lowest and the splitting is about 1 eV [1].

Similar arguments, and a similar Hamiltonian to (1) apply to crystal field splittings. For example the $j = 5/2$ state of Ce may be split into either a quartet and a doublet, or into 3 doublets by a crystal field (note that Kramers degeneracy applies, so all degeneracies are even) and such splittings are often observed experimentally [3]. In this case the $j = 5/2$ conduction band states may also be combined into states of corresponding symmetry to the crystal field levels and a Hamiltonian similar to (1) can be written (with one or more splittings) with the degeneracies $N_1, N_2, \ldots$ now those of the crystal field multiplets [4]. As crystal fields arise (either through electrostatic forces or through hybridisation with orbitals on neighbouring sites) because of the anisotropy of the environment, it would be possible to have different V's for each multiplet. At first, however, we consider only the splitting δE (a single splitting is treated, to exemplify more complex crystal field splittings) and the same V's for each multiplet.

Because of the single constraint on (1), there is only a single boson field b (and b^+), as in Chapter 2, and so the mean field theory again involves only 2 parameters. Introducing the Lagrange multiplier $\varepsilon_f - E_0$ the self-consistent equations for ε_f and Δ $(= \pi\rho V^2 |\langle b \rangle|^2)$ can be written down immediately, following Chapter 2, eq. (64). They are (at $T = 0$)

$$\frac{N_1}{\pi}\tan^{-1}\frac{\Delta}{\varepsilon_f} + \frac{N_2}{\pi}\tan^{-1}\frac{\Delta}{\varepsilon_f+\delta E} = 1 - \frac{\Delta}{\Delta_o} \tag{3}$$

$$\frac{N_1\Delta_o}{\pi}\ln\frac{(\varepsilon_f^2+\Delta^2)^{1/2}}{D} + \frac{N_2\Delta_o}{\pi}\ln\frac{((\varepsilon_f+\delta E)^2+\Delta^2)^{1/2}}{D}$$

$$= E_o - \varepsilon_f \tag{4}$$

The quasiparticle density of states has two Lorentzian resonances, one at ε_f (the N_1-fold degenerate multiplet) and one at $\varepsilon_f + \delta E$ (the N_2-fold degenerate multiplet); the first equation has on the left hand side the total occupation of these resonances. The second equation arises in a similar fashion. Notice that these equations are similar to those that arise at $T = 0$ in finite magnetic field h, (Chapter 2, §6). The interesting point is that there is *no renormalization of the splitting* δE, the quasiparticle resonances are split by the same splitting as in the original Hamiltonian.

Let us simplify the equations (3, 4) by keeping only the leading dependence on Δ on the left hand side of each. This will be valid when the degeneracy of the multiplets is large, or for small occupations of the multiplets, (compared with 1), or suitable combinations of these conditions. This gives

$$n_{f_1} \simeq \frac{N_1\Delta}{\pi\varepsilon_f}, \qquad n_{f_2} \simeq \frac{N_2\Delta}{\pi\varepsilon_f} \tag{5}$$

for the occupations of the two multiplets, and

$$n_f = n_{f_1} + n_{f_2} = 1 - \frac{\Delta}{\Delta_0} \tag{6}$$

$$\frac{N_1 \Delta_0}{\pi} \ln \frac{\varepsilon_f}{D} + \frac{N_2 \Delta_0}{\pi} \ln \frac{(\varepsilon_f + \delta E)}{D} = E_0 - \varepsilon_f \tag{7}$$

(6) can be rearranged to give

$$n_f = \left(1 + \frac{\pi \varepsilon_f (\varepsilon_f + \delta E)}{(N_2 \varepsilon_f + N_1 (\varepsilon_f + \delta E)) \Delta_0} \right)^{-1} \tag{8}$$

which corresponds to Chapter 2, eq. (70). Evidently, when $\delta E \to 0$ we recover the results of Chapter 2 with $N = N_1 + N_2$. When δE is large (8) tends to

$$n_f \simeq \left(1 + \frac{\pi \varepsilon_f}{N_1 \Delta_0} \right)^{-1} \tag{9}$$

so the occupation is dominated by the lowest multiplet. However, the energy scale ε_f is still affected by the higher multiplet as long as it remains inside the band. For $\delta E >> \varepsilon_f$, the interesting case is the Kondo regime $n_f \to 1$, where (4) gives (even for small N_1)

$$k_B T_K \equiv (\varepsilon_f^2 + \Delta^2)^{1/2} = D \exp\left(\frac{\pi E_0}{N_1 \Delta_0} \right) \cdot \left(\frac{D}{\delta E} \right)^{N_2/N_1} \tag{10}$$

(For $\delta E > D$ however, the last factor becomes 1.) This important result will be confirmed by scaling theory, showing that the factor

$(D/\delta E)^{N_2/N_1}$ is exact, even when other scaling corrections to T_k are included. Thus an additional spin-orbit or crystal field multiplet at an energy larger than T_k but inside the band acts to *increase* T_k, compared with that for the lower multiplet only. In fact, equation (7), simplified in the Kondo limit to

$$\frac{N_1\Delta_0}{\pi}\ln\frac{\varepsilon_f}{D} + \frac{N_2\Delta_0}{\pi}\ln\frac{(\varepsilon_f+\delta E)}{D} = E_0 \qquad (11)$$

shows that ε_f varies smoothly from

$$T_K^{(N)} = D\exp\frac{\pi E_0}{N\Delta_0} \qquad (12)$$

to

$$T_K^{(N_1)} = D\exp\frac{\pi E_0}{N_1\Delta_0} \qquad (13)$$

as δE varies from 0 to D. Notice that the condition for (10) to be valid is

$$\delta E > \varepsilon_f$$

but ε_f depends on δE, making this a self consistent condition, the form

$$\delta E > T_K^{(N_1)} \qquad (14)$$

for example, is incorrect, at least in principle.

We can easily obtain expressions for the impurity contributions to χ_0 and γ, as in Chapter 2. For γ, the density of states at the Fermi energy gives

$$\gamma = \frac{\pi^2}{3} k_B^2 \left(\frac{N_1 \Delta/\pi}{\varepsilon_f^2 + \Delta^2} + \frac{N_2 \Delta/\pi}{(\varepsilon_f + \delta E)^2 + \Delta^2} \right) \tag{15}$$

With the same approximations as above this becomes

$$\gamma \simeq \frac{\pi^2}{3} k_B^2 \left(\frac{N_1 \Delta}{\pi \varepsilon_f^2} + \frac{N_2 \Delta}{\pi (\varepsilon_f + \delta E)^2} \right)$$

$$= \frac{\pi^2}{3} k_B^2 \left(\frac{n_{f_1}}{\varepsilon_f} + \frac{n_{f_2}}{\varepsilon_f + \delta E} \right)$$

(16)

The calculation of χ_0 is a little more complicated as the Zeeman term becomes non-diagonal when expressed in the basis of crystal field eigenstates. In the spin-orbit case, the Zeeman term would be diagonal in the basis used above if the magnetic field coupled to $\underline{J}$ (the total angular momentum operator) but as in fact it couples to $\underline{L} + 2\underline{S}$ [5], the Zeeman term is again not diagonal. In either case the off-diagonal terms lead to the Van Vleck contribution [6]. We will give an expression for χ_0 only in the spin-orbit case, neglecting the Van Vleck contribution:

$$\chi_0 = \frac{1}{3} j_1(j_1+1) g_1^2 \mu_B^2 \frac{N_1 \Delta/\pi}{\varepsilon_f^2+\Delta^2}$$

$$+ \frac{1}{3} j_2(j_2+1) g_2^2 \mu_B^2 \frac{N_2 \Delta/\pi}{(\varepsilon_f+\delta E)^2+\Delta^2} \qquad (17)$$

where j_1 , j_2 are the j's of the multiplets, and g_1 , g_2 are the corresponding Landé factors ($j_1 = 5/2$, $g_1 = 6/7$, $j_2 = 7/2$, $g_2 = 8/7$ for Ce ; for Yb the two multiplets are exchanged). It is evident that the value of the ratio χ_0/γ now depends on the splittings between levels, and not only on the degeneracies as was the case in Chapter 2, eq. (90). Therefore it is important in experimental comparisons with Fermi liquid theories such as the present one that, especially when crystal field splittings are present, the χ_0/γ ratio is compared with the value obtained taking account of realistic values of the splittings, otherwise deviations of R (Chapter 2, eq. (89)) from 1 have little significance.

§2. Application of Scaling Theory

In this section we provide a check on the results of the previous section for the Hamiltonian (1) by the use of scaling theory, as described in Chapter 1 [7]. As explained there, in scaling theory we reduce the band width D by δD , compensating for the change by modifying parameters E_0 , Δ_0 ... (or J for the Kondo case) by the amount that they are perturbed by the states in the band that have been removed. The new ("renormalized") Hamiltonian should then give rise to the same thermodynamics as the original one, for temperatures much less than D , within certain approximations

discussed in Chapter 1 and below. The scaling procedure can therefore be regarded as a method for deriving an effective Hamiltonian for use at temperature T by reducing the bandwidth to the order of T. Reducing T is then equivalent to following the evolution of the Hamiltonian as the bandwidth is reduced, and the crossovers that occur as functions of D are directly related to different regimes in temperature. Similar considerations apply to dynamical properties as functions of frequency ω at say $T = 0$ (for example, the F-spectral function, or dynamical magnetic susceptibility).

We will need some new notation for the energies of the f states. Let

$$E^{(0)}, E^{(1)}, E^{(2)} \tag{18}$$

be the energies of, respectively, the unoccupied f orbital, the lower multiplet (degeneracy N_1) of singly occupied states of the f orbital, and the higher multiplet (degeneracy N_2) of singly occupied states of the f orbital. The energies of the previous section are therefore

$$\begin{aligned} E^{(1)} - E^{(0)} &= E_0 \\ E^{(2)} - E^{(1)} &= \delta E \end{aligned} \tag{19}$$

Following Haldane [7], we calculate the changes in the energies (18) of the f states due to hybridisation with states within δD of the band edge, and so eliminate those states. In effect, we are calculating the self-energies of Fig. 3.1. As found by Haldane,

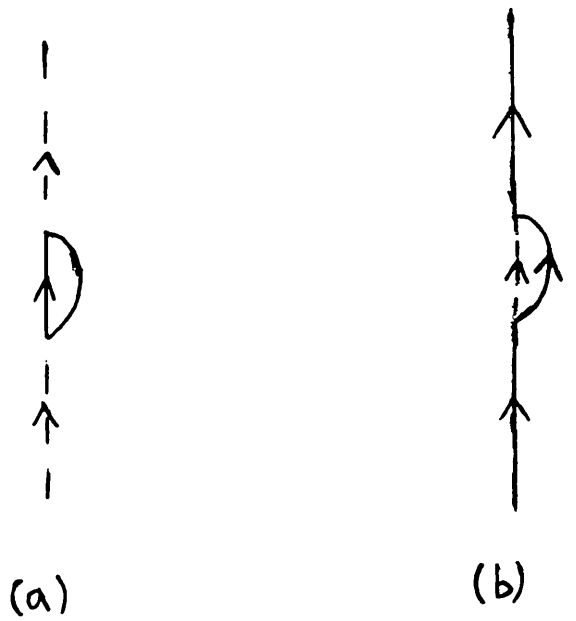


Figure 3.1 Self energies of f^0 and f^1 states involved in scaling. Dashed line: f^0 state. Straight line: f^1 state. Curved line: conduction electron or hole.

it is only necessary to work to order V^2, as corrections of higher order in V are not logarithmic and so not included in scaling theory (they give integrals which are convergent as $D \to \infty$). We first consider the regime

$$|E_0|, |E_0 + \delta D| \ll D \tag{20}$$

This corresponds to the usual scaling behaviour, just as if δE were zero. The f^0 energy $E^{(0)}$ is lowered by, from Fig. 3.1a,

$$N\rho V^2 \delta D/D$$

and $E^{(1)}$ and $E^{(2)}$ are each lowered by (Fig. 3.1b)

$$\rho V^2 \delta D/D$$

Note that the signs are fixed since, in second order Schrödinger perturbation theory, the effect of a virtual transition to a *higher* energy state is to *lower* the energy. We then have as our scaling transformation

$$\begin{aligned} D\frac{dE_f}{dD} &= -(N-1)\frac{\Delta_0}{\pi} \\ D\frac{d\delta E}{dD} &= D\frac{d\Delta_0}{dD} = 0 \end{aligned} \tag{21}$$

We have put $\bar{E}^{(1)} - \bar{E}^{(0)} = E_f$, whose initial value is E_0 (see below). The last equation follows from the absence of renormalisation of the states f^0 and f^1 themselves, leading to no change in the hybridisation matrix element in the Hamiltonian, as in [7].

The equations (21) confirm the idea that when (20) is satisfied, the splitting δE can be neglected, so that the scaling is identical to that for the model with zero splitting (full degeneracy N). Note that δE itself is invariant under scaling.

We integrate (21) to obtain

$$E_f(D) = E_f(D_0) + (N-1)\frac{\Delta_0}{\pi} \ln \frac{D_0}{D} \qquad (22)$$

Here D_0 is the initial bandwidth $(D < D_0)$, so that $E_f(D_0)$ is the E_0 of the previous sections. $E_f(D)$ is an "effective f level", and $E_f(D) + \delta E$ is the effective position of the upper multiplet.

Our perturbation theory breaks down when any of conditions (20) (for the renormalized E_f and D) or the condition

$$N\Delta_0 \ll D \qquad (23)$$

is not satisfied. Each possibility leads to a change in the scaling equations, and if the remaining conditions are still satisfied (well-separated energy scales) further scaling and further crossovers can take place. Evidently there are a number of possible scenarios (depending on the initial parameters) all of which need to be treated separately in scaling theory. Some of these will be considered here.

a) We first consider the case where the first crossover to occur is that where the condition

$$0 < E_f + \delta E \ll D$$

breaks down, the other conditions (20), (23) still being satisfied. As E_f is a function of D, eqn. (22), this occurs when D has been reduced to an energy T^* given by the condition

$$E_f(T^*) + \delta E = T^*$$

$$= E_f(D_0) + \delta E + (N-1)\frac{\Delta_0}{\pi} \ln \frac{D_0}{T^*} \qquad (24)$$

We suppose that this occurs when $|E_f(T^*)|$ is still small compared with T^*, so that in fact

$$T^* \simeq \delta E \qquad (25)$$

For energy scales less than T^*, fluctuations into the excited multiplet are effectively "frozen out", i.e. too high in energy to appear as real excitations. We may again apply scaling theory. For bandwidths D somewhat less than T^*, it is found that the reduction in $E^{(1)}$ on reducing the bandwidth by δD is still

$$\rho V^2 \delta D / D$$

that in $E^{(0)}$ is now

$$N_1 \rho V^2 \frac{\delta D}{D} + N_2 \rho V^2 \frac{\delta D}{T^*}$$

and that in $E^{(2)}$ is now

$$-\rho V^2 \frac{\delta D}{T^*}$$

The terms in $\delta D/T^*$ come from fluctuations between the excited multiplet of f^1 states and the f^0 states, and integrate up to terms of order D/T^*, which for small D can be neglected compared with the other terms behaving like $\ell n\ D$. The terms neglected here give rise to shifts in energies which are essentially constant, except near the crossover $D \simeq T^*$; provided the energy scales are well-separated they produce at worst numerical factors in the definition of T^* (eqn. (24)) which is to be used in calculating low energy effects. We are left with the scaling of E_f, which is that of a $U = \infty$ Anderson model with zero splitting (degeneracy N_1):

$$E_f(D) = E_f(T^*) + (N_1 - 1)\frac{\Delta_0}{\pi} \ln \frac{T^*}{D} \qquad (26)$$

We have put the initial values of E_f and D to be those at $D = T^*$, ignoring the non-logarithmic effects of the crossover we have just discussed.

From (26) we deduce the low temperature properties by comparison with Chapter 1. In particular, in the Kondo regime the next crossover occurs when $D \simeq \tilde{T}$ where

$$-\tilde{T} = E_f(T^*) + (N_1 - 1)\frac{\Delta_0}{\pi} \ln \frac{T^*}{\tilde{T}} \qquad (27)$$

at which point the f^0 state is frozen out, leaving a local moment described by a Coqblin-Schrieffer Hamiltonian with degeneracy N_1. The Kondo temperature can be written in various forms, using (24-27):

$$T_K \propto \tilde{T}\left(\frac{\Delta_0}{\pi\tilde{T}}\right)^{1/N_1} \exp -\frac{\pi\tilde{T}}{N_1\Delta_0}$$

$$= T^*\left(\frac{\Delta_0}{\pi T^*}\right)^{1/N_1} \exp \frac{\pi E_f(T^*)}{N_1\Delta_0}$$

$$= D_0\left(\frac{\Delta_0}{\pi D_0}\right)^{1/N_1}\left(\frac{D_0}{T^*}\right)^{N_2/N_1} \exp \frac{\pi E_f(D_0)}{N_1\Delta_0}$$

$$= D_0\left(\frac{\Delta_0}{\pi D_0}\right)^{1/N_1}\left(\frac{D_0}{\delta E}\right)^{N_2/N_1} \exp \frac{\pi E_0}{N_1\Delta_0} \qquad (28)$$

(using finally $\delta E \simeq T^*$ and $E_0 = E_f(D_0)$). This agrees with eqn. (10) from the mean field theory, except that the latter, as usual, does not give the $(\Delta_0/D_0)^{1/N_1}$ factor which comes from $1/N$ corrections (or next-leading logarithmic corrections in the scaling theory for the Coqblin-Schrieffer model).

b) We next consider another case which ultimately has $n_f \simeq 1$, but this time the freezing out of f^0 states and of the higher multiplet occurs at the *same* energy scale $\tilde{T}$, i.e.

$$-\delta E = -\tilde{T} = E_f(D_0) + (N-1)\frac{\Delta_0}{\pi}\ln\frac{D_0}{\tilde{T}} \qquad (29)$$

Here we cross directly into a Coqblin-Schrieffer model of degeneracy N_1 , cutoff $\tilde{T}$ and coupling $\rho J = -\Delta_0/\pi\tilde{T}$, and so we have

$$T_K \propto \tilde{T}\left(\frac{\Delta_0}{\pi\tilde{T}}\right)^{1/N_1} \exp -\frac{\pi\tilde{T}}{N_1\Delta_0}$$

$$= D_0\left(\frac{\Delta_0}{\pi D_0}\right)^{1/N_1}\left(\frac{D_0}{\tilde{T}}\right)^{N_2/N_1} \exp \frac{\pi E_f(D_0)}{N_1\Delta_0}$$

$$= D_0\left(\frac{\Delta_0}{\pi D_0}\right)^{1/N_1}\left(\frac{D_0}{\delta E}\right)^{N_2/N_1} \exp \frac{\pi E_0}{N_1\Delta_0}$$

(30)

Again the factor $(D_0/\delta E)^{N_2/N_1}$ found in mean field theory appears.

c) As a final example of a Kondo case ($n_f \simeq 1$) we consider the case where the first crossover freezes out the f^0 state, so that

$$0 < -E_f(D) \ll D$$

breaks down, but δE is still much smaller than D. This crossover occurs when D reaches the value $\tilde{T}$ where, as in (29)

$$-\tilde{T} = E_f(D_0) + (N-1)\frac{\Delta_0}{\pi}\ln\frac{D_0}{\tilde{T}} \qquad (31)$$

When D is reduced further below $\tilde{T}$, the f occupation is $n_f \simeq 1$ and the model is effectively a Coqblin-Schrieffer Hamiltonian with

$$\rho J = \frac{-\Delta_0}{\pi \tilde{T}} \quad , \text{ cutoff } \tilde{T} \tag{32}$$

as in case (b), but now, while all N scattering channels participate in the Hamiltonian, there is an energy splitting δE between states in the two manifolds of f^1 states (degeneracies N_1 and N_2). This problem, of a Kondo-type Hamiltonian with crystal field or spin-orbit splitting, was discussed by Nozières and Blandin [8]. They emphasized, as we did earlier in discussing eq. (10), that the important criterion for the importance of the splitting is its size compared with T_k. They did not, however, give an expression for T_k in the presence of a large splitting analogous to our expressions (28) and (30). The treatment of this case by Anderson's scaling method for the Kondo model has been done by Yamada *et al.* [9] and the next-leading logarithmic divergences included in a second paper [10]. They find

$$T_K \propto D_0 (\rho|J|)^{1/N_1} \left(\frac{D_0}{\delta E}\right)^{N_2/N_1} \exp\left(-\frac{1}{N_1 \rho |J|}\right) \tag{33}$$

where D_0 is the initial cutoff in their model. For our case this becomes

$$T_K \propto \tilde{T} \left(\frac{\Delta_0}{\pi \tilde{T}}\right)^{1/N_1} \left(\frac{\tilde{T}}{\delta E}\right)^{N_2/N_1} \exp\left(-\frac{\pi \tilde{T}}{N_1 \Delta_0}\right)$$

$$= D_0 \left(\frac{\Delta_0}{\pi D_0}\right)^{1/N_1} \left(\frac{D_0}{\delta E}\right)^{N_2/N_1} \exp\left(\frac{\pi E_f(D_0)}{N_1 \Delta_0}\right) \tag{34}$$

This holds provided $\delta E >> T_k$ (but note that T_k depends on δE as emphasized previously). If instead $\delta E \lesssim T_k$, the full degeneracy $N = N_1 + N_2$ of the Coqblin-Schrieffer model is recovered, and

$$T_k \propto D_0 \left(\frac{\Delta_0}{\pi D_0}\right)^{1/N} \exp \frac{\pi E_0}{N\Delta_0} \qquad (35)$$

Expressions (28), (30) and (34), which apply in apparently different regimes of scaling theory, are identical. From the point of view of T_k, and therefore of the main contributions to χ_0 and γ, it is as if the order of the two crossovers, one freezing out the f^0 state, the other freezing out the excited f^1 multiplet, does not make any difference. We might say that these crossovers "commute". However, at energies intermediate between the crossovers (if they are distinct, i.e. not case (b)) we are in different physical regimes (contrast cases (a) and (c)) and this can be expected to show up in some observable quantity (see discussion of spectral functions below).

We may explain the equality of (28), (30) and (34) by emphasizing the lack of dependence of T_k on the energy at which charge fluctuations into the f^0 state are frozen out. This is a feature of the $U = \infty$ Anderson model with zero splitting also (though not of the models we consider in §4). Fluctuations into the excited multiplet are always frozen out at $D \simeq \delta E$, and δE itself is never renormalized. The factor $(D_0/\delta E)^{N_2/N_1}$ is contributed by the extra spin fluctuations into the excited multiplet at energies between D_0 and δE.

d) We also mention a mixed-valence case as an alternative branch of case (a). After the crossover at T^* given by (24), the excited multiplet is frozen out, and scaling proceeds according to (26).

Suppose the next crossover is where

$$E_f(D) = D \tag{36}$$

thus freezing out the remaining f^1 states. This occurs at an energy

$$T_2^* = E_f(T_1^*) + (N_1 - 1)\frac{\Delta_0}{\pi} \ln \frac{T_1^*}{T_2^*} \tag{37}$$

T_1^* being the T^* of eq. (24). It is assumed that $E_f(T_1^*) << T_1^*$ in order that scaling is valid. In this case, it is natural to interpret T_1^* and T_2^* as the positions of peaks in the F-spectral function, with widths Δ_0 and weights N_2 and N_1 respectively. χ_0 and γ can be calculated directly from this picture, at least to leading order in Δ_0. We wish to emphasize that the *effective* splitting of these peaks is

$$T_1^* - T_2^* = \delta E + (N_1 - 1)\frac{\Delta_0}{\pi} \ln \frac{T_2^*}{T_1^*} \tag{38}$$

which is somewhat *less* than δE. The effective splitting is less than the bare splitting, though it can never be reduced to zero this way.

This result is in contrast with the result of the mean field theory, which had only a single self-consistent equation to determine the positions of both quasiparticle peaks (7), so that the splitting was precisely δE. Note, however, that the correction term in (38) is usually small compared with δE itself, since

$$T_1^* \simeq \delta E \tag{39}$$

here.

In a similar way we can discuss the F spectral function in the other cases (a)-(c). Apart from the "Kondo resonance" peak or peaks, which are within about T_K of the Fermi level, the positions, widths and weights of the peaks can be estimated on the basis of the scaling theory used so far. The results are summarised in Fig. 3.2.

a) At the first crossover, at $D \simeq T^*$, the excited multiplet was frozen out. We expect therefore that in the positive energy part of the spectrum, representing the density of states for adding a particle, there will be a peak at an energy T^*, since the added electron can go into the unoccupied f^1 states if it has energy T^*. There will be no corresponding peak for holes at $-T^*$. The width of the peak will be Δ_0, since once the electron has been added, it can decay into the band at a rate Δ_0. Note that this peak occurs in the F-spectral functions whose angular momentum suffix denotes a state lying in the excited multiplet (e.g.

$$\langle T\, b^+ f_m^{(7/2)}(\tau)\, f_m^{(7/2)+} b(0) \rangle$$

for the spin-orbit coupled case, where $j_2 = 7/2$ is the excited multiplet for Ce, with $N_2 = 2j_2 + 1$).

Continuing to decrease the energy, the next crossover occurs at $D \simeq \tilde{T}$ where the f^0 state is frozen out. Then the ground state is mainly f^1 in the j_1 (lower) multiplet. We then expect, as in the Kondo limit of the usual, unsplit model, that there is a peak at $-\tilde{T}$, corresponding to the possibility of removing an electron, provided an energy $\tilde{T}$ is provided. The hole so created has a lifetime $N_1\Delta_0$, as there are N_1 ways in which an electron

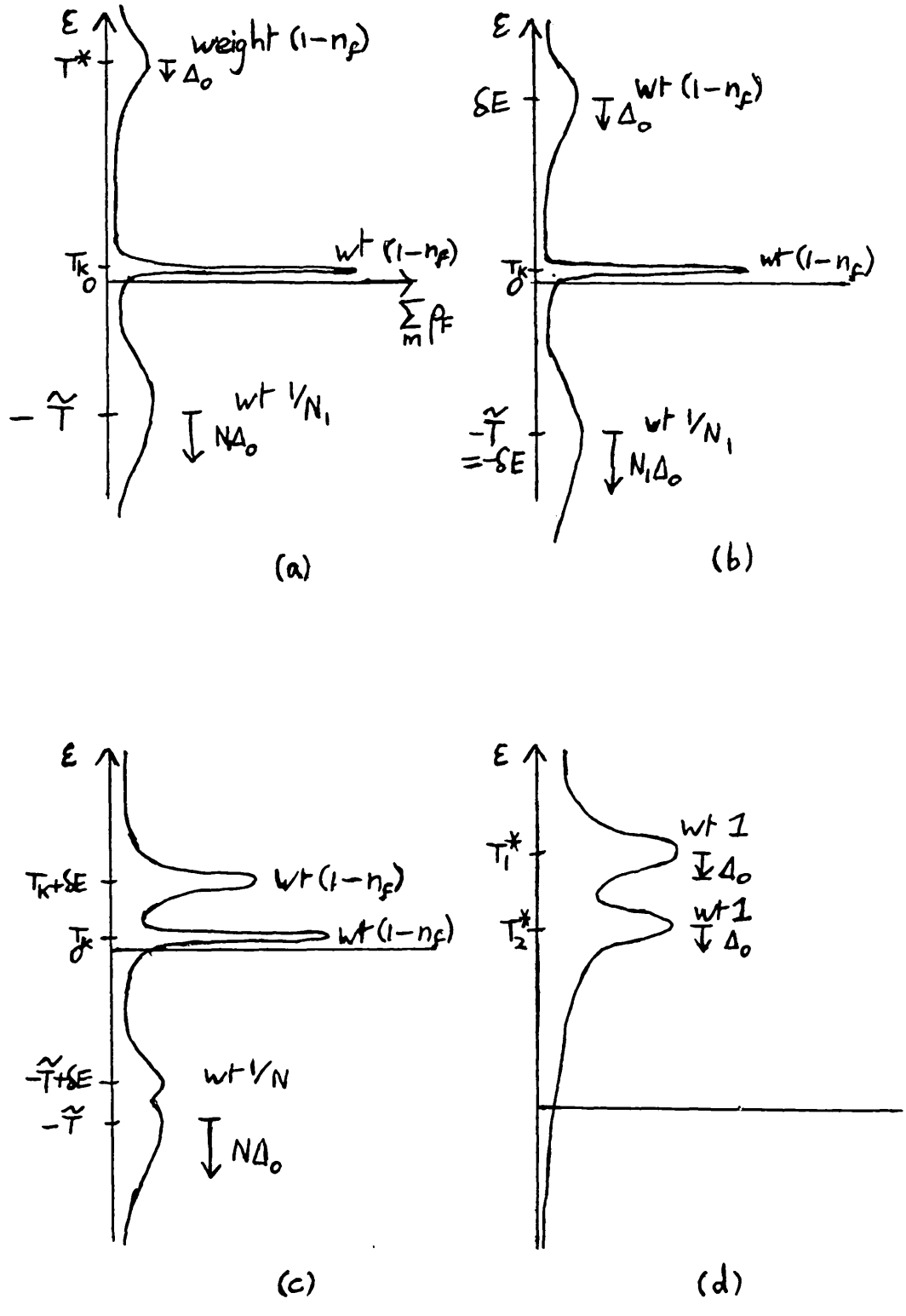


Figure 3.2 Schematic plot of the F-spectral function, shown summed over channels, for the cases described in the text. Weights are given per channel.

from the band can fall in and reoccupy the hole.

Finally, there will be a Kondo resonance at around T_k above the Fermi level, with width about $\pi T_k/N_1$ (for N_1 large), or at the Fermi level, with width T_k, if $N_1 = 2$, as in the quasi-particle resonance of Chapter 2. Both this Kondo peak and the lower, occupied peak at $-\tilde{T}$ are as expected, since we saw that the model scaled into the usual unsplit model with N replaced by N_1 when D was less than T^*.

As for the weights of the peaks, discussion is simplified by considering the sum rules for the two multiplets, analogous to that in Chapter 2, eq. (103). The total weight in the j_2 (excited) states, summed over the N_2 channels, is (rigorously)

$$n_{f_2} + N_2(1 - n_f) \tag{40}$$

and that in the j_1 states is

$$n_{f_1} + N_1(1 - n_f) \tag{41}$$

Note that it is n_f, not n_{f_i}, (i = 1 or 2) that appears in the bracket in (40), (41) since this factor describes the probability of find the ion in the f^0 state, and so is unity minus the *total* occupation n_f. Consequently, for the total weight, we find, on adding (40), (41)

$$n_f + N(1 - n_f) \tag{42}$$

which is the same as the unsplit case, (Chapter 2, eq. (103)) as one would expect.

In the present case, n_{f_2} is small, but $n_{f_1} \simeq n_f \simeq 1$. The peak at T^* in the "unoccupied" part of the spectrum therefore has weight $(1-n_f)$ per channel for states in the j_2 manifold, which is very small. To reiterate the previous paragraph, the weight is small because to excite this peak we must add an electron to the f states, which is hard as the occupation is close to one.

The weights of the other two peaks are as in the usual model, namely $1/N_1$ per channel in the j_1 manifold for the peak at $-\tilde{T}$ and $(1-n_f)$ for the Kondo peak, per channel.

The effective splitting between the "unoccupied" peaks is therefore of order

$$T^* - T_K \simeq T^* \simeq \delta E \tag{43}$$

using (25), as $T^* >> T_K$.

b) This case is similar to (a), but now T^* and $\tilde{T}$ have become equal. The widths and weights of the peaks are unaltered, and the effective splitting between the "unoccupied" peaks is

$$\tilde{T} - T_K \simeq \tilde{T} \simeq \delta E \tag{44}$$

c) In case (c), the first crossover, at $D \simeq \tilde{T}$, freezes out the f^0 states. It is further assumed that $\delta E << \tilde{T}$. Then we expect that the occupation is more or less evenly shared between the two multiplets:

$$n_{f_1} \simeq \frac{N_1}{N} \quad , \quad n_{f_2} \simeq \frac{N_2}{N} \tag{45}$$

An electron may therefore be removed from either multiplet, giving a

peak in the vicinity of $\tilde{T}$. Due to the splitting, however, this peak is split by δE , the j_2 states lying higher than the j_1 states, since less energy is needed to remove an electron from the former to the Fermi level than from the latter. Both these peaks have weight $1/N$ per channel and widths $N\Delta_0$, the latter arising since *all* channels can now contribute to the decay of the hole.

The Kondo resonance at T_k above the Fermi level is also expected to show the splitting, the j_2 states lying about δE above the j_1 states, and having a width intermediate between T_k/N and Δ_0 (for $T_k << \delta E << \tilde{T}$). As we have mentioned, we cannot deduce this from scaling theory for the Anderson model alone, and we have fallen back on consideration of the mean field theory of the previous section and the references given [8,9,10] for the Kondo model with crystal field splitting. The weight of each Kondo peak is expected to be again $(1-n_f)$ per channel.

As we move from case (a) to (b) to (c), then, with $\tilde{T}$ fixed and δE decreasing, the splitting of the quasiparticle peaks (those in the unoccupied part of the spectrum) gradually decreases, the upper one being about δE above the lower, and moving down to meet it as δE is decreased. The weights remain constant at $(1-n_f)$, but the width of the higher peak decreases from Δ_0 to $\pi T_k/N$ as $\delta E \to 0$. Case (b) seems to be the crossover point, where $\delta E \simeq \tilde{T}$, when the width first starts to decrease. For the peaks in the occupied part of the spectrum, as δE is decreased through $\tilde{T}$ (case (b)) we enter a regime where two peaks occur, one at $-\tilde{T}$ in the j_1 manifold and one at $-\tilde{T} + \delta E$ in the j_2 manifold. Presumably as δE is decreased, the width of *both* peaks increases from $N_1\Delta_0$ to $N\Delta_0$. Since when $\delta E \simeq \tilde{T}$ no broad peak is apparent at the Fermi energy, we suspect that the weight of the higher peak

is zero when $\delta E \simeq \tilde{T}$ and increases graudally to $1/N$ as $\delta E \to O(N\Delta_0)$.

We conclude that in this Kondo regime, two to four peaks may be observed, depending on the parameters. Needless to say, when the splitting of two peaks is smaller than their width, the peaks may be hard to distinguish. In the case of crystal field splittings, which are typically of order 10-20 meV , or less, in Ce and Yb compounds, the splitting of the lower peaks (case c) may be invisible; indeed the peak itself is broad and has little weight and so may not be seen in a photoemission experiment [11]. However, the splitting of the Kondo resonance when $\delta E > T_k$ may be observable though experimental broadenings are frequently larger than these splittings. A more favourable experiment would be neutron scattering, where splittings would also appear directly [12].

For spin orbit splittings, of order 270 meV (Ce) or 1 eV (Yb) we would probably be in case (a). Here the small weight $(1-n_f)$ of the peak, together with its relative broadness (the width would be Δ_0) leads us to predict that this peak would not be seen in a photoemission-type of experiment either.

The mean field theory of §1 has performed fairly well in obtaining the energy scales T_k and the positions and weights of the "unoccupied" peaks (that they each have weight $(1-n_f)$ in the F-spectral function follows from mean field theory exactly as in Chapter 2, §4). The widths of the higher peak in cases (a)-(b) and the lower peaks have not been obtained. The lower peaks we know to be a $1/N$ effect, obtained from fluctuations. The broadening of the higher quasiparticle peak is a fluctuation effect which should be obtained in leading order in $1/N$, as in the case of the unsplit model (Chapter 2, §5 and [11]). This is again expected to be

obtained on including fluctuations in the Bose field, in analogy with the variational calculation in [11].

We mention finally that our equation (7) was also obtained by Gunnarsson and Schönhammer [11] with their variational approach, with its corollary (10). A similar result was obtained by Yamada *et al.* [9, 10] for the Kondo case, also by a variational method.

§3. Models with both Configurations Magnetic

a) Introductory Remarks

In this and the following section we treat the problem of intermediate-valent ions whose f-occupation fluctuates between two configurations, both of which have non-zero angular momentum. Among the rare earths, the only element known definitely to fall into this class is Tm , though Pr and Tb have also been proposed as candidates. TmSe is the most studied example, being a semi-metallic compound which orders antiferromagnetically at 3K [3] and whose mean valence lies between divalent and trivalent at about 2.75 [3] (i.e. an f occupation of 12.25) as measured by interpolation of lattice constants. Varma [13] proposed that TmSe could be magnetic, unlike any known mixed-valent Ce , Yb , Sm or Eu compound, because both the f^{13} and the f^{12} configurations are magnetic, so that the moment is not completely lost during a valence fluctuation, as it is in for example a Ce compound. Some authors [14] suggested as a further consequence of this property that an isolated valence-fluctuating Tm ion would have a residual moment in its ground state, unlike the Ce-like cases previously discussed, where the ground state is always a singlet. This idea is lent some apparent support by the available results on a dilute Tm system,

TmLaSe [15] in which the neutron quasielastic linewidth varies linearly with temperature as $T \to 0$, in contrast with Ce-like impurities where it saturates [16], due to the formation of a singlet, Fermi-liquid ground state. However, as Varma *et al.* [17, 18] have recently pointed out, the model in [14] is not physically realistic for a valence-fluctuating Tm impurity. More realistic models studied in [17, 18] by a variational technique were found in all cases to have a singlet ground state analogous to that of a Ce or Yb impurity. These models are similar to those we will consider below. The implication of these results for the experiments is that either the characteristic temperature at which the singlet ground state sets in is below the temperatures reached, which would make it of the order of a few millikelvin, or else the impurity system studied is simply not mixed-valent, so that the impurity has either an f^{12} or an f^{13} stable moment, with perhaps only direct-exchange couplings to the conduction electrons (which are unlikely to lead to a singlet ground state). A search for other Tm compounds or dilute alloys showing mixed-valence behaviour, preferably in a true metallic host, seems desirable.

b) Models: LS versus jj Coupling Schemes

The construction of a model for a mixed-valent Tm impurity must begin with a discussion of the energy levels of the f^{12} and f^{13} states in the absence of a hybridisation matrix element. For the f^{13} state, there is a single hole in the f shell, as in the case of an Yb^{3+} impurity, whose energy is split by the spin orbit interaction into $j = 7/2$ and $j = 5/2$ multiplets, as in §1, with the $j = 7/2$ multiplet lowest (a spherically symmetric environment is assumed). The f^{12} state has two holes in the f-shell, and presents a new situation. It is conventional in the

rare earths, as in the lighter elements, to adopt the LS (or Russell-Saunders) coupling scheme [19] for the hierarchy of splittings of many-electron states of the f shell by electrostatic and spin-orbit coupling. In this scheme, as in Hund's rules [20], the largest couplings are electrostatic, so that at first the spin-orbit coupling can be neglected. Then L and S, the total orbital and total spin angular momentum are conserved separately. Hund's rules tell us to first form states with the maximum possible S, and of these to pick those with the largest possible L (consistent of course with the exclusion principle). This gives the lowest lying multiplet of states. Spin-orbit coupling, acting in this manifold only, splits these states, the total J value being $|L-S|$ in the first half of the rare earth series, and $|L+S|$ in the second half, as for Tm. Thus the lowest f^{12} state of the Tm ion is $^3H_6$ in spectroscopic notation, where $J = 6$, the first excited state is $^3H_4$, about 0.8 eV higher.

The possible hybridisation terms taking the Tm ion between the lowest multiplets of the two configurations can now be worked out. Hybridisation conserves both ℓ and s of the electron, so involves only $\ell = 3$ partial wave states, of either spin, in the conduction band. As the angular momentum of the two configurations is respectively $J = 6$ and $J = 7/2$, the difference is 5/2 and so *either* of the $j = 7/2$ or $j = 5/2$ conduction electron scattering channels can be involved, when ℓ and s are combined: $j = \ell \pm s = 3 \pm \frac{1}{2}$. This is in contrast with the case of Ce or Yb impurities, where one configuration has $J = 0$, and conservation of *total* angular momentum during hybridisation picks out either the $j = 5/2$ or $j = 7/2$ partial wave states. In the LS coupling

scheme, individual f electrons (or f holes) do not have well-defined j values, and so conduction electrons of *either* j value can hybridise with the impurity. A model Hamiltonian, keeping only the lowest multiplet for each valence state, is then

$$H_{LS} = \sum_{km} \varepsilon_k c^{(5/2)+}_{km} c_{km} + \sum_{km} \varepsilon_k c^{(7/2)+}_{km} c^{(7/2)}_{km}$$
$$+ \Big\{ V_{5/2} \sum_{km_1m_2M} \langle 6, M | \tfrac{7}{2} m_1, \tfrac{5}{2} m_2 \rangle X_{Mm_1} c^{(5/2)+}_{km_2}$$
$$+ V_{7/2} \sum_{km_1m_2M} \langle 6, M | \tfrac{7}{2} m_1, \tfrac{5}{2} m_2 \rangle X_{Mm_1} c^{(7/2)+}_{km_2}$$
$$+ \text{h.c.} \Big\}$$
$$+ \sum_m E_{13} X_{mm} + \sum_M E_{12} X_{MM} \qquad (46)$$

The notation for conduction electron states is as in §1, while the operators X_{Mm} are similar to those in Chapter 2, §1, taking the ion from its f^{13} to its f^{12} state:

$$X_{Mm} = |f^{12}: J=6, J_z=M\rangle\langle f^{13}: J=\tfrac{7}{2}, J_z=m|$$

etc. (Capital M runs from -6 to 6 , while lower case m runs from -7/2 to 7/2). The coefficients in the summations in the hybridisation terms in (46) are just conventional Clebsch-Gordan coefficients.

Hamiltonian (46) is the one we ultimately need to solve to understand mixed-valent Tm ions (neglecting crystal field splittings initially). However, as a preliminary step, we will study a simpler model, which originates from jj coupling. In the jj coupling scheme, we make the opposite assumption from that in the LS scheme, namely that the spin-orbit coupling is much larger than the electrostatic effects (we will term the latter "Hund's rule coupling"). We first form eigenstates of the spin-orbit coupling, so that each f electron has either $j = 5/2$ or $j = 7/2$. In the second half of the rare earth series, we can regard the 5/2 states as filled, leaving one or two $j = 7/2$ holes in the f shell for tne f^{13} or f^{12} states respectively. At this stage we can introduce hybridisation, which conserves total angular momentum, and neglecting the $j = 5/2$ excited states an Anderson-like Hamiltonian (written in terms of fermion operators) is

$$H_{SU(N)} = \sum_{km} \varepsilon_k c^+_{km} c_{km} + \sum_m E_o f^+_m f_m + V \sum_{km} \left(c^+_{km} f_m + h.c. \right) \tag{47}$$

Here *all* sums over m run from $-7/2$ to $7/2$, so we have dropped the 7/2 label on the conduction electron states once more. It is understood that (47) acts only between states where $n_f = 6$ or 7 (projection operators could be used to enforce this as in Chapter 2, §1). The Hamiltonian (47) is SU(N) invariant, $(N = 2j + 1)$ suggesting that a $1/N$ approach could be used. We will tackle (47) by a mean field approach in the next subsection, and by scaling

in the next section.

In the jj coupling scheme, the Hund's rule coupling acts only among the $j = 7/2$ states (for our case) and acts to line up the $\underline{j}$'s of the f electrons to the maximum. It could be simulated by a ferromagnetic $\underline{j} \cdot \underline{j}$ coupling. Neglecting the excited states once more, the final Hamiltonian becomes

$$H_{jj} = \sum_k \varepsilon_k c^+_{km} c_{km} + \sum_m E_{13} X_{mm} + \sum_M E_{12} X_{MM}$$
$$+ \left(\sqrt{2}\, V \sum_{km_1 m_2 M} \langle 6, M | \tfrac{7}{2} m_1, \tfrac{7}{2} m_2 \rangle X_{Mm_1} c^+_{km_2} \right.$$
$$\left. + \text{h.c.} \right) \qquad (48)$$

which is similar to H_{LS} except for the omission of $j = 5/2$ conduction electrons. The factor of $\sqrt{2}$ is included in (48) as a consequence of Fermi statistics in the f^{12} (two holes) state, in order that V in (47) agrees with that in (48), as will be seen in §4. Note that although the angular momentum of the f^{12} state is the same in both H_{LS} and H_{jj}, the actual wavefunctions are different, due to the different coupling schemes.

c) Mean Field Theory of $H_{SU(N)}$

It is convenient to perform a particle-hole inversion of our problem, and treat an f shell fluctuating between f^1 and f^2 states. We introduce an extension of Coleman's boson trick to treat (47):

$$H_{SU(N)} = \sum_{km} \varepsilon_k \, c^+_{km} c_{km} + \sum_m E_{21} f^+_m f_m$$
$$+ V \sum_{km} \left(c^+_{km} f_m b^+ a + f^+_m c_{km} a^+ b \right)$$
$$+ E - E_{21} \qquad (49)$$

The boson operators a , b will ensure that the constraint $n_f = 1$ or 2 is enforced provided we work in a subspace where the conserved quantities

$$Q_1 = n_f - a^+ a$$
$$Q_2 = a^+ a + b^+ b \qquad (50)$$

are both equal to 1 . These constraints may be introduced by integration over a *pair* of variables λ_1 , λ_2 , extending eq. (19) of Chapter 2. In (49) we have also used

$$E_{21} = E_2 - E_1 \qquad (51)$$

as the energy difference between the two configurations, and added constants to the Hamiltonian so that the energies of the f^1 and f^2 states are E_1 and E_2 respectively.

This extension of the boson trick generalises immediately to fluctuations between f^n and f^{n+1} by constraining Q_1 to be n instead of 1 . Two bosons are necessary whenever both

configurations are magnetic.

We will, in this section, treat (49) only in mean field theory, which is done by replacing a , b , a^+ , b^+ by their expectation values (chosen real and positive) which we denote by a and b for brevity:

$$\langle a \rangle, \langle a^+ \rangle \to a$$

$$\langle b \rangle, \langle b^+ \rangle \to b$$

In mean field theory the constraints are included through Lagrange multipliers only, so we add

$$(\varepsilon_f - E_{21})(Q_1 - 1) + B(Q_2 - 1) \tag{52}$$

to (49), ε_f and B being parameters, like a and b , to be found self-consistently.

Defining

$$\Delta_0 = \pi \rho V^2$$

$$\Delta = a^2 b^2 \Delta_0 \tag{53}$$

the ground state energy of (49) plus (52) is easily obtained by comparing with Chapter 2, eq. (63):

$$U(\varepsilon_f, B, a, b) = -\frac{N\Delta}{\pi} + \frac{N\varepsilon_f}{\pi}\tan^{-1}\frac{\Delta}{\varepsilon_f}$$

$$+ \frac{N\Delta}{2\pi}\ln\frac{\varepsilon_f^2+\Delta^2}{D^2}$$

$$+ (\varepsilon_f - E_{21})(-a^2-1)$$

$$+ B(a^2+b^2-1)$$

$$+ E_1 - E_{21} \qquad (54)$$

Varying ε_f , B , a^2 , b^2 gives 4 equations:

$$a^2+b^2 = 1$$

$$n_f = \frac{N}{\pi}\tan^{-1}\frac{\Delta}{\varepsilon_f} = 1+a^2$$

$$b^2\ln\frac{(\varepsilon_f^2+\Delta^2)^{1/2}}{D} = \frac{\pi}{N\Delta_o}(\varepsilon_f - E_{21} - B)$$

$$a^2\ln\frac{(\varepsilon_f^2+\Delta^2)^{1/2}}{D} = -\frac{\pi B}{N\Delta_o} \qquad (55)$$

Before manipulating these equations, we note that the mean field Hamiltonian again represents a non-interacting Fermi liquid, and

χ_0 and γ are proportional to the density of states at the Fermi energy as usual. For example,

$$\gamma = \frac{\pi^2}{3} k_B^2 \frac{N\Delta/\pi}{\varepsilon_f^2+\Delta^2}$$

$$= \frac{\pi^2}{3} k_B^2 \frac{N}{\pi\Delta} \sin^2 \frac{\pi n_f}{N}$$

$$= \frac{\pi^2}{3} k_B^2 \frac{N}{\pi} \frac{\sin^2 \pi n_f/N}{\Delta_0 (n_f-1)(2-n_f)} \tag{56}$$

using (55a,b), or alternatively, taking $N \to \infty$ with $N\Delta_0$ fixed,

$$\gamma \simeq \frac{\pi^2}{3} k_B^2 \frac{n_f}{T_A} \tag{57}$$

where we have introduced

$$T_A = (\varepsilon_f^2 + \Delta^2)^{1/2} \tag{58}$$

We see already from (56), (58), that χ_0 and γ diverge as $n_f \to 1$ or 2 , so that $T_A \to 0$ in these limits.

From (55c,d)

$$\frac{b^2}{a^2} = 1 + \frac{E_{21} - \varepsilon_f}{B} = \frac{1-a^2}{a^2} \tag{59}$$

Hence

$$a^2 = \frac{B}{2B + E_{21} - \varepsilon_f}$$

$$b^2 = \frac{B + E_{21} - \varepsilon_f}{2B + E_{21} - \varepsilon_f} \tag{60}$$

or

$$B = (E_{21} - \varepsilon_f)\frac{(n_f - 1)}{3 - 2n_f} \tag{61}$$

We will check the behaviour of B as $n_f \to 3/2$ below. Adding (55c) and (55d),

$$\ln \frac{T_A}{D} = \frac{\pi}{N\Delta_o}\frac{(E_{21} - \varepsilon_f)}{2n_f - 3} \tag{62}$$

From (62), as $E_{21} \to +\infty$, $n_f \to 1$, $B \to 0$ and

$$(\varepsilon_f^2 + \Delta^2)^{1/2} = T_K^{(1)} = D\exp -\frac{\pi E_{21}}{N\Delta_o} \tag{63}$$

When $E_{21} \to -\infty$, $n_f \to 2$, $B \to -E_{21}$ and

$$(\varepsilon_f^2 + \Delta^2)^{1/2} = T_K^{(2)} = D\exp \frac{\pi E_{21}}{N\Delta_o} \tag{64}$$

When $n_f \to 3/2$, $\varepsilon_f \to E_{21}$ (by equating (55)(c) and (d)) and so from (55d)

$$B \to \begin{cases} \dfrac{N\Delta_o}{2\pi} \ln \left| \dfrac{D\cos\frac{3\pi}{2N}}{E_{21}} \right| , & N > 3 \\ \dfrac{3\Delta_o}{2\pi} \ln \dfrac{4D}{\Delta_o} , & N = 3 \end{cases} \tag{65}$$

(The model reverts to that of Chapter 2 when $N = 2$, requiring the treatment given there.)

The f occupation is determined by a transcendental equation:

$$\frac{\Delta}{\Delta_0} = a^2 b^2 = (n_f - 1)(2 - n_f) = \frac{T_A}{\Delta_0} \sin\left(\frac{\pi n_f}{N}\right) \tag{66}$$

which simplifies for large N to a quadratic

$$(n_f - 1)(2 - n_f) = \frac{\pi T_A n_f}{N \Delta_0} \tag{67}$$

whose solution is

$$n_f = \frac{\left(3 - \frac{\pi T_A}{N\Delta_0}\right) \pm \sqrt{\left(3 - \frac{\pi T_A}{N\Delta_0}\right)^2 - 8}}{2} \tag{68}$$

The double-valuedness is an essential feature of this equation. The solution becomes complex when T_A is larger than

$$\frac{N\Delta_0}{\pi}\left(3 - 2\sqrt{2}\right) \simeq 0.17 \frac{N\Delta_0}{\pi} \tag{69}$$

which value is attained when $n_f = \sqrt{2} = 1.42 \ldots$

Near $n_f = 1$, from (67),

$$n_f \simeq 1 + \frac{\pi T_A}{N\Delta_0} + O\left(\left(\frac{\pi T_A}{N\Delta_0}\right)^2\right) \tag{70}$$

while near $n_f = 2$,

$$n_f \simeq 2\left(1 - \frac{\pi T_A}{N\Delta_o} + O\left(\left(\frac{\pi T_A}{N\Delta_o}\right)^2\right)\right) \tag{71}$$

The deviation from integral valence is exponentially small in $|E_{21}|$ in each case, similarly to the Kondo limit $(n_f \to 1)$ in the previous chapter.

We can define an F-spectral function as the imaginary part of the Fourier transform of

$$\langle T\, b^+ a\, f_m(\tau)\, f_m^+\, a^+ b\rangle \tag{72}$$

In the mean field approximation, we have

$$\rho_F(\varepsilon) = \frac{Z_f\, \Delta/\pi}{(\varepsilon-\varepsilon_f)^2+\Delta^2} \tag{73}$$

(cf. Chapter 2, eq. (102)) with

$$\frac{\Delta}{\Delta_o} = Z_f = a^2 b^2 = (n_f-1)(2-n_f) \tag{74}$$

In summary, the mean field theory has given a picture of the ground state and elementary excitations which is Fermi liquid-like, as in the model of Chapter 2. This means that the ground state of $H_{SU(N)}$ is a paramagnetic singlet. The quasiparticle density of states is Lorentzian, and the overall energy scale T_A of the resonance, given by (62) becomes small as *either* limit $n_f = 1$ or 2 is approached, and never exceeds a value given, for large N , by (69). In this model, and presumably also for H_{LS} and H_{jj} , *both*

integral-valent limits are Kondo limits where energy scales become small, due to the local moments which exist in each case (the question of whether H_{LS} and H_{jj} have singlet ground states cannot be settled this way, however, as we do not know how to include Hund's rule couplings in our mean field theory). In the F-spectral function, the weight of the resonance is reduced by a factor (74) which becomes small in each Kondo limit, analogous to the previous chapter. It would appear that a Langreth-type sum role [21]

$$\rho_F(0) = \frac{\sin^2 \frac{\pi n_f}{N}}{\pi \Delta_0} \tag{75}$$

(cf. Chapter 2, eq. (104)) holds for $H_{SU(N)}$ also, from which the first equality in (74) could be deduced.

In the following section, we form a critique of these results on the basis of scaling theory.

§4. Scaling Theory and Critique of Mean Field Theory

In this section we apply Haldane's scaling theory [7] to $H_{SU(N)}$, H_{jj}, and H_{LS}. In particular, for $H_{SU(N)}$ we are able to deduce the properties in the large N limit and compare them with the mean field theory of the previous section.

In the particle-hole-inverted form, we write the Hamiltonian as

$$\begin{aligned} H_{SU(N)} = & \sum_{km} \varepsilon_k c^+_{km} c_{km} + \sum_m f^+_m f_m E_{21} \\ & + V \sum_{km} \left(c^+_{km} f_m + f^+_m c_{km} \right) \\ & + E_1 - E_{21} \end{aligned} \tag{76}$$

where

$$E_{21} = E_2 - E_1 \tag{77}$$

and E_2 and E_1 are respectively the energies of the f^2 and f^1 states; it is again understood that no other states $(f^0, f^3, \ldots)$ are brought in by hopping.

For this model, scaling works very similarly to the Ce-like case treated by Haldane. The perturbation on low energy processes due to states within δD of the band edge D can be calculated perturbatively in powers of V. For the energies E_1 and E_2 we calculate self-energies to $O(V^2)$ due to hopping into the other valence configuration and emitting an electron or hole within δD of the band edge. In this way we reduce D but compensate for this by changing E_{21}, thus giving part of the scaling transformation. For $H_{SU(N)}$, the process shown in Fig. 3.3(a) lowers the energy of the f^1 state by

$$(N-1)\rho V^2 \delta D / D \tag{78}$$

while that in Fig. 3.3(b) lowers the energy of the f^2 state by

$$2\rho V^2 \delta D / D \tag{79}$$

Note that, in second order Schrödinger perturbation theory, excited states always *lower* the energy, thus fixing the sign, while the factors come from summing over possible internal states in (78) and from the two ways in which a transition to f^1 can be made in (79). The change in E_{21} is therefore

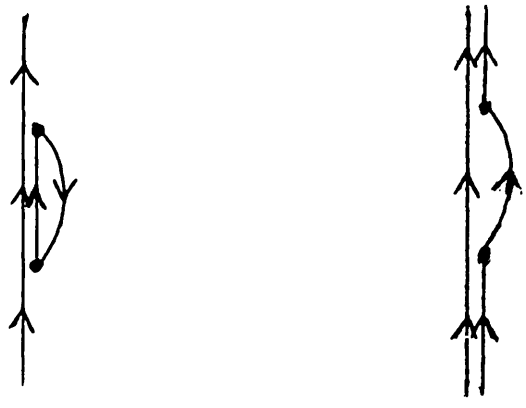


Figure 3.3 Self energies contributing to Haldane scaling

$$\delta E_{21} = (N-3)\rho V^2 \delta D/D \tag{80}$$

This can be integrated to give

$$E_{21}(D) = E_{21}(D_0) + (N-3)\frac{\Delta_0}{\pi} \ln \frac{D_0}{D} \tag{81}$$

Here D_0 is supposed to be the initial value of the bandwidth, and D the value to which it has been reduced; $E_{21}(D_0)$ is the initial value of the energy difference E_{21}. We define

$$\Delta_0 = \pi \rho V^2 \ , \tag{82}$$

the hybridisation width. As in Haldane [7] the width is unchanged on scaling, providing D is large. Higher order in V corrections to (81) are neglected as they vanish for large D, and the scaling of any other possible term in an effective Hamiltonian is either irrelevant (vanishes for large D) or can be expressed in terms of (81) in this regime ($D >> |E_{21}(D)|$, $N\Delta_0$). Then (81), and the D-independence of Δ_0 are all the information we need.

For completeness, we give a possible choice of scaling invariant, following Haldane,

$$E_{21}^* = E_{21}(D) + (N-3)\frac{\Delta_0}{\pi} \ln \frac{D}{N\Delta_0} \tag{83}$$

which together with Δ_0 can distinguish the different scaling trajectories.

In connection with (81) we note 2 special cases. In the case $N = 2$ the f^2 state is a singlet and the model is equivalent

to the model studied by Haldane, with our f^2 replacing his f^0 state. Our E_{21} is then equal to minus his E_d, and so our eqn. (81) agrees with his result.

Second, in the case $N = 3$, the change in E_{21} with D vanishes, which never happens in the Ce-like model for any N. It appears here because both the f^1 and f^2 states are triply degenerate for $N = 3$, and particle-hole inversion simply interchanges the two valence configurations. Therefore the change in E_{21} must vanish, since if it had a definite sign it would break this particle-hole symmetry. The case $N = 3$ is often a useful check on the results to be dervied below.

Scaling breaks down when D is roughly equal to either $|E_{21}(D)|$ or $N\Delta_0$ (or to temperature T). Suppose the first such crossover as D is reduced is when $E_{21}(D) = D >> N\Delta_0$ i.e. when $D = T^*$ where

$$T^* = E_{21}(D_0) + (N-3)\frac{\Delta_0}{\pi} \ln \frac{D_0}{T^*} \qquad (64)$$

T^* is undefined up to a number multiplying D_0 inside the log in (84); The number can be obtained by matching perturbation series for temperatures above and below T^* and is universal when $N\Delta_0 << T^* << D_0$ [22]. In this regime, as we will see below, the f-occupation n_f is close to 1, and if the bandwidth is reduced further below T^*, the scaling relations change. As E_{21} is now larger than D, a Schrieffer-Wolff transformation can be made, to obtain an effective interaction which is

$$H_{cs} = -J \sum_{\substack{kk' \\ mm'}} c^+_{k'm'} c_{km} \left(f^+_m f_{m'} - \frac{1}{N} \delta_{mm'} \sum_{m''} f^+_{m''} f_{m''} \right) \qquad (85)$$

the usual Coqblin-Schrieffer Hamiltonian [2], plus a potential scattering term which can be neglected. The parameters are now that the initial bandwidth is T^* while $\rho J = -\Delta_0/\pi T^*$. The new Hamiltonian is governed by the scaling equation of the Coqblin-Schrieffer Hamiltonian [23], mentioned earlier, and gives rise to a single invariant energy scale which is now given by

$$T_K = T^* \left(\frac{N\Delta_0}{\pi T^*}\right)^{1/N} \exp\left(-\frac{\pi T^*}{N\Delta_0}\right)$$

$$= D_0 \left(\frac{N\Delta_0}{\pi D_0}\right)^{1/N} \left(\frac{T^*}{D_0}\right)^{2(1-\frac{2}{N})} \exp\left(-\frac{\pi E_{21}(D_0)}{N\Delta_0}\right) \qquad (86)$$

on using (84). We conclude that, at least over some range of values $E_{21}^* >> N\Delta_0$, the groundstate of $H_{SU(N)}$ is a singlet, with magnetic susceptibility χ and linear coefficient of specific neat γ proportional to the inverse of (86). The point to note is the factor

$$(T^*/D_0)^{2(1-\frac{2}{N})} \qquad (87)$$

in (86) which would not be present if the f^2 level was replaced by an f^0 level at the same energy difference from E_1, and Δ_0 and D_0 were unchanged, which would be the usual Ce-like $U = \infty$ Anderson moel. Note also that the factor (87) survives in the $N \to \infty$ limit (taken with $N\Delta_0$ fixed).

Now suppose instead that we are in the opposite regime, where the first crossover is when $-E_{21}(D) = D >> N\Delta_0$, i.e. where $D = \tilde{T}$ where

$$-\tilde{T} = E_{21}(D_0) + (N-3)\frac{\Delta_0}{\pi} \ln \frac{D_0}{\tilde{T}} \quad . \tag{88}$$

The low-temperature f-occupation n_f is now close to 2 and a Schrieffer-Wolff transformation can again be made to obtain Hamiltonian (85) with $n_f = 2$, with bandwidth $\tilde{T}$ and $\rho J = -\Delta_0/\pi\tilde{T}$. For this model the scaling equation is the same as for the $n_f = 1$ case, and it again scales into a singlet, Fermi liquid ground state, as may be seen by applying Nozières-Blandin-type arguments [8] for the stability of the strong-coupling fixed point (indeed, this conclusion, for each integer value of n_f in H_{cs} , seems to have been reached by Nozières and Blandin themselves; see footnote on p.209 of their paper).

Then χ at $T = 0$ and γ are given by the inverse of

$$T_k = \tilde{T}\left(\frac{N\Delta_0}{\pi\tilde{T}}\right)^{1/N} \exp\left(-\frac{\pi\tilde{T}}{N\Delta_0}\right)$$

$$= D_0\left(\frac{N\Delta_0}{\pi D_0}\right)^{1/N}\left(\frac{\tilde{T}}{D_0}\right)^{2/N} \exp\left(\frac{\pi E_{21}}{N\Delta_0}\right) \tag{89}$$

In this case, the $\tilde{T}/D_0$ prefactor tends to unity as $N \to \infty$.

We have now shown that the groundstate of H_{cs} is a singlet with Fermi liquid properties whether $|E_{21}|$ is larger or smaller than D_0 , provided in the latter case that $|E_{21}^*| >> N\Delta_0$. The

remaining possibility, where the latter condition is not satisfied, is that the first crossover occurs when $D \simeq N\Delta_0$. In this case we expect that the system scales directly into a strongly mixed-valent ($n_f \simeq 3/2$) singlet, Fermi liquid ground state. This conclusion is plausible since this case lies between two limiting cases which are both singlets. It may also be possible to show that a *mixed-valent* strong coupling regime ($D \ll N\Delta_0$) exists and is a stable fixed point in the renormalization group sense [26] analogous to the strong coupling fixed points of the Kondo regimes [25]. In this regime, X and γ will be proportional to the inverse of an energy of the order of $N\Delta_0$.

For the special case $N = 3$, the logarithmic corrections in (84) and (88) vanish, so that $\tilde{T}$ or T^* are given by $|E_{21}|$ in the respective regimes, while

$$T_k = |E_{21}| \left(\frac{3\Delta_0}{\pi |E_{21}|} \right)^{1/3} \exp\left(-\frac{\pi |E_{21}|}{3\Delta_0} \right) \quad (90)$$

for either limiting case, which again shows the particle-hole symmetry for $N = 3$. We see that the bandwidth drops out of thermodynamic quantities, for $T \ll D$ in this model.

We may also obtain from the scaling transformation, with little extra work, the deviation of n_f from 1 or 2 due to valence fluctuations to leading order in Δ_0 .

As in Haldane [7], the transformation that leads to (78) and (79) also renormalises each of the two valence configurations by mixing them with the other configuration plus an electron or hole within δD of the band edge, as in Fig. 3.3. The renormalised states take the form:

$$|\widetilde{f^1,m}\rangle = |f^1,m\rangle - \sum_{\substack{D-\delta D<|\varepsilon_k|<D \\ m'\neq m}} \frac{V}{|\varepsilon_k|} c_{km'}|f^2,mm'\rangle \tag{91}$$

$$|\widetilde{f^2,m_1m_2}\rangle = |f^2,m_1,m_2\rangle - \sum_{D-\delta D<|\varepsilon_k|<D} \frac{V}{|\varepsilon_k|}\left(c^+_{km_1}|f^1,m_2\rangle - c^+_{km_2}|f^1,m_1\rangle\right)$$

Scaling of these states effectively stops when a crossover $|E_{21}(D)| \simeq D$ takes place, and the system is frozen into one or other renormalized configuration. The actual occupation is then found from (91) by taking matrix elements of n_f and integrating down to T^* or $\tilde{T}$ (neglecting $O(\Delta_0/D_0)$), and is

$$n_f = 1 + (N-1)\frac{\Delta_0}{\pi T^*} \tag{92}$$

or

$$n \quad n_f = 2 - \frac{2\Delta_0}{\pi \tilde{T}} \tag{93}$$

respectively, up to corrections of order Δ_0^2. At very low temperatures ($T \lesssim T_n$) there will also be terms of order $T_k/N\Delta_0$, but these are dominated by (92) or (93) when T^* or $\tilde{T} >> N\Delta_0$. Typically, in either limit (n_f close to 1 or 2) quantities involving charge fluctuations, for example the f occupation or the charge susceptibility are governed by the "charge fluctuation energy scale" T^* or $\tilde{T}$, as appropriate, while quantities involving spin fluctuations are governed by the "spin fluctuation energy" T_k, as in the case of spin susceptibility χ. Only when $|E^*_{21}| \lesssim N\Delta_0$ ($n_f \simeq 3/2$) can

there be a single energy governing both change and spin effects.

All the above conclusions for fluctuations between states with one or two f electrons, each carrying angular momentum j , and no $\underline{j} \cdot \underline{j}$ coupling can be generalised to fluctuations between states with n and n + 1 f electrons ($0 \leq n \leq N - 1$) . We give only the generalization of (81):

$$E_{n+1,n}(D) = E_{n+1,n}(D_0) + \left(N-(2n+1)\right)\frac{\Delta_0}{\pi}\ln\frac{D_0}{D} \qquad (94)$$

For example, for the case n = 2 , which may be relevant to the light actinides, we find that the particle-hole symmetric case where the log corrections disappear is N = 5 .

Now we approach the Hamiltonian H_{jj} in which an infinite, ferromagnetic coupling of the form $\underline{j} \cdot \underline{j}$ between f electrons has been added to (76). In the Kondo regimes $|E_{21}| >> D$ of this model the *most general* Kondo Hamiltonian consistent with rotational symmetry has 2j [8] coupling constants for spin-flip type terms, whether we consider the f^1 case or the f^2 case, and so the general scaling equations are complex. The Schrieffer-Wolff transformation picks out a single line in the space of coupling constants as possible initial values of the couplings, and the Kondo temperature must be found by integrating the general scaling equations along a trajectory intersecting the physical line, a calculation we have not attempted. Therefore, in this thesis we consider only the simpler Haldane scaling regime.

We first evaluate the self energy Fig. 3.3b for an electron within δD of the band edge, using the matrix elements in (48). Here the initial (doubly occupied) f state has total angular momentum J = 2j - 1 (= 6 for Tm where j = 7/2) and

$J_Z = \mu$, say. Then use of the completeness relation

$$\sum_{mm'} |\langle J,\mu | jj\, m m'\rangle|^2 = 1 \tag{95}$$

gives for the lowering of E_2 ,

$$2\rho V^2 \delta D/D \tag{96}$$

That the factor is 2 (because we included $\sqrt{2}$ in (48)) as for the case of $H_{SU(N)}$ is verification of the matrix elements in (48), as we explain below.

To evaluate Fig. 3.3a we rewrite the Clebsch-Gordan coefficients as

$$\langle J,\mu | jj\, m m'\rangle = \sqrt{\frac{2J+1}{2j+1}}\, \langle J j \mu, -m | j\, m'\rangle \tag{97}$$

and use now the completeness relation

$$\sum_{\mu,m} |\langle J j, \mu, -m | j\, m'\rangle|^2 = 1$$

and hence the lowering of E_1 is

$$\frac{2J+1}{\frac{1}{2}(2j+1)}\, \rho V^2 \frac{\delta D}{D} \tag{98}$$

The coefficients in (96) and (98) deserve some comment. Had the infinite Hund's rule coupling not been included, (98) would have included a sum over alternate integer values of J up to $J = 2j - 1$ and we would have recovered (78). The total number of f^2 states satisfying the Pauli principle is $\frac{1}{2}N(N-1)$; therefore we would

have had

$$N-1 = \frac{\frac{1}{2}N(N-1)}{\frac{1}{2}(2j+1)} \quad ; \tag{99}$$

we deduce that in (98) we have simply weighted the result (78) to account for the reduced number of possible f^2 states. However, (96) is the same as (79) since the initial f^2 state was assumed to be in the $J = 2j - 1$ manifold and there are then no further restrictions on the intermediate states.

Combining these coefficients we find for the scaling relation itself

$$E_{21}(D) = E_{21}(D_0) + 2\frac{(N-3)}{N}\frac{\Delta_0}{\pi}\ln\frac{D_0}{D} \tag{100}$$

For the Tm case $j = 7/2$, the log term in (100) has been multiplied by $1/4$. The charge fluctuation energies T^* or $\tilde{T}$ can now be deduced in analogy with (84) and (88). As discussed above, we cannot at present obtain the Kondo temperatures, as the Coqblin-Schrieffer formulas (86a), (89a) no longer apply. The only exception is the $N = 3$ case, where the Hund's rule coupling has no effect whatsoever. (100) may easily be generalized to H_{LS}, as the effect of the $j = 5/2$ conduction electrons is the same as that of the $j = 7/2$ electrons included above, and so the widths due to $V_{5/2}$ and $V_{7/2}$ add:

$$E_{21}(D) = E_{21}(D_0) + \frac{2(N-3)}{N}\left(\Delta_{5/2} + \Delta_{7/2}\right) \tag{101}$$

in an obvious notation.

For H_{jj} we expect the ground state to be a singlet much as for $H_{SU(N)}$, with similar Fermi liquid properties. For H_{LS}, however, if we consider arbitrary values of the ratio $V_{5/2}/V_{7/2}$ (strictly, if LS coupling is used, this ratio is fixed) then when $V_{5/2} \to 0$ we recover H_{jj}, but if $V_{7/2} \to 0$, we have coupling only to the $j = 5/2$ conduction electrons. We expect that this is not enough to screen the impurity moment. Two $j = 5/2$ holes have a moment of only $J = 5$ at most, while the f^2 state has $J = 6$, and so we cannot form a singlet variational state along the lines of Varma and Yafet. For general values of $V_{5/2}/V_{7/2}$, we must be in one regime or the other, suggesting that there must be a boundary separating the two cases. Hamiltonians lying exactly on this boundary may scale to a non-trivial fixed point, (rather than the $J = \infty$ strong coupling fixed point of the Kondo problem) analogous to that in the problem of the spin-$\frac{1}{2}$ Kondo impurity coupled equally to two spin-$\frac{1}{2}$ conduction band scattering channels [25, 8] where a non-trivial fixed point with non-trivial exponents appears (e.g. $\chi(T) \sim T^{1-\tau}$ as $T \to 0$, $\tau = \frac{4}{n+2}$ where n is the number of scattering channels). We do not know on which side of such a line Tm itself would lie. It is possible that the boundary line coincides with $V_{7/2} = 0$, in other words infinitesimal coupling to the $j = 7/2$ electrons is sufficient to give a singlet ground state; in this case Hamiltonians lying at $V_{7/2} = 0$ would scale to a degenerate groundstate, without the non-trivial fixed point. We suspect that, whether the latter possibility is in fact the case or not, the true Tm Hamiltonian lies on the same side of the boundary as H_{jj} and scales to a singlet ground state.

We now compare our results for $H_{SU(N)}$ from scaling theory with those obtained from mean field theory in the previous section.

Comparing (63) and (64) with the $N \to \infty$ limits of (86) and (89) we see that in the $n_f \simeq 2$ Kondo limit, the Kondo temperatures agree for large N :

$$T_K^{(2)} = D \exp\left(\frac{\pi E_{21}}{N\Delta_0}\right) \tag{102}$$

However, for $n_f \simeq 1$, the mean field theory fails to produce the extra prefactor in

$$T_K^{(1)} = D\left(\frac{T^*}{D}\right)^2 \exp\left(-\frac{\pi E_{21}}{N\Delta_0}\right) \tag{103}$$

From an examination of the diagrams of scaling theory we see that this factor is associated with the self energy of the f^1 state, which would appear as a fluctuation correction to the mean field theory. In fact, by comparing the Hamiltonian (49) with the analysis of Chapter 2 §3, and the following chapter, we see that the *two* bosons emitted at each hybridisation in (49), as opposed to one in the $U = \infty$ Anderson model, spoil the $1/N$ analysis, so that the mean field theory need not be the large-N limit.

Similarly, the results (92) and (93) for the valence show that the mean field theory is reasonable at large N near $n_f = 2$, since the power law term in (93), though dominating the exponential behaviour (71), is formally of order $1/N$. On the other hand, near $n_f = 1$, the power law term (92) is of order 1 , and so should be present in the leading-order-in-$1/N$ results, in addition to the mean field term (70).

We conclude that the mean field theory gives reasonable results for the large-N limit of $H_{SU(N)}$ near $n_f = 2$, but is quantitatively (but not qualitatively) wrong near $n_f = 1$.

REFERENCES

1. R.J. Elliott, "Rare Earth Metals", Plenum Press, 1972.
2. B. Coqblin and J.R. Schrieffer, Phys. Rev. *185* (1969) 847.
3. J.M. Lawrence, P.M. Riseborough and R.D. Parks, Rep. Prog. Phys. *44* (1981) 1.
4. A. Bringer and H. Lustfeld, Z. Physik B *28* (1977) 213.
5. L. Schiff, "Quantum Mechanics", 3rd Edition, (McGraw-Hill) p.440.
6. J.H. Van Vleck, "Theory of Electric and Magnetic Susceptibilities" (Oxford) 1932.
7. F.D.M. Haldane, Phys. Rev. Lett. *40* (1978) 416.
8. Ph. Nozières and A. Blandin, J. Physique (Paris) *41* (1980) 193.
9. K. Yamada, K. Yosida and K. Hanzawa, Prog. Theor. Phys. (Kyoto) *71* (1984) 450.
10. K. Yamada *et al.*, 4th International Conference on Valence Fluctuations, J. Magn. Magn. Materials, to be published.
11. O. Gunnarsson and K. Schönhammer, Phys. Rev. Lett. *50* (1983) 604; Phys. Rev. B *28* (1983) 4315.
12. E. Holland-Moritz, D. Wohlleben and M. Loewenhaupt, Phys. Rev. B *25* (1982) 7482, §4D.
13. Ch. Varma, Rev. Mod. Phys. *48* (1976) 219.
14. J. Mazzaferro, C.A. Balseiro and B. Alascio, Phys. Rev. Lett. *47* (1981) 274.
15. M. Loewenhaupt and E. Holland-Moritz, J. Appl. Phys. *50* (1979) 7456; Ref. 12 §4E; E. Holland-Moritz and M. Prager, J. Magn. Magn. Mats. *31-34* (1983) 395.
16. Ref. 12, §4A,C.

17. Ch. Varma and Y. Yafet, Preprint.

18. Y. Yafet and B. Jones, preprint.

19. See e.g. Schiff, ref. 5, p.434.

20. C. Kittel, "Introduction to Solid State Physics", (Wiley) 1976, p.442.

21. D. Langreth, Phys. Rev. *150* (1966) 712.

22. F.D.M. Haldane, J. Phys. C *11* (1978) 5015.

23. P. Schlottmann, Z. Phys. *51* (1983) 3.

24. H.R. Krishnamurthy, J.W. Wilkins and K. Wilson, Phys. Rev. B *21* (1980) 1003, 1044.

25. N. Andrei and C. Destri, Phys. Rev. Lett. *52* (1984) 364.
P.B. Wiegmann and A.M. Tsvelick, J.E.T.P. Lett. *38* (1983) 489; Adv. Phys. *32* (1983) 453.

CHAPTER 4. CORRECTIONS TO MEAN FIELD THEORY

§1. Expansion of Effective Action to Second Order

In this chapter we consider the effects of fluctuations about the mean field theory of Chapter 2. The expansion of the effective action S_{eff} of Chapter 2 about the stationary values of s_0 and λ and the evaluation of functional integrals over these fields generates a diagram expansion for the fluctuations in the Bose fields b and λ. We carry the expansion as far as the contribution of gaussian fluctuations in b (and b^+) to the free energy which we find to be correct to $O(1/N)$ in accordance with power-counting arguments (Chapter 2, §3). We also make use of the calculation of the fluctuations to prove a result concerning "perfect screening" of the quantum number Q carried by the quasiparticles; we find for *on shell* excitations that the change in Q on adding a quasiparticle to the system is zero. Finally we show that non-Gaussian fluctuations in the free energy are of higher order in $1/N$ and can be systematically classified in powers of $1/N$ according to the number of boson loops they contain, as in the simple power-counting in Chapter 2 §3. Fluctuations in λ are also discussed.

A technical aspect of the calculation, discussed more fully below, is the appearance of infrared-divergent integrals in some of the expressions. While divergences cancel in measurable quantities, they appear explicitly in certain (unmeasurable) symmetry breaking quantities, in particular the order parameter $\langle b \rangle$. We argue that in this way the symmetry broken by the mean field theory is restored by the fluctuations, though without affecting the attractive physical

picture of the resonant density of states obtained from the mean field theory.

Our starting point is eqns. (49-51) of Chapter 2 which we write, on defining

$$\sigma = Vb \tag{1}$$

as

$$Z = Z_0 \int_{-\pi/\beta}^{\pi/\beta} \frac{\beta d\lambda}{2\pi} \int \mathcal{D}\sigma \mathcal{D}\sigma^* \exp\left[-S_{eff}\right] \tag{2}$$

with

$$\begin{aligned} S_{eff}[\sigma(\tau), \sigma^*(\tau), \lambda] &= -N \mathrm{Tr} \ln\left[\frac{d}{d\tau} + \varepsilon_f + i\lambda - \sigma \sum_k \left(\frac{d}{d\tau} + \varepsilon_k\right)^{-1} \sigma^*\right] \\ &\quad + \int_0^\beta d\tau \left[\frac{1}{V^2} \sigma^* \left(\frac{d}{d\tau} + \varepsilon_f - E_0 + i\lambda\right)\sigma \right. \\ &\quad \left. - (\varepsilon_f - E_0 + i\lambda)\right] \end{aligned} \tag{3}$$

and

$$Z_0 = \exp N \mathrm{Tr} \sum_k \ln\left(\frac{d}{d\tau} + \varepsilon_k\right) \tag{4}$$

We have shifted $i\lambda$ by $\varepsilon_f - E_0$ so that the stationary point found in Chapter 2 occurs at $\lambda = 0$.

We now expand (3) to second order in the deviation of σ and σ^* from their stationary point values, which we take to be real and equal to s_0. The linear terms will vanish on account of the

stationarity condition to be imposed at each stage. Introducing the operators

$$G_f = \left(-\frac{d}{d\tau} - \varepsilon_f - s_0^2 G_k\right)^{-1}$$
$$G_k = \sum_k \left(-\frac{d}{d\tau} - \varepsilon_k\right)^{-1} \tag{5}$$

the expansion of the Tr&n expression in (3) yields the second order terms

$$N\,\mathrm{Tr}(\sigma - s_0) G_k (\sigma^* - s_0) G_f$$
$$+\frac{1}{2} N\,\mathrm{Tr}\Big\{\left[s_0 G_k(\sigma^* - s_0) + (\sigma - s_0) G_k s_0\right] G_f$$
$$\times \left[s_0 G_k (\sigma^* - s_0) + (\sigma - s_0) G_k s_0\right] G_f\Big\} \tag{6}$$

Each term in (6) can be represented as a diagram (Fig. 4.1). G_f, the f propagator, is represented by a double line, G_k by a single line and insertions of s_0 by a filled circle. Dashed lines indicate σ or σ^*; the arrow emerging *from* the diagram being a σ^* leg, the opposite a σ leg (thus arrows run continuously across an f - b vertex, corresponding to the conservation of Q by the hybridisation term).

Each trace in (6) is now to be evaluated as in Chapter 2 eqns. (53-6). We set

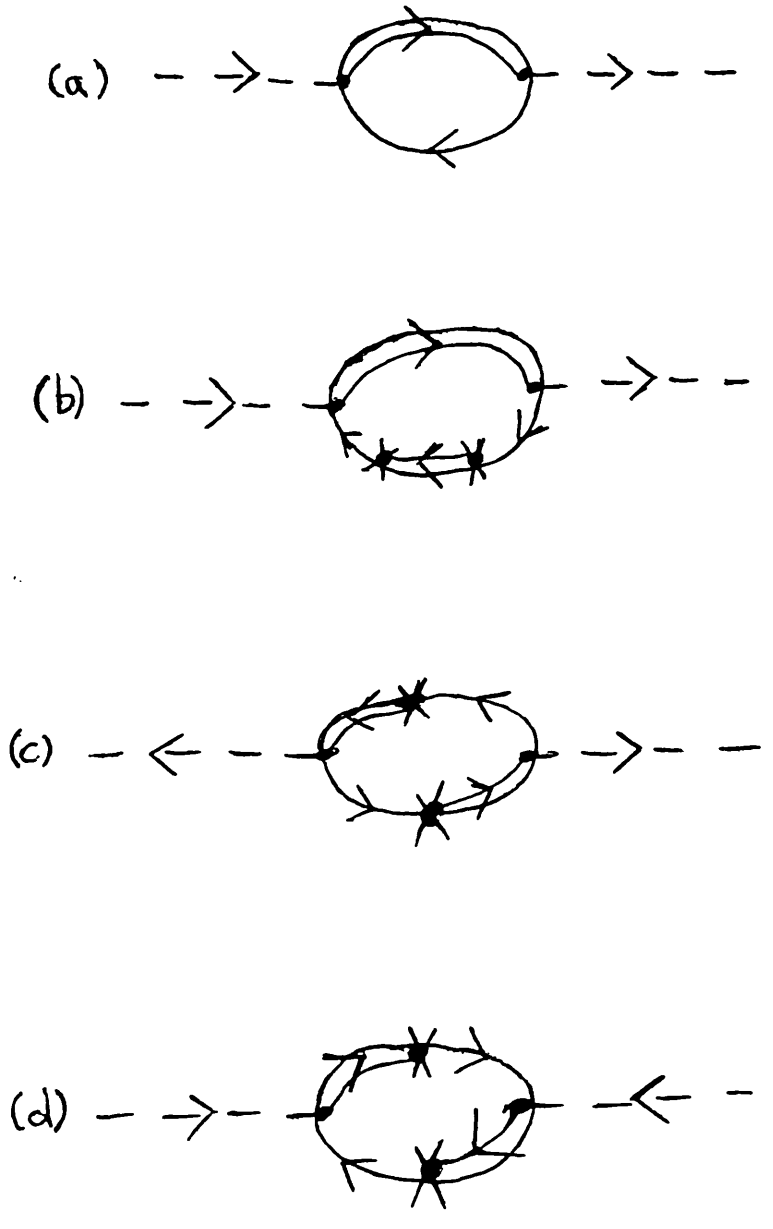


Fig. 4.1 Diagrams resulting from expansion of S_{eff} to second order in $\sigma(\omega)$, $\sigma^*(\omega)$.

$$\sigma(\tau) - s_0 = \frac{1}{\beta} \sum_{\omega_\nu} \sigma(\omega_\nu) e^{-i\omega_\nu \tau}$$

$$\sigma^*(\tau) - s_0 = \frac{1}{\beta} \sum_{\omega_\nu} \sigma^*(\omega_\nu) e^{-i\omega_\nu \tau} \qquad (7)$$

and work in the Fourier representation.

The first term in (6) (Fig. 4.1a) then gives the contribution to S_{eff}

$$N \mathrm{Tr}(\sigma - s_0) G_k (\sigma^* - s_0) G_f$$

$$= N \int_0^\beta d\tau \frac{1}{\beta^3} \sum_{\omega_n} \sum_{\substack{\omega_{\nu_1} \\ \omega_{\nu_2}}} \frac{\sigma(\omega_{\nu_1}) \sigma^*(\omega_{\nu_2}) e^{-i(\omega_{\nu_1} + \omega_{\nu_2})\tau}}{i\omega_n - \varepsilon - s_0^2 \sum_k \frac{1}{i\omega_n - \varepsilon_k}}$$

$$\times \sum_k \frac{1}{i\omega_n + i\omega_{\nu_2} - \varepsilon_k} \qquad (8)$$

Here $\omega_\nu = 2\pi\nu/\beta$ (for $\nu = \nu_1$ or ν_2), $\omega_n = (2n+1)\pi/\beta$ and n, ν_1, ν_2 are integers. We again approximate

$$\sum_k (i\omega - \varepsilon_k)^{-1} \simeq -i\pi\rho \,\mathrm{sgn}\, \omega \qquad (9)$$

as in Chapter 2 eq. (57). The integral over τ can be done yielding a Kronecker delta, thus eliminating a Bose frequency sum, so that we can write (8) as

$$\frac{1}{\beta} \sum_{\omega_\nu} \sigma^*(-\omega_\nu) \sigma(\omega_\nu) \Gamma^{(1)}(i\omega_\nu) \qquad (10)$$

where

$$\Gamma^{(1)}(i\omega_\nu) = N\frac{1}{\beta}\sum_{\omega_n}\frac{-i\pi\rho\,\mathrm{sgn}(\omega_n-\omega_\nu)}{i\omega_n-\varepsilon_f+i\Delta\,\mathrm{sgn}\,\omega_n}$$

$$=\frac{-N}{2\pi i}\int d\varepsilon f(\varepsilon)\frac{-i\pi\rho\,\mathrm{sgn}(\mathrm{Im}\varepsilon-\omega_\nu)}{\varepsilon_f-\varepsilon_f+i\Delta\,\mathrm{sgn}\,\mathrm{Im}\varepsilon} \tag{11}$$

Here $f(\varepsilon) = (e^{\beta\varepsilon}+1)^{-1}$ is the Fermi function and the contour C surrounds the imaginary ε axis. The integrand of (11) has cuts at $\mathrm{Im}\,\varepsilon = 0$ and $\mathrm{Im}\,\varepsilon = \omega_\nu$. The contour C and the cuts are shown in Fig. 4.2. We may now distort the contour to surround the cuts, yielding after some algebra the result at $T = 0$

$$\Gamma^{(1)}(i\omega_\nu) = \frac{1}{2}N\rho\ln\frac{\varepsilon_f^2+(|\omega_\nu|+\Delta)^2}{D^2}$$

$$-i\,\rho N\,\mathrm{sgn}\,\omega_\nu\left(\tan^{-1}\frac{|\omega_\nu|+\Delta}{\varepsilon_f}-\tan^{-1}\frac{\Delta}{\varepsilon_f}\right) \tag{12}$$

Here the inverse tangent is defined to lie in the range

$$0 \le \tan^{-1}x \le \pi$$

and we have assumed ε_f, Δ, $|\omega| \ll D$ in evaluating (12).

The results for the remaining diagrams Fig. 4.1 b-d at $T = 0$ are, for diagram (b)

$$\frac{1}{\beta}\sum_{\omega_\nu}\sigma^*(-\omega_\nu)\,\sigma(\omega_\nu)\,\Gamma^{(2)}(i\omega_\nu)$$

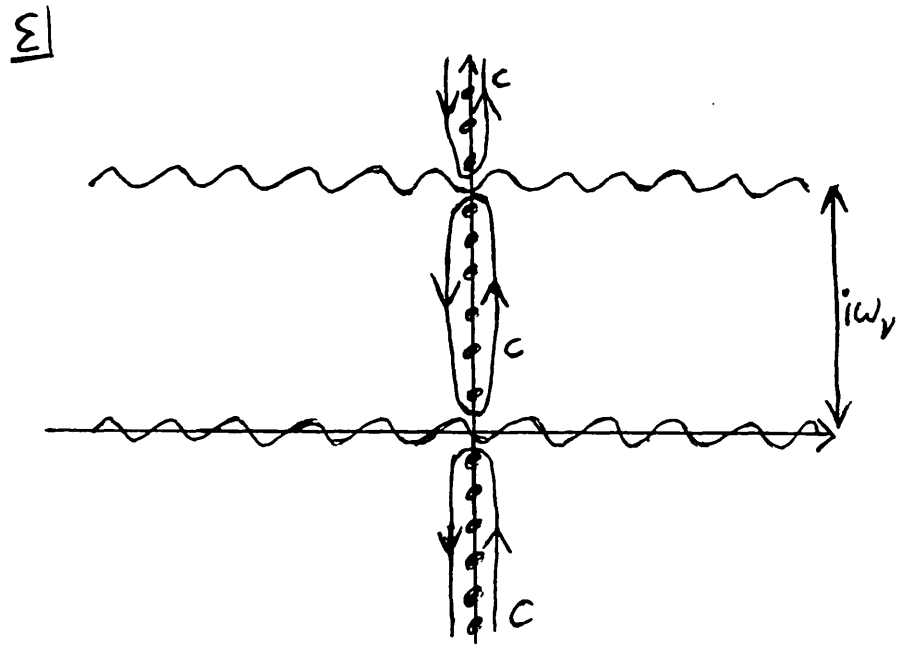


Fig. 4.2 Analytic structure and contour of eq. (11).

where

$$\Gamma^{(2)}(i\omega_\nu) = \frac{N\rho\Delta^2}{|\omega_\nu|(|\omega_\nu|+2\Delta)} \ln\left[1 + \frac{|\omega_\nu|(|\omega_\nu|+2\Delta)}{\varepsilon_f^2+\Delta^2}\right] \tag{13}$$

and for (c) and (d)

$$\frac{1}{2\beta}\sum_{\omega_\nu}\left(\sigma(-\omega_\nu)\sigma(\omega_\nu)+\sigma^*(-\omega_\nu)\sigma^*(\omega_\nu)\Gamma^{(3)}(i\omega_\nu)\right. \tag{14}$$

where

$$\Gamma^{(3)}(i\omega_\nu) = \frac{N\rho\Delta(|\omega_\nu|+\Delta)}{|\omega_\nu|(|\omega_\nu|+2\Delta)} \ln\left[1 + \frac{|\omega_\nu|(|\omega_\nu|+2\Delta)}{\varepsilon_f^2+\Delta^2}\right] \tag{15}$$

We note that (14) describes "anomalous" terms, where two σ lines enter or leave a Fermion loop, analogous to those in the theory of superfluidity, and resulting from the breaking of the symmetry in the mean field theory. However, neither $\Gamma^{(2)}$ nor $\Gamma^{(3)}$ needs to be included in the calculation of the correction to the free energy below, since the factors of Δ and Δ^2 in (13) and (15) compared with (12) make them of higher order in $1/N$ and so they can be ignored.

We then have finally for the second order terms in S_{eff},

$$S_{eff}^{(2)} = \frac{1}{\beta}\sum_{\omega_\nu}\sigma^*(-\omega_\nu)\sigma(\omega_\nu)\left(\frac{1}{V^2}\left(-i\omega_\nu+\varepsilon_f-E_0\right)+\Gamma^{(1)}(i\omega_\nu)\right) \tag{16}$$

§2. Corrections to Free Energy

It is now straightforward to do the complex Gaussian functional integral over $\sigma(\omega)$, $\sigma^*(\omega)$. The correction to the free energy, reinstating the normalization of $\sigma = Vb$, is

$$\Delta F = \frac{1}{\beta} \sum_{\omega_\nu} \ln \left[i\omega_\nu - \left(\varepsilon_f - E_0 + \frac{N\Delta_0}{\pi} \ln \frac{(\varepsilon_f^2 + \Delta^2)^{1/2}}{D} \right) \right.$$

$$\left. - \frac{N\Delta_0}{\pi} \ln \left(\frac{i\omega_\nu - \varepsilon_f + i\Delta \operatorname{sgn} \omega_\nu}{-\varepsilon_f + i\Delta \operatorname{sgn} \omega_\nu} \right) \right] \tag{17}$$

This represents the sum of the RPA-like diagrams shown in Fig. 4.3. Replacing the sum by a contour integral and bending the contour around the negative real axis gives, at $T = h = 0$,

$$\Delta F = \frac{-1}{2\pi i} \int_{-D}^{0} d\varepsilon \, 2i \tan^{-1} \left[\frac{\frac{N\Delta_0}{\pi} \left(\tan^{-1} \frac{\Delta}{\varepsilon_f - \varepsilon} - \tan^{-1} \frac{\Delta}{\varepsilon_f} \right)}{\varepsilon - \left(\varepsilon_f - E_0 + \frac{N\Delta_0}{\pi} \ln \frac{((\varepsilon - \varepsilon_f)^2 + \Delta^2)^{1/2}}{D} \right)} \right]$$

$$= \frac{N\Delta_0}{\pi} \int_{-D}^{0} d\varepsilon \, \frac{\Delta}{\pi} \left(\frac{1}{\varepsilon - \varepsilon_f} + \frac{1}{\varepsilon_f} \right) \left\{ \varepsilon - \left(\varepsilon_f - E_0 \right.\right.$$

$$\left.\left. + \frac{N\Delta_0}{\pi} \ln \left| \frac{\varepsilon - \varepsilon_f}{D} \right| \right\}^{-1} \right. \tag{18}$$

to leading order in $1/N$. We must now correct the self-consistent equations for ε_f and Δ by requiring the new free energy to be

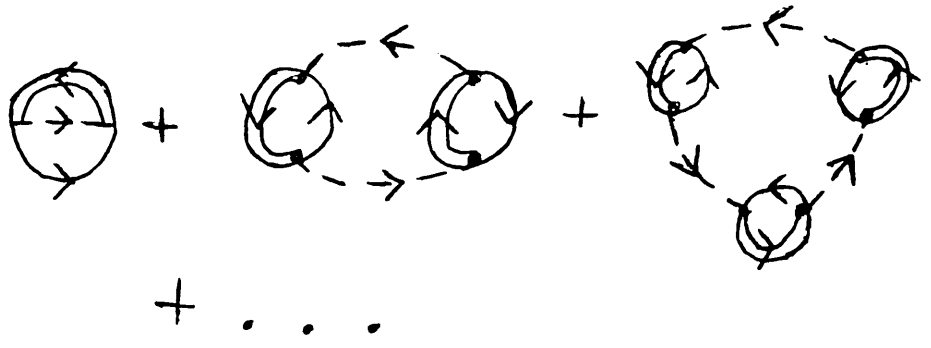


Fig. 4.3 RPA-like diagrams resulting from Gaussian functional integral over fluctuations in σ and σ^* .

stationary with respect to variations in ε_f and s_0. Differentiating with respect to ε_f yields

$$\frac{N}{\pi}\tan^{-1}\frac{\Delta}{\varepsilon_f}+\frac{\Delta}{\Delta_0}-1-\frac{N\Delta_0}{\pi}\frac{\Delta}{\pi}\int_{-D}^{0}d\varepsilon\left(\frac{1}{\varepsilon_f^2}-\frac{1}{(\varepsilon-\varepsilon_f)^2}\right)$$
$$\times\left(\varepsilon-\frac{N\Delta_0}{\pi}\ln\left|\frac{\varepsilon-\varepsilon_f}{\varepsilon_f}\right|\right)^{-1}$$
$$-\frac{N\Delta_0}{\pi}\frac{\Delta}{\pi}\int_{-D}^{0}d\varepsilon\left(\frac{1}{\varepsilon-\varepsilon_f}+\frac{1}{\varepsilon_f}\right)\left[-1+\frac{N\Delta_0}{\pi(\varepsilon-\varepsilon_f)}\right]\left\{\varepsilon-\frac{N\Delta_0}{\pi}\ln\left|\frac{\varepsilon-\varepsilon_f}{\varepsilon_f}\right|\right\}^{-2}$$
$$=0 \qquad (19)$$

The last integral is infrared divergent; we discuss this problem below. Differentiating with respect to Δ yields, to $O(1/N)$

$$\varepsilon_f-E_0+\frac{N\Delta_0}{\pi}\ln\frac{\varepsilon_f}{D}$$
$$+\frac{1}{N}\left(\frac{N\Delta_0}{\pi}\right)^2\int_{-D}^{0}d\varepsilon\left(\frac{1}{\varepsilon_f}+\frac{1}{\varepsilon-\varepsilon_f}\right)\left(\varepsilon-\frac{N\Delta_0}{\pi}\ln\left|\frac{\varepsilon-\varepsilon_f}{\varepsilon_f}\right|\right)^{-1}=0 \qquad (20)$$

Notice that Δ does not appear in this equation.

These equations are represented diagrammatically in Fig. 4.4, the first two terms in each case being the representation of the mean field theory only, the remainder the fluctuation corrections. Note that differentiation with respect to ε_f is represented by an external wavy leg, which is our symbol for a λ fluctuation. Likewise, differentiation with respect to s_0 corresponds to a σ (or σ^*) tadpole diagram as shown. Since

$$d\Delta=2\pi\rho s_0\,ds_0$$

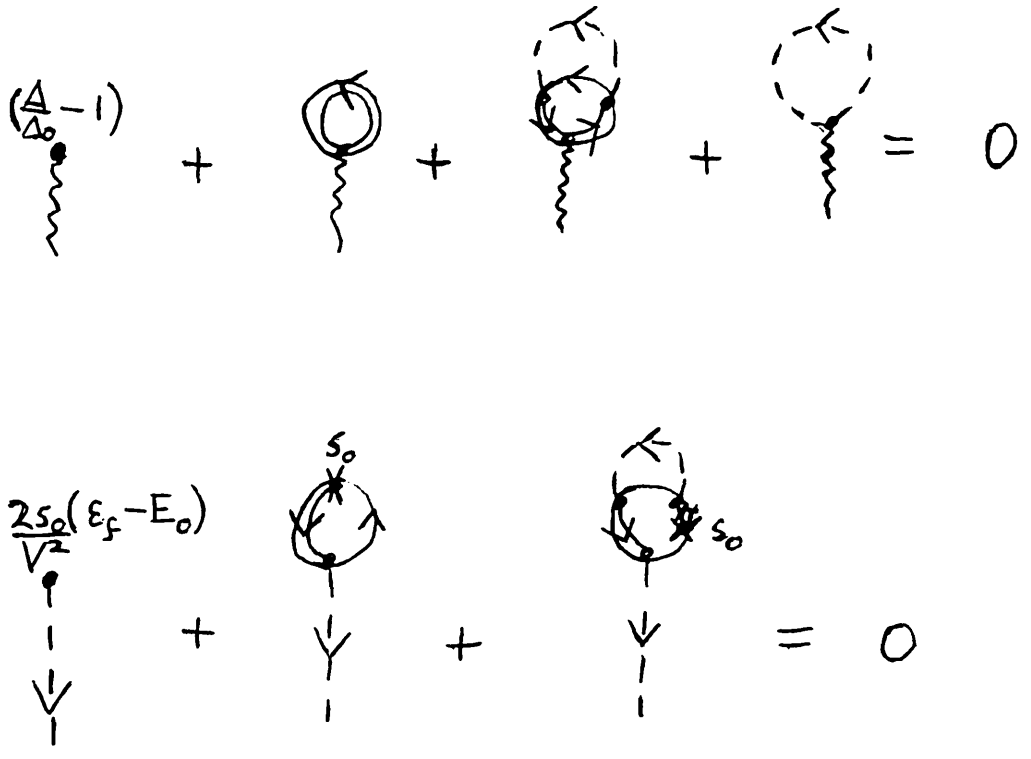


Fig. 4.4 Diagrammatic representation of equations (19) and (20) respectively. First two terms in each case are mean field result; rest are fluctuation corrections. Wavy line is a λ fluctuation, corresponding to differentiation with respect to ε_f .

equation (20) is then obtained by dividing the diagram by $2\pi\rho s_0$, and multiplying by Δ_0. There are no factors associated with the external legs, while the dashed internal line in each equation, representing a σ fluctuation, denotes the σ propagator which is the inverse of (16), namely

$$\langle \sigma^*(-\omega)\sigma(\omega)\rangle = \frac{-\beta V^2}{i\omega - \frac{N\Delta_0}{\pi} \ln \frac{i\omega - \varepsilon_f + i\Delta \operatorname{sgn}\omega}{-\varepsilon_f + i\Delta \operatorname{sgn}\omega}} \qquad (21)$$

correct to the order to which we said we were working in §1.

Incidentally, note that in the Kondo regime $n_f \to 1$ the spectral function corresponding to (21) has a broad peak (width $N\Delta_0$) at an energy which is the large positive root of

$$\varepsilon = \frac{N\Delta_0}{\pi} \ln \frac{\varepsilon - \varepsilon_f}{\varepsilon_f}$$

namely $\varepsilon \simeq \tilde{T}$, with

$$\tilde{T} = -E_0 + \frac{N\Delta_0}{\pi} \ln \frac{\tilde{T}}{D}$$

which, like $|E_0|$, is large compared with ε_f. This is the version of Haldane's charge fluctuation energy scale (see Chapter 1) appropriate to large N, showing up for the first time.

Using this diagrammatic representation, it is straightforward to check that the terms $\Gamma^{(2)}$ and $\Gamma^{(3)}$ which we ignored lead only to higher order (in $1/N$) corrections to the free energy and self-consistent equations.

Adding eq. (18) to the expression from mean field theory, Chapter 2 eq. (63), we see that most terms can be eliminated using (20) to leave for the ground state energy E_G ,

$$E_G = E_0 - \varepsilon_f + O\left(\frac{1}{N^2}\right) \tag{22}$$

where ε_f is given by (20). In this way we have avoided (19) with its infrared divergence for the time being. Eqs. (22) and (20) are the same as the recent work of Rasul and Hewson [1] who used a Goldstone diagram method to obtain the $1/N$ expansion.

We note here that our derivation is correct for the Anderson model with E_0 well inside the band; however for E_0 outside the band (E_0 larger than D) , which is the Kondo (Schrieffer-Wolff) limit, it is incorrect. A more careful evaluation of the fluctuation corrections in Fig. 4.4b starts with a double integral which is the same as Ref. [1b], eq. 2.11:

$$\varepsilon_f - E_0 + \frac{N\Delta_0}{\pi} \ln \frac{\varepsilon_f}{D}$$

$$+ \frac{1}{N}\left(\frac{N\Delta_0}{\pi}\right)^2 \int_{-D}^{0} \frac{d\varepsilon_1}{(\varepsilon - \varepsilon_f)^2} \int_{-D}^{0} \frac{d\varepsilon_2}{\varepsilon_1 + \varepsilon_2 - \frac{N\Delta_0}{\pi} \ln \left| \frac{\varepsilon_1 + \varepsilon_2 - \varepsilon_f}{\varepsilon_f} \right|}$$

$$= 0 \tag{23}$$

By shifting the ε_2 integral by ε_1 , and integrating by parts, one obtains the single integral in (20), plus a term which vanishes for large D and

$$\frac{1}{N}\left(\frac{N\Delta_0}{\pi}\right)^2 \int_{-D}^{0} \frac{d\varepsilon}{(\varepsilon-\varepsilon_f)\left(-D+\varepsilon-\frac{N\Delta_0}{\pi}\ln\left(\frac{D+|\varepsilon|+\varepsilon_f}{\varepsilon_f}\right)\right)} \tag{24}$$

When E_0 is inside the band, this term vanishes as $D \to \infty$. However, in the Schrieffer-Wolff limit, E_0 is much larger than D, and we may neglect $-D+\varepsilon$ compared with the log term. Then for large D, (24) is of order

$$-\Delta_0/\pi \tag{25}$$

which must be added to (20). For the other integrals encountered below, there are no such corrections.

Returning to the case of E_0 inside the band, 1/N corrections to n_f can now be obtained using the formula

$$n_f = \frac{dE_G}{dE_0}$$

from (20) and (22), giving after some algebra:

$$n_f = \frac{\mu}{1+\mu}\left(1 + \frac{\mu}{N(1+\mu)}\left(L_2 - \mu k - \frac{\mu}{1+\mu}L_1\right)\right)$$

$$L_p = \int_0^{D/T_A} \frac{dx}{(x+\mu\ln(1+x))}\left[1 - \frac{1}{(1+x)^p}\right]$$

$$k = \int_0^{D/T_A} \frac{dx}{(x+\mu\ln(1+x))^2}\frac{x^2}{(1+x)^2} \tag{26}$$

where

$$\mu = \frac{N\Delta_o}{\pi T_A}$$

and

$$T_A = E_o - \frac{N\Delta_o}{\pi} \ln \frac{T_A}{D} > 0$$

is the value of ε_f to leading order in $1/N$.

The result (26) is of course identical to that of Rasul and Hewson [1], who showed that it contains a power law correction to $1 - n_f$ as $n_f \to 1$ consistent with the form expected from scaling theory:

$$1 - n_f = \frac{\pi D}{N\Delta_o} \exp \frac{\pi E_o}{N\Delta_o} + \frac{\Delta_o}{\pi \tilde{T}} \qquad (27)$$

where $\tilde{T}$ is the large-N version of the charge fluctuation energy scale:

$$-\tilde{T} = E_o + \frac{N\Delta_o}{\pi} \ln \frac{D}{\tilde{T}} \qquad (28)$$

Note that while the "power law" term in (27) is formally of order $1/N$, as $E_0 \to -\infty$ it dominates the exponentially-small leading order term, a point emphasized by Schlottmann [2].

We can now obtain the $1/N$ corrections to Δ in closed form. Eq. (19) can be written to $O(1/N)$ using (20), (26) as

$$\frac{N\Delta}{\pi T_A} + \frac{\Delta}{\Delta_0} - 1 + \left(n_f - \frac{\mu}{1+\mu}\right)(1+\mu) + \frac{\mu^2}{N} I = 0$$

$$I = \int_{\Lambda}^{D/T_A} dx \, \frac{x}{1+x} \, \frac{1}{(x + \mu \ln(1+x))^2} \tag{29}$$

where an infrared cut-off Λ has been introduced.

Hence, rearranging (29)

$$\frac{\Delta}{\Delta_0} = 1 - n_f - \frac{\mu^2}{N(1+\mu)} I + O\left(\frac{1}{N^2}\right)$$

$$= (1 - n_f)\left(1 - \frac{\mu^2}{N} I\right) + O\left(\frac{1}{N^2}\right) \tag{30}$$

The infrared divergence due to I is

$$\frac{\mu^2}{N} \int_{\Lambda}^{\infty} dx \, \frac{x}{1+x} \, \frac{1}{(x + \mu \ln(1+x))^2} \sim -\frac{n_f^2}{N} \ln \Lambda \tag{31}$$

where the leading order result for n_f has been used. We will discuss the significance of (30) and (31) later.

§3. Corrections to χ and γ

We now turn to the calculation of $1/N$ corrections to the zero temperature magnetic susceptibility χ_0 and the linear coefficient of specific heat γ. The magnetic field h is introduced into the fermion bubble $\Gamma^{(1)}$ (eq. (11) and Fig. 4.1a) through the substitution $\varepsilon_f \to \varepsilon_f - hg\mu_B m$ in each angular momentum channel m :

$$\Gamma^{(1)}(i\omega_\nu;h,T) = \frac{1}{\beta}\sum_{m\omega_n} \frac{(-i\pi\rho)\,\mathrm{sgn}(\omega_n-\omega_\nu)}{i\omega_n-(\varepsilon_f-hg\mu_B m)+i\Delta\,\mathrm{sgn}\,\omega_n} \tag{32}$$

This can be evaluated to order h^2 and T^2 as

$$\Gamma(i\omega_\nu;h,T) = \Gamma(i\omega_\nu;h,T) + N\rho\left[\frac{-1}{(i\omega_\nu-\varepsilon_f+i\Delta\,\mathrm{sgn}\,\omega_\nu)^2}+\frac{2i\Delta\varepsilon_f\,\mathrm{sgn}\,\omega_\nu}{(\varepsilon_f^2+\Delta^2)^2}\right] \times\left(\frac{1}{6}j(j+1)(g\mu_B)^2h^2+\frac{\pi^2}{6}k_B^2T^2\right) \tag{33}$$

where $\Gamma^{(1)}(i\omega_\nu;0,0)$ was given in (12). The free energy correction (18) now becomes

$$\Delta F = -\int_{-D}^{D}\frac{d\varepsilon}{\pi}\,b(\varepsilon)\tan^{-1}\left[\frac{-V^2\,\mathrm{Im}\,\Gamma(\varepsilon+i0^+;h,T)}{\varepsilon-(\varepsilon_f-E_0+V^2\,\mathrm{Re}\,\Gamma(\varepsilon+i0^+;h,T)}\right] \tag{34}$$

where $b(\varepsilon) = (e^{\beta\varepsilon}-1)^{-1}$ is the Bose function. χ_0 and γ are obtained to order $1/N$ by differentiating the total free energy twice with respect to h or T respectively, neglecting the implicit dependence of ε_f and Δ on h and T as before. To pick up all terms of order $1/N$, it is essential to use the corrected ε_f and Δ, determined by (19) and (20), in the mean field terms (Chapter 2, Eqns. (82) and (87)); in calculating contributions from

ΔF , the leading order results (Chapter 2, Eq. (71)) can be used. It is easily verified that h^2 and T^2 terms in $\Gamma^{(1)}(\varepsilon)$ give rise to infrared divergent integrals when ΔF is differentiated; these divergences are cancelled by that in Δ , eq. (30), coming in through the leading order terms, as just mentioned. The results are

$$\chi_o = \frac{1}{3}(g\mu_B)^2 j(j+1)\frac{\mu}{T_A(1+\mu)}\left\{1 + \frac{\mu^2}{N(1+\mu)}\left[\frac{2(1+\mu)}{\mu}L_3 - L_2 - M - \left(2 - \frac{\mu}{1+\mu}\right)L_1\right]\right\}$$

$$\gamma = \frac{\pi^2 k_B^2}{3}\frac{\mu}{T_A(1+\mu)}\left\{1 + \frac{\mu^2}{N(1+\mu)}\left[\frac{2(1+\mu)}{\mu}L_3 - L_2 - M - \left(2 - \frac{\mu}{1+\mu}\right)L_1\right] + \frac{1}{N}\left(\frac{1}{(1+\mu)^2} - 1\right)\right\} \tag{35}$$

where

$$M = \int_0^{\Delta/T_A} dx \; \frac{x^2(2+\mu+x)}{(x+\mu\ln(1+x))^2}\,\frac{1}{(1+x)^3} \tag{36}$$

The result for χ_0 agrees with that of [1]. The result for γ contains an extra term not present in χ_0 , which we can rewrite as

$$\Delta\gamma = \frac{\pi^2}{3} k_B^2 \frac{n_f}{N T_A} \left[(n_f - 1)^2 - 1 \right] \tag{37}$$

(using the leading order result (Chapter 2, eq. (70)) for n_f) which originates from the Bose function in (34), using

$$\int_{-\infty}^{\infty} d\varepsilon\, b(\varepsilon) A(\varepsilon) = -\int_{-\infty}^{0} A(\varepsilon) d\varepsilon + \frac{\pi^2}{3} (k_B T)^2 A'(0) + O(T^4) \tag{38}$$

Hence the χ_0/γ ratio R (Chapter 2, eq. (89)) becomes

$$R = N/(N - 1 + (n_f - 1)^2) \tag{39}$$

We can also check the relation between χ_0, γ and the charge susceptibility χ_c found by Yoshimori [3], generalized to the spin-orbit coupled case treated here:

$$\gamma = \frac{\pi^2}{3} k_B^2 \left[\frac{1}{N} \chi_c + \frac{N-1}{N} \tilde{\chi} \right] \tag{40}$$

where

$$\chi_o = \frac{1}{3} j(j+1)(g\mu_B)^2 \tilde{\chi} \tag{41}$$

Using the large-N result for χ_c (Chapter 2, eq. (100))

$$\chi_c = \frac{\pi}{N\Delta_o} n_f^2 (1 - n_f) \tag{42}$$

we find that (40) is satisfied up to errors of order $1/N^2$.

The reduction (37) in γ by fluctuations in σ is highly significant, as it shows that, far from being extra degrees of freedom, these fluctuations describe the *removal* of degrees of freedom from the system. Now in the mean field theory, fluctuations in the occupation of each angular momentum channel in the resonance can occur, and contribute to γ. It is evident, however, because of the occupation restriction expressed by

$$Q \equiv n_f + b^+ b = 1$$

that fluctuations in the *total* occupation of the resonance should contribute little to γ as $n_f \to 1$ (the Kondo limit). Thus on specifying the occupation numbers of $N - 1$ channels, the last is fixed (for $n_f \simeq 1$) suggesting that in the Fermi liquid expression for γ the density of states in the resonance should be multiplied by $N - 1$, not N. Another way of expressing this is to say that the f-charge n_f associated with the (low energy) quasiparticles becomes small as $n_f \to 1$, a point we take up again in following sections. At small values of n_f, however, the f electrons are hardly sensitive to the occupation restriction (infinite interaction U) at all, since their density is low, and so

$$\gamma \propto N \rho_f(0) \tag{43}$$

with $\rho_f(0)$ having approximately the bare width Δ_0.

Note that our argument, supported by our $1/N$ calculation, predicts a reduction in γ, not an increase in χ_0 to enhance the χ_0/γ ratio (39). Simple Fermi liquid arguments ([4], see also [3]) seem to predict an enhancement of χ_0, but are nonetheless quite

compatible with ours, since strictly they give only R .

We now give for completeness some analysis of (35) for the Kondo limit, based on [1]. In this limit we let

$$\mu \to \infty$$

and in σ-fluctuation denominators keep only the log's, as we did in eq. (24), which is equivalent to working in the Schrieffer-Wolff limit,

$$-E_o \gg D$$

In this limit, we reinstate the term (25), and the integrals can be performed analytically [1]. One finds

$$\chi_o = \tfrac{1}{3} j(j+1)(g\mu_B)^2 \frac{1}{T_K}\left[1 - \frac{1}{N}(1 - C + \ln \rho J_o) + O\left(\frac{1}{N^2}\right)\right] \tag{44}$$

where as before

$$T_K = D \exp(-1/\rho J_o)$$

$$\rho J_o = \frac{N\Delta_o}{\pi |E_o|} \tag{45}$$

and C is Euler's constant. The log term in (44) is consistent with the expansion to O(1/N) of the exact scaling result for T_K ,

already used repeatedly in Chapter 3:

$$T_K^{(exact)} = D(\rho J_0)^{1/N} \exp(-1/\rho J_0) \tag{46}$$

Rasul and Hewson [1], by comparing with exact Bethe Ansatz results, argued conclusively that the other $1/N$ terms in (44) arise from the expansion to $O(1/N)$ of the expression:

$$e^{1/N}\ \Gamma\left(1+\frac{1}{N}\right) \tag{47}$$

where Γ is Euler's gamma function. They write the *exact* result for χ_0 as

$$\chi_0 = \frac{1}{3} j(j+1)(g\mu_B)^2 \frac{W(N)}{T_K^{(T=\infty)}} \tag{48}$$

where

$$T_K^{(T=\infty)} = \exp\left(1+C-\frac{1}{2N}\right) T_K^{(exact)} \tag{49}$$

is the Kondo temperature appearing in high temperature expansions, and

$$W(N) = \frac{\exp(1+C-3/2N)}{2\pi\,\Gamma(1+1/N)} \tag{50}$$

is a universal number (the Wilson number) for the limit $D \to \infty$ with T_K fixed, independent of the precise form of the cutoff. (50) is in very good agreement for $N = 2$ with the numerical result of Wilson [5], $W = 0.4128 \pm 0.002$.

For the Anderson model in the Kondo limit, (25) drops out, leading to the disappearance of $\exp(1/N)$ factors in (47); the term $\ell n\ \rho J_0$ becomes [1]

$$\ln \frac{N\Delta_o}{\pi D} \tag{51}$$

consistent with the result of scaling

$$T_K = D\left(\frac{N\Delta_o}{\pi D}\right)^{1/N} \exp \frac{\pi E_o}{N\Delta_o} \tag{52}$$

for the Anderson model. The universal number (50) is unchanged, as it should be, since $\exp(1/N)$ drops out [1] from the high temperature result (49) calculated in the local moment regime:

$$T_K \ll T \ll \tilde{T}$$

Finally in this section, we mention a slightly different way of calculating χ_0 or γ. One inserts (33) into (18) to obtain a version of (20) correct to order h^2 or T^2, giving ε_f as a function of h or T, and hence the free energy to order h^2 or T^2 replacing (22). χ_0 and γ are then obtained by differentiation, giving the same result as (35). This route is more like that of [1] but less like our Fermi liquid approach of Chapter 2. Conversely, n_f can be obtained by a method more like that of Chapter 2 by separating in (19) and Fig. 4.4 the expectation value of n_f onto one side (namely the second and third diagrams in Fig. 4.4a) and the expectation of $1 - b^+b$ onto the other (first and fourth diagrams in Fig. 4.4a). Equation (30) then appears directly and Δ can be eliminated from the remaining equation to give the explicit result (26) for n_f.

§4. Role of Infrared Divergences

We must now explain the meaning of equation (30). First let us recall that in assuming the non-zero expectation value

$$\langle b \rangle$$

(or s_0/V) we have broken the symmetry of the Hamiltonian under the simultaneous transformations:

$$f_m \to e^{i\theta} f_m \ , \ b \to e^{i\theta} b, \ c_{km} \to c_{km} \tag{53}$$

and their conjugates, where θ is an arbitrary real number. However in our low dimensional model, which is most closely analogous to a quantum field theory in only 1 spatial dimension, no continuous symmetry can be broken in the ground state, by the usual deep theorems [6]. This may seem to cast doubt on our mean field theory, which we wish to allay. Similar questions were raised by the large-N limit of the Gross-Neveu model [7] and were resolved by Witten [8] on whose ideas the following comments are closely based. Witten's solution of the problem is confirmed by the exact solution of the Gross-Neveu model [9] which is itself related to the Bethe Ansatz solution of the Coqblin-Schrieffer model, providing further support for our parallel with the Gross-Neven model.

Now in previous sections we have calculated $1/N$ corrections to n_f , χ_0 , γ and the ground state energy E_G due to fluctuations in σ . The σ propagator itself (21) has a pole at $\omega = 0$, which gives a $1/|\varepsilon|$ singularity in the spectral density at $\varepsilon = 0$. This pole is a direct consequence of symmetry breaking, as in Goldstone's theorem, as the symmetry guarantees that real transverse fluctuations

(i.e. those normal to <b>) can be made at low frequencies. The pole gives rise to the infrared divergence in (30). Had divergences appeared in the physical quantities calculated, n_f , χ_0 etc., we would have known that the mean field theory was wrong, and that the fluctuations were trying to produce a true ground state of a kind different from the mean field theory. We would at best have had a series to sum of divergent terms, perhaps finding a power law divergence of χ as $T \to 0$, or else we would have had to start again with another approach. In fact, we saw that divergences cancelled in the observable quantities, with physically satisfying results. This is evidence that we have not started in the wrong place in using the mean field theory as the basis of our expansion, with its Fermi liquid picture of the ground state and excitations.

Now we turn to eq. (30) itself, which was

$$\frac{\Delta}{\Delta_0} \equiv |\langle b \rangle|^2 = (1 - n_f)\left(1 + \frac{n_f^2}{N} \ln \Lambda\right) + O\left(\frac{1}{N^2}\right) \tag{54}$$

where we neglected regular terms coming from I and $\Lambda \to 0$ is the infrared cutoff. Following Witten we believe that higher order terms will sum into an exponential series of the form

$$|\langle b \rangle|^2 = \frac{\Delta}{\Delta_0} \sim c\, \Lambda^{n_f^2/N} \tag{55}$$

where c is some constant ($c = 1 - n_f$ to leading order in $1/N$) . This means that the symmetry is restored by the fluctuations, since now <b> tends to zero as $\Lambda \to 0$. In Witten's case the reason for the exponentiation of the series is that the *phase* of σ produces the infrared divergence, which can be exponentiated as the fluctuating phase is a free field (i.e. non-interacting):

$$\langle e^{i\theta(\tau)} \rangle = \exp\left(-\tfrac{1}{2}\langle \theta(0)\,\theta(0)\rangle\right)$$

$$\sim \Lambda^{\alpha/2} \qquad (56)$$

as $\Lambda \to 0$, for some $\alpha > 0$. This behaviour is characteristic of the two-dimensional XY model at low temperatures and we term it Kosterlitz-Thouless-like behaviour [10] (the vortex excitations of [10] seem not to appear in our problem).

While it is in effect the fluctuations in the phase of σ which produce the infrared divergences in our case also, we have preferred not to use an argument like (56) so far, as it would require a change to polar variables for σ which would be hard to justify properly.

In our case we have found that to order $1/N$ the exponent in (55) agrees with the Nozières-de Dominicis (ND) result [11] for the infrared exponent

$$\alpha = \sum \left(\frac{\delta}{\pi}\right)^2$$

when the Friedel sum rule [12] for the f phase shifts is used:

$$\alpha = N\left(\frac{n_f}{N}\right)^2 = \frac{n_f^2}{N} \qquad (57)$$

An analogous renormalized hybridization width which vanished like (55) with the ND exponent due to infrared effects was obtained by Hewson and Newns [13]. For the related problem of the "orthogonality catastrophe" (vanishing of the overlap of perturbed and unperturbed groundstates in models of impurities in a metallic host) Yamada and Yosida [14] have proved that it is governed by the ND exponent in

a number of situations involving general scattering potentials and/or interactions among the electrons. In view of the generality of (57), then, we think that (55) is likely to be exact. We disagree with the result of Coleman [15], found within the non-crossing approximation, where the exponent was independent of n_f.

To understand why the mean field theory can be physically correct, even though $\langle b \rangle$ vanishes, it is helpful to consider the b (or σ) correlation function

$$\langle T\sigma(\tau)\,\sigma^*(0)\rangle \tag{58}$$

True symmetry breaking would mean that this correlation function tends to a constant at large $|\tau|$:

$$\langle T\sigma(\tau)\sigma^*(0)\rangle \to |\langle b\rangle|^2 V^2 \tag{59}$$

In fact, as we have just shown (Eq. (55)) the right hand side of (59) vanishes. To find the actual τ-dependence of (58), we calculate the fluctuation corrections to the mean-field behaviour (59). Fluctuations in σ about s_0 have the propagator given by (21)

$$\langle \sigma^*(-\omega)\,\sigma(\omega)\rangle = \frac{-\beta V^2}{i\omega - \frac{N\Delta_{on}}{\pi}\left(\frac{i\omega - \varepsilon_f + i\Delta\,\mathrm{sgn}\,\omega}{-\varepsilon_f + i\Delta\,\mathrm{sgn}\,\omega}\right)} \tag{60}$$

plus corrections of order $1/N^2$. The inverse Fourier transform is infrared divergent because of the pole at $\omega = 0$ in (60), which results from the fluctuations transverse to $\langle b \rangle$, as a consequence of the symmetry (53). With the same cutoff Λ as before we obtain

$$\langle T\sigma(\tau)\sigma^*(0)\rangle \sim V^2|\langle b\rangle|^2 - V^2\frac{n_f^2}{N}(1-n_f)\ln(\Lambda T_A|\tau|) \tag{61}$$

as $|\tau| \to \infty$ and $\Lambda \to 0$. Using the result (54) for $|\langle b\rangle|^2$, the dependence on Λ is cancelled, and again assuming that the series exponentiates we find

$$\langle T\sigma(\tau)\sigma^*(0)\rangle \sim cV^2(T_A|\tau|)^{-\alpha} \tag{62}$$

where $c = 1 - n_f$ to leading order in $1/N$ as in (55).

The behaviour (62) is a key result. It shows that correlations in σ decay only slowly. We have argued above that only the phase of σ decays, while the correlation function for $|\sigma|$ presumably approaches a constant at large τ. In this situation, we may imagine that over moderately long times (of order T_A^{-1}) to very long times ($>> T_A^{-1}$), the electrons see the mean field value of σ, and respond as in the mean field theory. Thus the "almost long-range order" (62) (Kosterlitz-Thouless behaviour) accounts for the pleasing successes of the mean field theory. In particular, the elementary excitations (exact eigenstates of the many-body Hamiltonian) are expected to be fermions with a resonant density of states not too different from that in the mean field theory. The physical resonance width is non-zero, contrary to naive expectations from (55), since it is a physical quantity, and so infrared divergences must cancel whenever it is calculated, for example by deducing it from the $1/N$ corrected values of χ_0 or γ via Fermi liquid arguments. The quantity Δ, as it appears for example in (30), is merely a parameter of our theory and cannot be identified with the physical resonance width except in the mean field theory.

Corroboration for our picture of the elementary excitation spectrum comes from the Coqblin-Schrieffer model (the limit $-E_0 >> D$ of our model). Here the exact excitation spectrum can be obtained analytically from the exact solution [16] and is found (neglecting bound states of fermions and density modes) to have an exactly Lorentzian density of states, with the density of states at the Fermi energy agreeing with the Fermi liquid interpretation of the thermodynamics [17].

A similar relation between a physically reasonable mean field theory for a fermion system, and power law decay of correlations occurs in a solid state context in the study of the one dimensional interacting electron gas (for a review, see [18]). Indeed, a special case is the "backscattering model", which is identical to the Gross-Neveu model. More generally, various phases (e.g. antiferromagnetic, superconducting) can occur in which a mean field theory yields a physically reasonable description, but the order parameter (e.g. Cooper pair density) vanishes because of symmetry while the correlation function (e.g. for Cooper pairs) decays as a power law at large distances. Haldane [19] has argued, for systems without a gap in the excitation spectrum, that these decays are characteristic of one dimension, and that the exponents are universally related to a small number of parameters (such as velocities of collective modes).

To return to the Anderson model, if as we have argued, the exact quasiparticle excitations have a resonant density of states with finite width, their symmetry properties must be different from those of the bare fields (53), again as argued by Witten. If the quasiparticle excitations (whose exact creation operators we do not know) transformed like the bare fields (53), then a hybridisation term in their effective low-energy Hamiltonian would always be impossible, as

it would break the symmetry. Therefore, the f quasiparticle states must carry zero $Q = n_f + b^+b$, since Q is the generator of the symmetry (53). It is remarkable that this requirement is in fact satisfied, as far as on-shell matrix elements are concerned, even by the mean field theory, thanks to a kind of "perfect screening" effect of the transverse fluctuations in σ. The proof of this, based on an argument by Berg and Weisz, [20], is given in the next section.

§5. Quantum Numbers of Elementary Excitations

In this section we prove the result mentioned previously that in the mean field theory, properly interpreted, the quasiparticle excitations carry zero quantum number $Q = n_f + b^+b$. Since the result concerns *on shell* matrix elements, we require knowledge of the exact eigenstates of the quasiparticle (mean field) Hamiltonian H_{qp}, in zero magnetic field:

$$H_{qp} = \sum_{km} \varepsilon_{km} c_{km}^+ c_{km} + \sum_m \varepsilon_f f_m^+ f_m + s_0 \sum_{km} \left(c_{km}^+ f_m + f_m^+ c_{km} \right) \tag{63}$$

Defining one electron states

$$|f\rangle = f_m^+ |0\rangle$$

$$|k\rangle = c_{km}^+ |0\rangle \tag{64}$$

where $|0\rangle$ is the zero electron state of (63), the eigenstates are created by

$$c_{\mu m}^{+} = \sum_{k} \langle k|\mu\rangle c_{km}^{+} + \langle f|\mu\rangle f_{m}^{+} \tag{65}$$

in an obvious notation. As the index m is conserved throughout, it is dropped in labelling the states. On requiring (65) to create eigenstates of (63), we find

$$\langle k|\mu\rangle = \frac{s_0}{\varepsilon_\mu - \varepsilon_f} \langle f|\mu\rangle \tag{66}$$

$$\varepsilon_\mu - \varepsilon_f = s_0^2 \sum_{k} \frac{1}{\varepsilon_\mu - \varepsilon_k} \tag{67}$$

where

$$H_{qp} = \sum_{\mu m} \varepsilon_\mu c_{\mu m}^{+} c_{\mu m} \quad .$$

The eigenvalue equation (67) is best interpreted using a discrete set of energies ε_k, in which case one root ε_μ lies between each pair of ε_k's, and one extra root lies outside the ε_k's at each end of the spectrum, giving the required total number of ε_k. The normalisation is

$$|\langle f|\mu\rangle|^2 = \left(1 + s_0^2 \sum_{k} \frac{1}{(\varepsilon_\mu - \varepsilon_k)^2}\right)^{-1} \tag{68}$$

We introduce many-particle states by filling the states (65) up to the Fermi energy, and calling the (normalized) ground state of (63)

$$|\phi\rangle$$

with parameters as calculated in Chapter 2. Now defining

$$|\phi,\mu\rangle = c^{+}_{\mu m}|\phi\rangle \tag{69}$$

etc., the overlaps are

$$\langle\phi,f|\phi,\mu\rangle = \langle f|\mu\rangle$$

$$\langle\phi,k|\phi,\mu\rangle = \langle k|\mu\rangle$$

The result we are to prove is, for ε_μ , $\varepsilon_{\mu'} > 0$

$$\langle\phi,\mu'|\,Q(\omega)|\phi,\mu\rangle = \langle\phi|\,Q(0)|\phi\rangle\,\delta_{\mu\mu'} \tag{70}$$

when $i\omega = \varepsilon_{\mu'} - \varepsilon_\mu$, together with the corresponding results for hole-hole matrix elements, and for Q acting on $|\phi\rangle$ to create a particle and hole. (70) means that on-shell matrix elements of Q are zero, apart from the ground state term (which is constrained to be 1) ; we drop this groundstate term hereafter. The "proper interpretation" of mean-field theory, mentioned above, means the inclusion of all diagrams of the form shown in Fig. 4.5. Here the wavy line means the insertion of $Q(\omega)$. Apart from the naive term (a), they include the "screening" effect of the σ propagator in diagrams (b) to (e). The screening turns out to be exact, giving result (70).

In this derivation we only use the leading order σ propagator, eq. (21) for the dashed lines in Fig. 4.5. As mentioned after

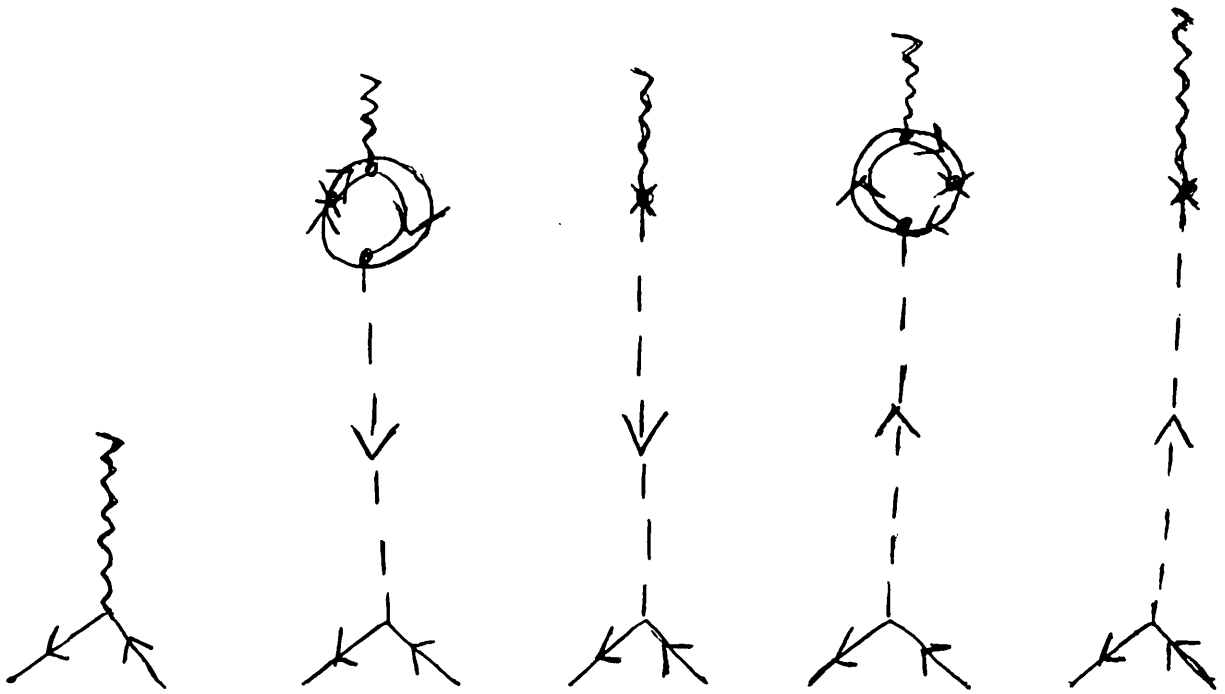


Fig. 4.5 Diagrams contributing to matrix elements of Q to leading order in $1/N$: wavy line represents insertion of $Q(\omega)$.

eq. (15), there are other terms in the expansion of S_{eff} to second order in σ , σ^* , which are higher order in $1/N$ (Fig. 4.1 b-d) these include "anomalous" terms proportional to $\sigma(-\omega)\sigma(\omega)$ and its conjugate. These terms give rise to corrections to (21) of order $1/N^2$ and to an "anomalous" propagator $\langle\sigma(-\omega)\sigma(\omega)\rangle$ of order $1/N^2$. When these corrections are included in Fig. 4.5, the cancellation of diagrams of the form shown is exact for any N .

The contribution of diagram (a) is just the naive matrix element,

$$\langle \mu' | Q(\omega) | \mu \rangle = \langle \mu' | f \rangle \langle f | \mu \rangle \tag{71}$$

as $Q = n_f + b^+ b$.

Fig. 4.5 (b) and (d) involve a fermion loop, which for diagram (b) is

$$\Gamma^{Q\sigma}(i\omega) = \frac{N}{\beta} \sum_{\omega_n} \frac{s_0(-i\pi\rho \operatorname{sgn} \omega_n)}{(i\omega_n + i\omega - \varepsilon_f + i\Delta \operatorname{sgn}(\omega_n+\omega))(i\omega_n - \varepsilon_f + i\Delta \operatorname{sgn} \omega)}$$

$$= -\frac{N\rho s_0}{i\omega}\left(\frac{|\omega|}{2(|\omega|+2\Delta)} \ln\left(1 + \frac{|\omega|(|\omega|+2\Delta)}{\varepsilon_f^2 + \Delta^2}\right)\right.$$

$$\left. - i \operatorname{sgn} \omega \left(\tan^{-1}\frac{|\omega|+\Delta}{\varepsilon_f} - \tan^{-1}\frac{\Delta}{\varepsilon_f}\right)\right) \tag{72}$$

at $T = 0$. To be consistent with our use of only the leading order σ propagator, we drop Δ (which is order $1/N$) in the prefactor of

the first term to give

$$\Gamma^{Q\sigma}(i\omega) = -\frac{N\rho s_0}{i\omega} \ln\left(\frac{i\omega - \varepsilon_f + i\Delta \operatorname{sgn}\omega}{-\varepsilon_f + i\Delta \operatorname{sgn}\omega}\right) \tag{73}$$

If this approximation is not made, the extra contributions cancel when the non-leading terms in $\langle\sigma^*(-\omega)\sigma(\omega)\rangle$ and $\langle\sigma(-\omega)\sigma(\omega)\rangle$, and its conjugate, are included, as mentioned above. The fermion loop in Fig. 4.5(d) gives $\Gamma^{Q\sigma}(-i\omega)$.

Diagrams (c) and (e) involve the direct coupling of Q to σ, through

$$b^+b = \frac{s_0^2}{V^2} + (\sigma^* - s_0)\frac{s_0}{V^2} + (\sigma - s_0)s_0/V^2 + (\sigma^* - s_0)(\sigma - s_0)/V^2 \tag{74}$$

Thus the linear coupling of Q to σ or σ^* fluctuations about s_0 is s_0/V^2. Diagrams (b) and (c) add to give

$$-\left(\frac{s_0}{V^2} + \Gamma^{Q\sigma}(i\omega)\right)\frac{1}{\beta}\langle\sigma^*(-\omega)\sigma(\omega)\rangle\sum_k \langle\mu'|f\rangle\langle k|\mu\rangle \tag{75}$$

the minus arising from the coupling of σ to $f_m^+ c_{km}$. Diagrams (d) and (e) give similarly

$$-\left(\frac{s_0}{V^2} + \Gamma^{Q\sigma}(-i\omega)\right)\frac{1}{\beta}\langle\sigma^*(\omega)\sigma(-\omega)\rangle\sum_k \langle\mu'|k\rangle\langle f|\mu\rangle \tag{76}$$

Using (21) and (66), we have

$$\langle \mu' | f \rangle \langle f | \mu \rangle \left(1 - \frac{S_0^2}{i\omega} \sum_k \frac{1}{\varepsilon_{\mu'} - \varepsilon_k} + \frac{S_0^2}{i\omega} \sum_k \frac{1}{\varepsilon_\mu - \varepsilon_k} \right)$$

$$= \frac{\langle \mu' | f \rangle \langle f | \mu \rangle}{\varepsilon_{\mu'} - \varepsilon_\mu} \left(\varepsilon_{\mu'} - \varepsilon_f - S_0^2 \sum_k \frac{1}{\varepsilon_{\mu'} - \varepsilon_k} - \left(\varepsilon_\mu - \varepsilon_f - S_0^2 \sum_k \frac{1}{\varepsilon_\mu - \varepsilon_k} \right) \right) \tag{77}$$

on continuing to $i\omega = \varepsilon_{\mu'} - \varepsilon_\mu \neq 0$. Using (67) this is zero.

When $\mu = \mu'$ this argument breaks down, as the matrix elements for coupling of $|\mu\rangle$ to the transverse σ mode, which appear in (77), cancel before the limit $\omega \to 0$ is taken. Instead their place is taken by the fluctuation in λ which exists only at $\omega = 0$, by definition (see eq. 2). The corresponding diagrams are used, involving longitudinal fluctuations in σ , λ , and their cross terms. In fact, at $\omega = 0$, the cancellation of diagrams takes place even off-shell.

Thus we have shown that matrix elements of $Q(\omega)$ between quasi-particle excitations are zero in the large N limit. At finite N , the diagrams of the type shown still cancel, as stated above, though we have not attempted higher order calculations, involving fermion self energies, vertex corrections, etc. The cancellation is the result of a gauge property, as the "screening" effect in (77) is due to the fluctuations transverse to $\langle b \rangle$ (i.e. in the phase of σ) which couple to Q through gauge transformation, (see Chapter 2 § 2), guaranteeing the cancellation of numerator and denominator in (75) and (76) apart from the factors left in (77). The result is therefore exact also at finite temperatures and magnetic fields. Similarly, though we calculated the fermion loops in (12) and (73) for a constant density of k states, the result (70) holds for

arbitrary density of states.

As a further corollary, we may omit diagrams (c) and (e) to study matrix elements of $n_f(\omega)$ alone. In the Kondo regime $T_k = T_A << N\Delta_0/\pi$, it is found that for $|\omega| << \tilde{T}$, the same charge fluctuation energy for large N given by

$$-\tilde{T} = E_o + \frac{N\Delta_o}{\pi} \ln \frac{D}{\tilde{T}} \tag{78}$$

the matrix elements of n_f are still small, while for $|\omega| >> \tilde{T}$, the matrix elements of n_f tend to 1.

We have shown then that the change in Q on adding a quasiparticle to the system is zero. If this had not been so, the constraint $Q = 1$ on the system would have vetoed the excitation and spoiled our Fermi liquid picture. It seems quite consistent, as a result, to ignore the constraint at low temperatures, except for its role in providing the self-consistent equation (by varying ε_f), and where a line is constrained to zero frequency, as in the calculation just done when $\omega = 0$, where the λ fluctuation had to be included. In fact we point out that the static charge susceptibility χ_c can be obtained in either of these ways: either by differentiating the equation for n_f, or by considering "screening" contributions to the $n_f - n_f$ response function at $\omega = 0$ (involving a λ line).

That the f-charge n_f carried by a quasiparticle becomes small as $\langle n_f \rangle \to 1$ indicates that the quasiparticle is mainly an excitation of the conduction band and of spin degrees of freedom in this limit. Consequently, the spin response (e.g. χ_0) sees the quasiparticle resonance but the charge response (e.g. χ_c) does not, so the former is much larger than the latter. In the case of γ, we again conclude that the charge degree of freedom does not count towards the Kondo specific heat: $\gamma \propto (N-1)/T_K$

§6. Proof that Expansion in Number of Boson Loops is a 1/N Expansion

In Chapter 2 §3 we saw that, if our model was modified to constrain Q (or n_f) to be of order N , rather than 1 , then it has a straightforward 1/N expansion, in which diagrams with r boson loops (i.e. with r sums over Bose-type Matsubara frequencies) for, say, the free energy are of order N^{1-r} ; that is the mean field terms are of order N , the one-loop corrections (Gaussian fluctuations) are of order 1 , and higher numbers of loops (non-Gaussian corrections) are of higher order in 1/N . We call this assignment of powers of 1/N to a diagram "naive" or "nominal" power-counting. However, for the case of interest to us, we constrain Q to be 1 , and we found that the free energy and its derivatives at T , h = 0 were of order 1 . We might have then been concerned that Gaussian fluctuations would be of the same order as the mean field terms, but in fact we have found in this chapter that the Gaussian corrections are of order 1/N . Again we may be concerned that some non-Gaussian terms are the same order as these. In this section we prove that this is not the case, and that a diagram with r boson loops contributes to the free energy to order

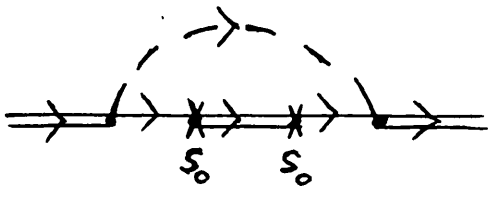
$$N^{-r}$$

at most; thus we show that the nominal power counting is correct, except that it is possible to pick up (at least) one extra factor of 1/N in each diagram. The reason for this will be that Δ is of

order $1/N$, not 1 as in the theory of Chapter 2 §3, and that it is always possible to take at least one integration in each diagram to be over a density of states of order $1/N$. The proof will be by induction on the number of boson loops. Finally we discuss fluctuations in λ , which have been omitted in the free energy calculation.

a) Proof by induction

Suppose that the expansion has already been established to order N^{-r} (we will see for which quantities this can be done below). By assumption the diagrams involved contain r boson loops, or less. There are various sources of terms at order $N^{-(r+1)}$: (i) The diagrams with r loops or less contain f propagators with Δ in the denominators. These denominators may be expanded in powers of Δ to give higher order corrections (in some places, the range of integration may cross $\varepsilon = \varepsilon_f$, where this expansion breaks down. Nonetheless, the integrals involved may be expanded in powers of $1/N$; their $N \to \infty$ limits certainly exist, by our inductive assumption). Note that this applies to the σ propagator (21) as well. (ii) Some diagrams with r loops or less are of order $N^{-(r+1)}$ or higher because they contain extra, explicit factors of s_0 , as in the case of diagrams 4.1 (b)-(d) or the self energy diagram below:



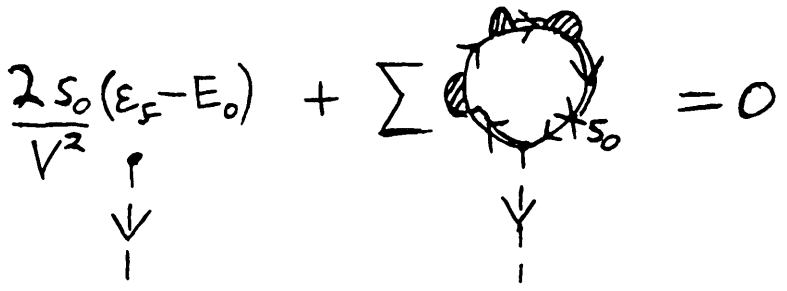
where the whole expression is multiplied by $s_0^2 \sim 1/N$. These factors are *in addition to* the factors whose existence we demonstrate below for level $r + 1$. Note that neither (i) nor (ii) appears in the type of theory of Chapter 2 §3, where Δ was of order 1 .

(iii) Where ε_f and Δ appear in diagrams with r loops or less, they are given their values to order N^{-r} ($N^{-(r+1)}$ for Δ) found from the stationary point conditions (e.g. (19,20) of this chapter). This process also generates terms of order $N^{-(r+1)}$ and higher in the free energy. We regard the substitution of higher order corrections to ε_f or Δ as a purely formal expansion of the integrals which contain them; in particular denominators containing ε_f or Δ are just expanded up. This might generate additional infrared divergent integrals, rather in the manner that (20) appeared; we will just *assume* that the divergences cancel in physical quantities $(F,\chi,\gamma,n_f\ldots)$ and sum up to make Δ vanish, as discussed in §4.

(iv) The last source of terms of order $N^{-(r+1)}$ are the "new" diagrams containing $r + 1$ boson loops. As we have seen, the contributions of effects (i)-(iii) from the "old" (r loop) diagrams are of order $N^{-(r+1)}$, so we are left with the "new" diagrams, which we must prove are indeed of order $N^{-(r+1)}$ as far as the free energy is concerned, and not of order N^{-r} as suggested by "nominal" power-counting. At this stage we can use leading order expressions for ε_f and Δ , and drop Δ^2 in f denominators, as the terms left out will appear through processes (i)-(iii) at a later stage in the expansion.

We first consider the self consistent equations arising from the condition that the free energy be stationary with respect to ε_f and Δ (for s_0 assumed non-zero). Taking the latter first, we

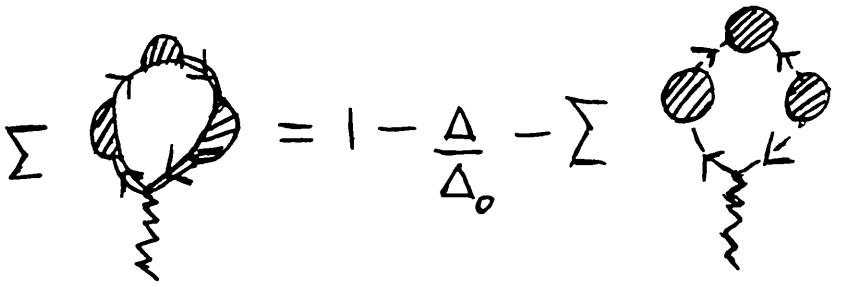
differentiate with respect to s_0 to obtain, (as in 4.4b to Gaussian order) the symbolic result:



(80)

where the diagrams summed contain $r + 1$ or less boson loops. The shaded areas represent various self-energy insertions on the fermion loop; the fermion lines may be either f or conduction electrons, except near the external leg where f appears on one side of the leg and conduction on the other. Now we observe, as a consequence of the last remark, that all such diagrams contain at least one s_0 factor, as does the first term in (80). We divide this factor off, whereupon we observe that the first term in (80), and the no-loop term in the sum of fermion loop diagrams, (cf. first two terms in Fig. 4.4b) are of order N, the one-boson loop terms of order 1, and so on. In other words, *naive power counting is valid* for this equation.

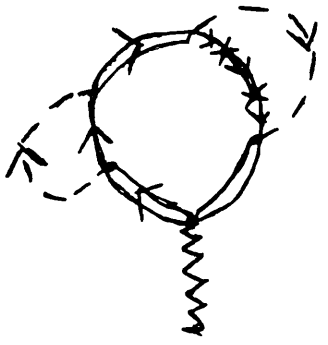
Now consider the other self-consistent equation, found by varying ε_f (compare Fig. 4.4a). We will consider first zero temperature and magnetic field. The equation takes the form



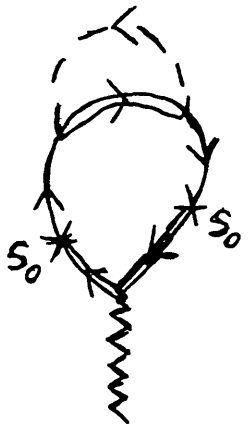
(81)

Again the summations are over diagrams containing $r + 1$ or less boson loops, the shaded semicircles represent possible self-energy insertions on the fermion loop, and the shaded circles represent self-energies for the boson (including possible anomalous terms; arbitrary numbers of self energies are allowed in the summation, of course, though only three are shown).

In our diagrams, the arrow on an f line can be followed onto a boson line, and thence back onto an f line and so on, so that the flow of Q through a diagram can be traced. Note that our σ propagator includes only the fermion loop Fig. 4.1a; the others, including the "anomalous" loops must be included as explicit diagrammatic corrections. Let us start at the wavy line insertion of an $r + 1$ loop diagram on the left hand side of (81) and attempt to follow the flow of Q continuously right round the loop. One of two things must happen: either the line can be traced, as in the example of



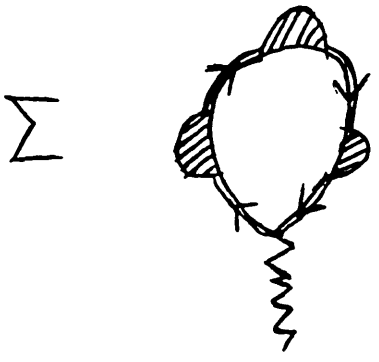
or else the line ends in an s_0 insertion, as in the following:



In the latter case, we could also start at the other end of the loop, and follow the arrows in reverse, to find another factor of s_0, so in fact we find a factor of $s_0^2 = O(1/N)$, which makes the diagram of order $N^{-(r+1)}$ (or higher). So we need only consider diagrams where the flow of Q can be traced unbroken around the fermion loop.

The same argument applies to the sum of diagrams involving boson self energies on the right hand side of (81), since we have specified that "anomalous" self energies, which involve the breakage (and reversal) of the flow of Q, must be drawn explicitly.

The general diagram remaining on the left hand side of (81) is now of the form



(82)

where all the lines between the (irreducible) self energies are f lines by assumption. Now (82) is to be evaluated by bending the contour around the negative real axis of the energy running round the loop, picking up the integral of the imaginary part of an expression like

$$G_f \Sigma_1 G_f \Sigma_2 \cdots \Sigma_n G_f \tag{83}$$

($n \geq 1$) where G_f is the f propagator for the resonance of the mean field theory, as usual. Note that each self energy Σ_i may contain less than $r + 1$ boson loops (but at least 1) ; only the total number of loops in the Σ_i must total $r + 1$.

The imaginary part of (83) must contain at least one imaginary part of either G_f or one of the Σ_i . If it is G_f , we are done, since at negative frequencies, the imaginary part is

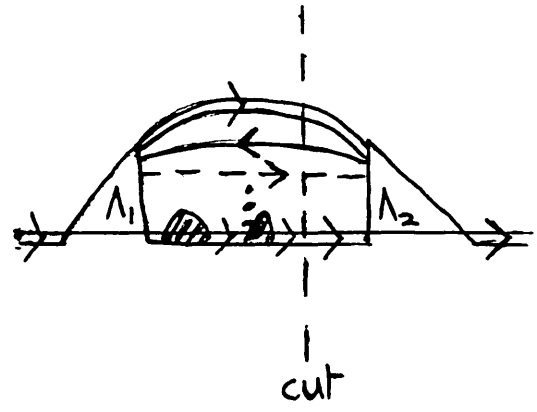
$$\frac{-\Delta}{(\varepsilon - \varepsilon_f)^2 + \Delta^2}$$

which is of order $1/N$ for $\varepsilon < 0$, so we have found our factor of $1/N$.

Otherwise, consider the imaginary part, for an incoming frequency $\varepsilon < 0$, of an f self-energy Σ_i . We wish to show that it is $1/N$ smaller than the nominal value N^{-r_i} , where r_i is the number of boson loops in Σ_i . Now it is well-known that for any self energy diagram, the imaginary part can be obtained by cutting across the diagram in each possible way, taking the imaginary part of each line cut and summing over the (real) frequencies running through these lines in the usual way. This expresses the fact that the imaginary part of the self energy represents physically the sum of amplitudes for decay into many real excitations, which are

represented by their density of states. The sum of the energies in the excitations so created must equal that of the original excitation. Consider a particular cut of the diagram Σ_i :

$$\mathrm{Im}\,\Sigma_i = \sum_{\substack{\text{possible}\\ \text{cuts}}}$$



The lines cut may be conduction, f electron or boson, running in either direction. As we have assumed that Q can be traced continuously from one side of the diagram to the other, it must cross the cut from left to right at least once. We choose one such crossing and show this line at the bottom of our figure; it has been taken to be an f line. The expression for $\mathrm{Im}\,\Sigma_i$ has the form

$$\mathrm{Im}\,\Sigma_i = \int \cdots \int \prod_i d\varepsilon_i \, \Lambda_1(\varepsilon_i)\Lambda_2(\varepsilon_i)\rho_1\rho_2 \cdots$$

$$\times \mathrm{Im}(G_f\Sigma_1 G_f \Sigma_2 \cdots G_f) \qquad (84)$$

where $\rho_1, \rho_2, \ldots$ are the imaginary parts of the other lines (including possible self-energy insertions) and the last factor is the bottom line, with its possible insertions of f self-energies.

Now the argument ε of $\mathrm{Im}\,\Sigma_i$ is supposed to be negative. We choose to make it run along the line along which Q is traced, and so it runs from left to right along the bottom cut line. The integration contours for the frequency sums in the diagram can be bent around the real axis on either the positive or negative side, as the integrals always converge fast enough at infinity. We choose the contours such that all the frequencies running through the bottom cut line in the direction of the arrow are negative. Now the total frequency in the line is negative, and the last imaginary part in (84) is evaluated at negative energies, as we had in (83). Again, if the imaginary part of G_f is taken, we have finished. If the imaginary part of a Σ_j inside (84) is taken, then the self energy Σ_j certainly contains fewer boson loops than Σ_i. If Σ_i contains $r+1$ boson loops, then Σ_j contains r or less, and by our inductive hypothesis, the imaginary part of Σ_j, and hence of Σ_i, is multiplied by an extra factor of $1/N$. The same argument applies when boson self energies are involved. This completes the proof for the second self-consistent equation, at $T = h = 0$, and incidentally shows that f and b self-energies with r boson loops have imaginary parts of order $N^{-(r+1)}$ at most, at frequencies $\varepsilon < 0$.

Now consider non-zero magnetic fields and temperatures. A magnetic field is included, at $T = 0$, by changing $\varepsilon_f \to \varepsilon_f - g\mu_B hm$ in an f line of angular momentum m. Now it is clear that the proof just given can be extended to show that for frequencies $\varepsilon \lesssim T_A$ (and zero field) the imaginary parts of f and b self energies are of order $N^{-(r+1)}$, at most, when they contain r loops, since the f density of states is of order $1/N$ everywhere below the peak in the Lorentzian at $\varepsilon = T_A$. Thus if the magnetic field

satisfies the condition $h_j < T_A$, the integrations are still over imaginary parts of order $1/N$ smaller than given by naive power counting, and so the proof goes through. In the case of finite temperature, the fermi or bose function has some amplitude at $\varepsilon \simeq T_A$, but this is small provided $T \lesssim T_A/\ell n\ N$ (the same crossover temperature found in Chapter 2 §6). We saw in Chapter 2 that at high temperatures or fields, $\Delta = 0$ and

$$\varepsilon_f = k_B T \ln(N-1) \tag{85}$$

(for $h = 0$, high T). (85) means that at high temperatures, the contribution of the peak in the f density of states (or corresponding step in that for the boson) is only of order $1/N$. It is possible that, starting from (85), a proof could be constructed for high temperatures and fields also, but we will avoid this. At low temperatures, the contribution from thermal occupation of the peak is exponentially small, and expansion in powers of T (and of h) samples only the low energy region where the density of states is of order $1/N$. Therefore we assert that the proof holds for the terms in the Sommerfeld expansion (in powers of T and h) of the self energies (at $\varepsilon \lesssim T_A$) and self consistent equations.

The occupation n_f can be obtained directly from the second self consistent equation, and the magnetization $M(h,T)$ can be found from similar diagrams. Hence these quantities have Sommerfeld expansions in which each coefficient can be expanded in powers of $1/N$, with terms to order N^{-r} given by consideration of diagrams involving up to r boson loops only. Other thermodynamic quantities are obtained similarly, as the free energy itself can be shown to be given by integration over negative frequencies of f and boson

propagators and self energies, with appropriate combinatoric factors, so that arguments similar to those given above can be used. We conclude that *all* thermodynamic quantities (the free energy and its derivatives) possess Sommerfeld expansions for which the coefficients can be obtained to order N^{-r} by consideration of diagrams involving up to r boson loops. These expansions are, however, only valid in the low temperature, low field region, which shrinks in size as N increases (see Chapter 2, §6d).

b) Discussion of fluctuations in λ

So far in this chapter we have made no reference to the integration of the partition function over λ, which in principle is necessary to impose the constraint $Q = 1$, other than the use of the stationary point condition on ε_f. We now consider diagrammatic expansion in the fluctuations of $i\lambda$ about its stationary point value $\varepsilon_f - E_0$.

In analogy with the use of Fourier transformed variables $\sigma(\omega)$, $\sigma^*(\omega)$ we use the variable

$$\tilde{\lambda} = \int_0^\beta \lambda(\tau)\, d\tau = \beta\lambda$$

as λ is constant. The integration limits on $\tilde{\lambda}$ are therefore $(-\pi, \pi)$ which are temperature independent. The effective action can be expanded in powers of $\tilde{\lambda}$ and diagrams evaluated using the quadratic terms in the expansion to provide the Gaussian weight in the usual way. Note that $\tilde{\lambda}$ mixes with $\sigma(0)$, $\sigma^*(0)$, and that the finite limits on $\tilde{\lambda}$ are replaced by infinity in order to do the integrals. The latter approximation is expected to be acceptable at low temperatures. The rules for the diagrams are the same as usual, except that the frequency in a $\tilde{\lambda}$ line must be zero.

When the effective action S_{eff} is expanded in powers of $\tilde{\lambda}$, $\sigma(\omega)$, $\sigma^*(\omega)$, an important property arises from the gauge invariance discussed in Chapter 2 §2. The invariance of the model under transformations (25), (27) of Chapter 2 means that there is a correspondence

$$\lambda \leftrightarrow \dot{\theta} \tag{86}$$

between diagrams with λ legs and others where the λ legs are replaced by fluctuations in the phase θ of σ , plus an extra factor of ω for each such leg. For example, at the level of second order terms, the expansion of S_{eff} in (16) tends to zero as $\omega \to 0$, which is how the pole in the σ propagator arises. If σ is decomposed into longitudinal and transverse fluctuations relative to s_0 , it is found that it is the terms involving transverse fluctuations which vanish. This remains true when the other terms, Fig. 4.1 b-d are included. Here we are substituting the stationary point values of ε_f , Δ into (16). If instead we calculate the corresponding terms for longitudinal fluctuations in σ , fluctuations in $\tilde{\lambda}$, and the mixing between them, we find that terms involving λ are finite and equal to the $\omega \to 0$ limit of the terms involving transverse fluctuations divided by ω for each transverse fluctuation leg. This relation is a result of the gauge symmetry of Chapter 2 §2.

However, quantities such as the free energy are gauge invariant, and the factors of ω cancel between fermion bubbles and propagators, so at $\omega = 0$ identical expressions are apparently obtained from Gaussian fluctuations in either of the variables just described. We begin to wonder whether the fluctuations in λ lead

to an overcounting of the $\omega = 0$ fluctuations in the transverse part of σ. We will see, though we will not give a full proof, that this is not the case, and that results such as those obtained earlier in this chapter can be justified.

The crucial point is the regularisation of the pole in the σ propagator. The best way to do this is to add to the effective action a term

$$-\mu^2\left(\sigma(\tau) - \sigma^*(\tau)\right)^2 \qquad (87)$$

where μ is small and positive, which explicitly breaks the symmetry, and will appear as a small "mass" for the transverse fluctuations. The infrared divergences are rendered finite by this trick, as long as $\mu \neq 0$.

In the diagrams for the free energy, there are no divergences, because the pole in the σ propagator is always cancelled by factors of ω in the fermion loops which form the vertices. In the presence of the regulator (87) the propagators are modified, but at $\omega \neq 0$, μ is eventually smaller than ω and we recover the expressions for $\mu = 0$. At $\omega \equiv 0$, however, the fermion loops (vertices) are now zero, while the σ propagators are finite at non-zero μ. Hence *terms due to transverse fluctuations in* σ *vanish at* $\omega = 0$ *when properly regularised.* Their place is taken up by the fluctuations involving $\tilde{\lambda}$, so that gauge invariant quantities, for which $\omega \to 0$ in the summations presents no problem, take the same value as obtained by continuity, without regularisation.

In the self consistent equations, λ lines may be differentiated, but their imaginary part is always zero, so the $\omega \simeq 0$ part of the integral vanishes, and infrared divergences are here regulated by μ instead of the cruder Λ.

In conclusion, it appears that the treatment earlier in this Chapter, where λ fluctuations were neglected, and regularisation was done in a rather *ad hoc* way, is perfectly effective in producing correct results for thermodynamic quantities. We emphasize that the correspondence (86) can only hold when $\langle b \rangle \neq 0$, otherwise θ cannot be defined, so this treatment does not hold in the high temperature region where $\langle b \rangle = 0$, but does hold throughout the low temperature, low field region.

To see intuitively why λ fluctuations are of little importance, consider the partition function without integration over λ. It has the form

$$Z' = \sum_{Q=-\infty}^{\infty} e^{-\beta F(Q)} \tag{88}$$

The parameter ε_f is chosen to make $\langle Q \rangle = 1$ and presumably the $Q = 1$ part has the lowest free energy for this value of ε_f. As the free energies of different Q differ by an amount independent of the size of the system, the subspaces with $Q \neq 1$ are suppressed exponentially at low temperatures and do not contribute to the Sommerfeld expansion. This argument assumes that the symmetry is unbroken, so that the partition function splits as in (88). Since we have seen above that symmetry is restored in the $1/N$ expansion in each order in $1/N$, this argument can be applied to our approximate results as well as to the exact form (88).

§7. Summary of Results of Chapter 4

a) The effective action was expanded to second order in the deviations in σ and σ^* from their stationary point values, and simplifying to leading order in $1/N$, Gaussian functional integrals were carried out to find $1/N$ corrections to

(i) self-consistent equations for ε_f and Δ

(ii) ground state energy

(iii) χ_0, γ and n_f at $T = h = 0$.

b) Ground state energy, χ_0, γ, n_f were found to be finite and in agreement with available predictions including the relation [3] between χ_0, γ and χ_c to order $1/N$.

c) The parameter Δ had corrections of the form

$$\frac{\Delta}{\Delta_0} = (1-n_f)\left(1 + \frac{n_f^2}{N}\ln\Lambda\right)$$

where $\Lambda \to 0$, which, it was argued, signify restoration of symmetry and the vanishing of Δ:

$$\frac{\Delta}{\Delta_0} \sim c\,\Lambda^{n_f^2/N}$$

The exponent n_f^2/N was related to that of Nozières and de Dominicis and so is likely to be exact.

d) It was shown that the quasiparticle excitations carry zero $Q = n_f + b^+b$, because of a "perfect screening" effect, confirming the physical picture of a resonance of one-electron excitations.

e) It was shown that diagrams for the free energy containing r boson loops contribute to order N^{-r} at most, by an inductive argument. It was argued that careful regularisation leads to the disappearance of zero frequency fluctuations in σ transverse to $\langle b \rangle$ and their replacement by fluctuations in λ otherwise omitted. Alternatively, fluctuations in λ may simply be omitted at low temperatures and fields.

REFERENCES

1. J.W. Rasul and A.C. Hewson, J. Phys. C *16* (1983) L933; *ibid 17* (1984) 2555, 3337.
2. P. Schlottmann, Phys. Lett. A *100* (1984) 509.
3. A. Yoshimori, Progr. Theor. Phys. (Kyoto) *55* (1976) 67.
4. P. Nozières and A. Blandin, J. Physique *41* (1980) 193.
5. K.G. Wilson, Rev. Mod. Phys. *47* (1975) 773.
6. N.D. Mermin and H. Wagner, Phys. Rev. Lett. *22* (1966) 1133. S. Coleman, Commun. Math. Phys. *31* (1973) 259.
7. D.J. Gross and A. Neveu, Phys. Rev. D *10* (1974) 3235.
8. E. Witten, Nucl. Phys. B *145* (1978) 110.
9. N. Andrei and J.H. Lowenstein, Phys. Rev. Lett. *43* (1979) 1698.
10. J.M. Kosterlitz and D.J. Thouless, J. Phys. C *6* (1973) 1181.
11. P. Nozières and C.T. de Dominicis, Phys. Rev. *178* (1969) 1097.
12. D. Langreth, Phys. Rev. *150* (1966) 712.
13. A.C. Hewson and D.M. Newns, J. Phys. C *13* (1980) 4477.
14. K. Yamada and K. Yosida, Prog. Theor. Phys. (Kyoto) *68* (1982) 1504.
15. P. Coleman, Phys. Rev. B *29* (1984) 3035.
16. N. Andrei, K. Furuya and J.H. Lowenstein, Rev. Mod. Phys. *55* (1983) 331.
17. J.W. Rasul, Proc. Int. Conf. Valence Instabilities (Zurich), ed. Wachter and Boppart (Amsterdam: North Holland).
18. D. Jérome and H.J. Schulz, Adv. in Phys. *31* (1982) 299.
19. F.D.M. Haldane, J. Phys. C *14* (1981) 2585.
20. B. Berg and P. Weisz, Nucl. Phys. B *146* (1978) 205.

CHAPTER 5. APPLICATION OF MEAN FIELD THEORY TO ANDERSON LATTICE AND HUBBARD MODELS

§1. The $U = \infty$ Anderson lattice model

In this chapter we consider models of many f-orbitals lying on the sites of a lattice. In the following section we discuss a mean field theory for a $U = \infty$, $SU(N)$ invariant Hubbard model. In the present section we generalize our previous treatment of a $U = \infty$ Anderson impurity to the so-called Anderson lattice model.

The Anderson lattice model consists of an Anderson-type ion situated on each site of a periodic lattice, with local hybridisation between the f and conduction states. If the environment of each ion is taken to be spherically symmetric, we can again use a partial wave decomposition about each site. We will, for simplicity, drop the spin of the conduction electrons, so as to emphasize the role of orbital angular momentum. Following Coqblin and Schrieffer [1] (who included spin and spin-orbit coupling) we end up with

$$H = \sum_{\underline{k}} \varepsilon_{\underline{k}} c^{\dagger}_{\underline{k}} c_{\underline{k}} + E_o \sum_{im} f^{\dagger}_{im} f_{im} + V \sum_{im} (4\pi)^{1/2} \left[f^{\dagger}_{im} b_i \sum_{\underline{k}} Y_L^m(\Omega_{\underline{k}}) e^{i\underline{k}\cdot\underline{R}_i} c_{\underline{k}} + h.c. \right] \quad (1)$$

We have again used Coleman's boson to introduce an infinite U interaction between f electrons at the same site, the usual constraint

$$Q_i = \sum_m f_{im}^+ f_{im} + b_i^+ b_i = 1 \qquad (2)$$

for each site being understood.

a) SU(N) invariant model and mean field solution

The model we will treat in this chapter is a simplified version of (1), in which conduction electrons are regarded as carrying angular momentum j (whereas in (1) the angular momentum becomes scrambled as electrons move from site to site). Matrix elements are taken to conserve J_Z and hybridisation is assumed to transfer an f electron to the conduction band state at the same site. The Hamiltonian is

$$H = \sum_{\underline{k}m} \varepsilon_{\underline{k}} c_{\underline{k}m}^+ c_{\underline{k}m} + E_o \sum_{im} f_{im}^+ f_{im} + V \sum_{im} \left[f_{im}^+ c_{im} b_i + c_{im}^+ f_{im} b_i^+ \right] \qquad (3)$$

We will now follow our previous treatment of the impurity at $T = 0$ and introduce the constraints (2) through Lagrange multipliers, which because of translational invariance of the system we take to be independent of position. The expectation value of b_i and b_i^+ we also take to be independent of the site label i. We therefore have a self-consistent band structure problem with the one-electron Hamiltonian:

$$H_{qp} = \sum_{\underline{k}m} \varepsilon_{\underline{k}} c^{+}_{\underline{k}m} c_{\underline{k}m} + \varepsilon_f \sum_{\underline{k}m} f^{+}_{\underline{k}m} f_{\underline{k}m} + s_0 \sum_{\underline{k}m} \left(f^{+}_{\underline{k}m} c_{\underline{k}m} + h.c. \right) \tag{4}$$

All sums over $\underline{k}$ are, in this model, over a single Brillouin zone. Fig. 5.1 shows a cross-section through the bands of a typical solution of (4).

At this point we mention a related calculation by Lacroix and Cyrot [2] who decoupled the spin $\frac{1}{2}$ Kondo lattice Hamiltonian by a modified version of the Yoshimori-Sakurai functional integral method [3]. Their scheme differs slightly from the $N = 2$, Kondo limit of our model, but provides some useful calculational tools for our purposes. In contrast with Lacroix and Cyrot, we are able not only to make the extension to the Anderson lattice, but also to justify our method since it is exact in the large-N limit.

First we obtain expressions for the densities of states of (4) in terms of that of the non-hybridised conduction band. For the conduction electrons, the local propagator is obviously

$$G_k(i\omega) = \sum_{\underline{k}} \left(i\omega - \varepsilon_{\underline{k}} - \frac{s_0^2}{i\omega - \varepsilon_f} \right)^{-1} \tag{5}$$

and so the density of states per channel is

$$\rho_c(\varepsilon) = \rho_0 \left(\varepsilon - \frac{s_0^2}{\varepsilon - \varepsilon_f} \right) \tag{6}$$

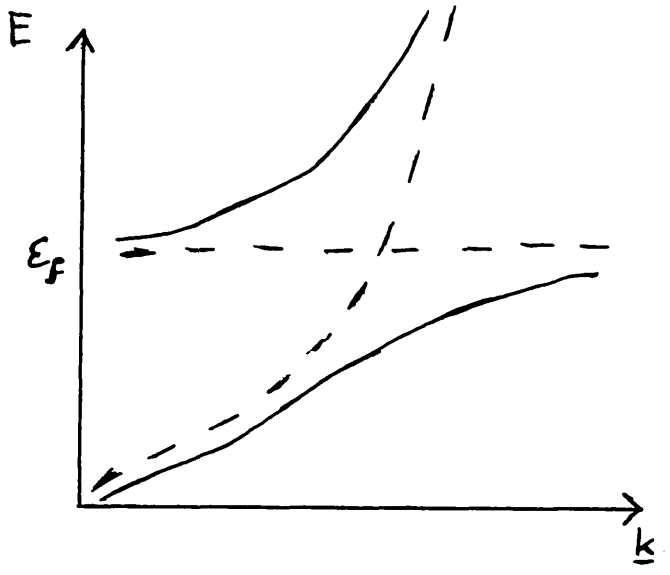


Fig. 5.1. Hybridised bands of H_{qp} , eq. (4); dashed lines, f and conduction bands without hybridisation, solid lines including hybridisation s_0 .

where $\rho_0(\varepsilon)$ is the density of states of the conduction band without hybridisation. For the f electrons, the local propagator is

$$G_f(i\omega) = \frac{s_0^2}{(i\omega-\varepsilon_f)^2} G_k(i\omega) + \sum_{\underline{k}} \frac{1}{i\omega-\varepsilon_f} \qquad (7)$$

and the density of states is

$$\rho_f(\varepsilon) = \frac{s_0^2}{(\varepsilon-\varepsilon_f)^2} \rho_0\left(\varepsilon - \frac{s_0^2}{\varepsilon-\varepsilon_f}\right) \qquad (8)$$

We now specialise to a constant, rectangular density of states ρ_0 :

$$\rho_0(\varepsilon) = \begin{cases} \frac{1}{2D} , & -D < \varepsilon < D \\ 0 & \text{otherwise} \end{cases} \qquad (9)$$

The density of states has been normalised to give one state per site, and the energy zero is put at the centre of the band.

Substituting (9) into (6) and (8) we see that in the vicinity of ε_f , the argument of $\rho_0(\varepsilon)$ becomes large and because (9) is zero outside $\pm D$, a gap appears around ε_f . Also, the edges of the bands are shifted. The 4 band edges are the solutions of

$$\varepsilon - \frac{s_0^2}{\varepsilon-\varepsilon_f} = \pm D \qquad (10)$$

and are, in ascending order,

$$\varepsilon_a = \tfrac{1}{2}\left[\varepsilon_f - D - \sqrt{(\varepsilon_f+D)^2+4s_0^2}\right] \simeq -D - \frac{s_0^2}{|\varepsilon_f+D|}$$

$$\varepsilon_b = \tfrac{1}{2}\left[\varepsilon_f + D - \sqrt{(\varepsilon_f-D)^2+4s_0^2}\right] \simeq \varepsilon_f - \frac{s_0^2}{|\varepsilon_f-D|}$$

$$\varepsilon_c = \tfrac{1}{2}\left[\varepsilon_f - D + \sqrt{(\varepsilon_f+D)^2+4s_0^2}\right] \simeq \varepsilon_f + \frac{s_0^2}{|\varepsilon_f+D|}$$

$$\varepsilon_d = \tfrac{1}{2}\left[\varepsilon_f + D + \sqrt{(\varepsilon_f-D)^2+4s_0^2}\right] \simeq D + \frac{s_0^2}{|\varepsilon_f-D|} \qquad (11)$$

The densities of states are shown in Fig. 5.2. In (11) we have expanded the solutions on the assumption that $s_0^2 \ll |\varepsilon_f - D|$, $|\varepsilon_f + D|$ which will be valid for most cases when the conduction band is about half filled and we do not go too far towards $n_f = 0$.

It is now straightforward to write down the self-consistent equations obtained by requiring that ε_f and s_0 minimise the ground state energy. For the lattice case, an important difference is that the chemical potential μ must also be determined self-consistently to fix the total number of electrons in the system.

The self-consistent equations are, at $T = 0$:

i) From varying ε_f :

$$n_f = \frac{Ns_0^2}{2D}\int_{\varepsilon_a}^{\mu} d\varepsilon \, \frac{1}{(\varepsilon-\varepsilon_f)^2} = \frac{Ns_0^2}{2D}\left[\frac{1}{\varepsilon_a-\varepsilon_f} - \frac{1}{\mu-\varepsilon_f}\right]$$

$$= 1 - \frac{s_0^2}{V^2} \qquad (12)$$

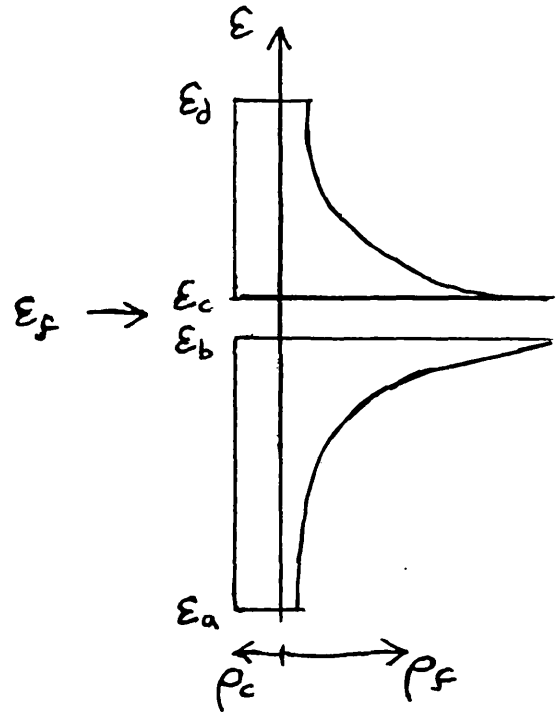


Fig. 5.2. Density of states corresponding to Fig. 5.1, showing $\rho_f(\varepsilon)$, $\rho_c(\varepsilon)$ and positions of band gap, edges and ε_f .

ii) From varying μ ,

$$n_c + n_f = \frac{N}{2D}(\mu - \varepsilon_a) + n_f = n \tag{13}$$

Here n_c is the number of conduction electrons per site, and n the total number of electrons per site.

iii) From varying s_0^2

$$\frac{N}{2D}\int_{\varepsilon_a}^{\mu} d\varepsilon \frac{1}{\varepsilon - \varepsilon_f} = \frac{N}{2D} \ln\left(\frac{\varepsilon_f - \mu}{\varepsilon_f - \varepsilon_a}\right)$$

$$= -\frac{(\varepsilon_f - E_0)}{V^2} \tag{14}$$

As mentioned above, we consider mainly the case $n_c \simeq N/2$ and $\varepsilon_f - \mu \ll D$, when $\varepsilon_f - \varepsilon_a \simeq D$ and we can simplify the equations to

$$n_f = \frac{N\Delta}{\pi T_A} = 1 - \frac{\Delta}{\Delta_0} \tag{12'}$$

$$\frac{N}{2D}(\mu + D) + n_f = n \tag{13'}$$

$$-\frac{N\Delta_0}{\pi} \ln \frac{T_A}{D} = T_A - \tilde{E}_0 \tag{14'}$$

where we have introduced the familiar notations

$$T_A = \varepsilon_f - \mu$$

$$\tilde{E}_0 = E_0 - \mu$$

$$\Delta_0 = \pi V^2/2D$$

$$\Delta = \pi s_0^2/2D \qquad (15)$$

to emphasize the similarity with the equations for a single impurity. From (12′) we deduce

$$n_f = \left(1 + \frac{\pi T_A}{N\Delta_0}\right)^{-1} \qquad (16)$$

Because of the self-consistency, and because ε_f , Δ and μ vary as constant $+ aT^2$ as $T \to 0$ (or $h \to 0$) we can as in previous chapters use Fermi liquid theory to write χ_0 and γ in terms of the densities of states at μ :

$$\chi_0 = \frac{1}{3} j(j+1)(g\mu_B)^2\left[\frac{N}{2D} + \frac{n_f}{T_A}\right]$$

$$\gamma = \frac{\pi^2}{3} k_B^2\left[\frac{N}{2D} + \frac{n_f}{T_A}\right] \qquad (17)$$

Here we have included the conduction band contributions, including in the case of X_0 a coupling of h to conduction electrons with the same g factor as for the f electrons. Obviously the X_0/γ ratio R is 1, whether conduction band parts are omitted or not.

The charge response of the system is modified by the self-consistency of μ (13′) as well as that of the f band. First we may consider the change in total number of electrons on changing μ at fixed E_0. It is given by

$$\frac{dn}{d\mu} = \frac{N}{2D} + \frac{dn_f}{d\mu}$$

$$= \frac{N}{2D} + n_f^2(1-n_f)\frac{\pi}{N\Delta_0} \qquad (18)$$

on using (14′), (16) and

$$\frac{d\tilde{E}_0}{d\mu} = -1.$$

(18) is simply the response of the conduction band plus the charge susceptibility found for impurities in Chapter 2, (100).

Now we consider the change in n_f with E_0 when n is fixed. (13′) gives

$$\frac{N}{2D}\frac{d\mu}{dE_0} + \frac{dn_f}{dE_0} = 0 \qquad (19)$$

while

$$\frac{dn_f}{dE_o} = \frac{dn_f}{d\tilde{E}_o}\frac{d\tilde{E}_o}{dE_o} = \frac{dn_f}{d\tilde{E}_o}\left(1 - \frac{d\mu}{dE_o}\right)$$

$$= -n_f^2(1-n_f)\frac{\pi}{N\Delta_o}\left(1 - \frac{d\mu}{dE_o}\right) \tag{20}$$

From (19) and (20),

$$\frac{dn_f}{dE_o} = \frac{-n_f^2(1-n_f)\frac{\pi}{N\Delta_o}}{1 + n_f^2(1-n_f)\frac{\pi}{N^2\Delta_o}} \tag{21}$$

b) Discussion

Except when $n_f \simeq 0$ or 1, (21) is strongly modified by its denominator. The effect occurs because when E_0 is raised, electrons flow into the conduction band, which has a lower density of states in general, so raising μ, which tends to suppress the reduction in n_f. This is a well-known effect in the Anderson lattice model which has been discussed by many authors [3] (though never treated in full). It tends to pin the f level ϵ_f near the Fermi energy. (21) could be integrated to find n_f as an explicit function of E_0. Taking $E_0 << -D$ initially, so $n_f \simeq 1$, (21) implies that as the mixed valence regime is reached, n_f does not decrease as rapidly when E_0 is raised as it does in the single impurity model, so E_0 must become more positive to reach a given value of n_f. However, in a

real material one has Coulomb interactions between conduction electrons, and between conduction electrons and f electrons. The latter interaction tends to mean that when an f electron hops into the band, the hole in the f shell attracts a conduction electron which screens the change in charge. Outside a distance of order the screening length (perhaps less than 1 Angstrom) there is no apparent change in the charge in the vicinity of the impurity (apart from the weak oscillatory tail). As f ions would be perhaps 2-4 A apart, each would be independent of the valence of its neighbours. In other words, the attractive interaction between f holes and conduction electrons tends to counteract the change in μ [4,5]. In the Anderson lattice model, where this interaction is ignored, changes in n_f with temperature would also be suppressed; however, significant changes in n_f with increasing temperature can be clearly seen in measurements of anomalous thermal expansion (Chapter 1). This is evidence for the existence of the f-hole-conduction electron interaction.

Now in our mean field theory, the only additional approximation so far has been to neglect the correction to the band edge ε_a (11) (working in the case μ , $\varepsilon_f - \mu$ small compared with D , $n_c \simeq N/2$). The correction in (11) is of order

$$\frac{S_o^2}{2D} = \frac{\Delta}{\pi} = \frac{n_f T_A}{N}$$

which is small under our assumptions, especially when N is large (Δ is never larger than Δ_0 , which is always assumed much smaller than D in the Anderson lattice model). From this we obtained (12'-14') which differed from the single impurity results of Chapter 2

only in the self-consistency of the chemical potential. As we have just argued that the valence-pinning effects of the latter would be counteracted in a real material (or in a model with the extra attractive interaction), we have found some justification in the large-N approach for application of single-impurity results for thermodynamics to concentrated systems. Comparisons of single-impurity results, approximate or exact, with experimental data have been remarkably successful [6,7].

The physical reason for the similarity of (12′-14′) to the equations for one impurity in the large-N limit may be seen by expanding $\rho_f(\varepsilon)$ (or $G_f(\varepsilon)$) in powers of s_0^2 :

$$G_f(\varepsilon) = \sum_k \Bigg(\frac{1}{\varepsilon - \varepsilon_f + i\delta} + \frac{s_0}{\varepsilon - \varepsilon_f + i\delta} \frac{1}{\varepsilon - \varepsilon_k + i\delta} \frac{s_0}{\varepsilon - \varepsilon_f + i\delta}$$

$$+ \frac{s_0}{\varepsilon - \varepsilon_f + i\delta} \frac{1}{\varepsilon - \varepsilon_k + i\delta} \frac{s_0^2}{\varepsilon - \varepsilon_f + i\delta} \frac{1}{\varepsilon - \varepsilon_k + i\delta} \frac{s_0}{\varepsilon - \varepsilon_f + i\delta}$$

$$+ \cdots \Bigg) \tag{22}$$

To leading order in $1/N$, only the second term contributes to $\rho_f(\varepsilon)$, *provided* $\varepsilon - \varepsilon_f$ is large compared with $s_0^2/2D$. The density of states ρ_c in (6), (8) is slowly varying except when ε approaches the gap, where it becomes sensitive to variations in $\rho_0(\varepsilon)$ at $\varepsilon = \pm D$ (which we took to be step functions). Thus the leading term is sufficient at energy ε provided

$$\varepsilon - \frac{s_0^2}{\varepsilon - \varepsilon_f} \ll D$$

for ε below the gap. Then with $n_c \simeq N/2$, μ near zero, $\rho_f(\varepsilon)$ is the same as the impurity f density of states at large N for energies at μ or below, which were all that were needed for the self-consistent equations (12′-14′). We see that, although the bands show that intersite propagation is fully coherent in our approach, the f density of states is dominated by *local* hybridisation to leading order in 1/N at the energies we are interested in. Quantities other than thermodynamic variables, such as Fermi surface masses, will reveal the existence of f quasiparticle bands with large mass enhancements near the Fermi level.

c) Insulating case

We now consider the possibility of an insulating ground state for (4). This will occur when the chemical potential lies in the gap. The total number of electrons in such a state is

$$n = N\int_{\varepsilon_a}^{\varepsilon_b} d\varepsilon \left(1 + \frac{\xi_0^2}{(\varepsilon-\varepsilon_f)^2}\right)\rho_0\left(\varepsilon - \frac{\xi_0^2}{\varepsilon-\varepsilon_f}\right) \qquad (23)$$

for a general density of states ρ_0. Now let

$$x = \varepsilon - \frac{\xi_0^2}{\varepsilon-\varepsilon_f} \qquad (24)$$

then

$$n = N \int_{-D}^{D} dx\, \rho_0(x) \tag{25}$$

This was to be expected, since we have filled a Brillouin zone. Since $n_f \leq 1$, we have $n_c \geq N - 1$ and so μ lies rather close to the upper band edge (when N is large) - see Fig. 5.3. Taking μ at ε_b, we see from (12-14) that the gap is

$$\varepsilon_c - \varepsilon_b \cong \varepsilon_f - \varepsilon_b \doteq T_A \tag{26}$$

for large N.

It is found experimentally [8] that SmB_6 and the high pressure phase of SmS are semiconductors with a small gap at low temperatures. In these, basically ionic, compounds the S or B_6 valence bands are thought to be filled and the only bands near the Fermi energy are the hybridised Sm f and d bands. The only electrons in the d bands (less than 1 electron per Sm) come out of the f^6 (Sm^{2+}) filled shell. Thus, performing electron-hole inversion, it would appear that (25) is satisfied. This phenomenon of the hybridisation gap as the explanation of semiconducting behaviour is well known [9], however our renormalised bands can give a very small gap (26) so that it may be possible to explain the electronic structure of SmS and SmB_6 in terms of the Anderson lattice (using no doubt a more realistic form such as (1)).

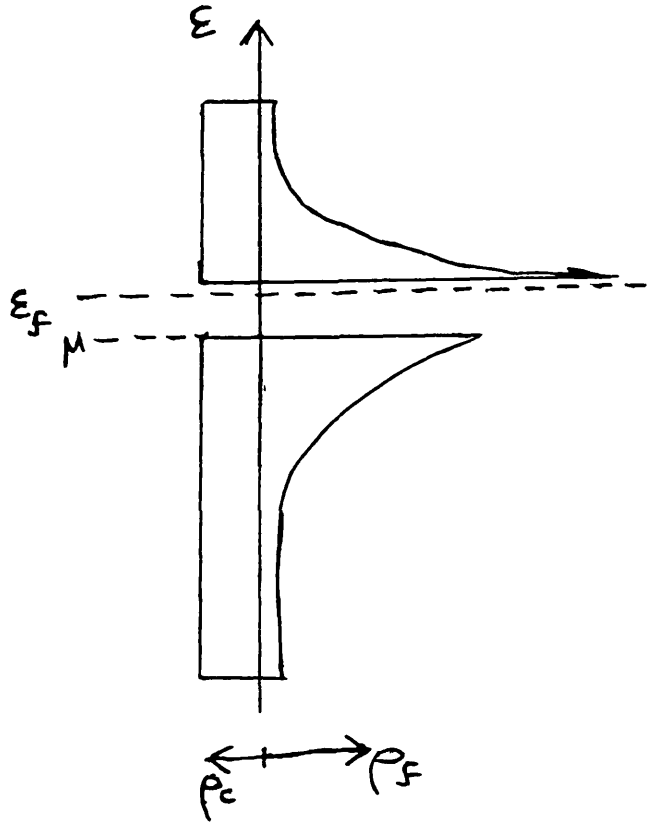


Fig. 5.3. Densities of states for insulating case

d) RKKY interactions in the Kondo limit

Let us return to the conducting situation $n_c \simeq N/2$ and compare the groundstate energy of our mean field theory in the Kondo limit with that of a totally ordered magnetic state (neglecting the Kondo effect on the latter) as in [2]. The ground state energy of the Kondo lattice, treated in mean field theory is of order $-T_k$ per site compared with that for non-interacting bands. The Kondo coupling is again $\rho J = \Delta_0/\pi E_0 = O(1/N)$ and the RKKY interaction between two moments, neglecting the Kondo effect on the moments, is of the form

$$J^2 f(R_{ij})$$

where $f(R)$ is analogous to the usual RKKY function and does not depend on J or N. Hence the energy of a magnetically ordered state is of order $1/N^2$. Following Doniach [10] we argue that the Kondo lattice becomes magnetic when these energies are comparable, which is when

$$D \exp \frac{-2D}{J_0} = \left(\frac{J_0}{2D}\right)^2 \frac{1}{N^2} A \qquad (27)$$

(using $J_0 = -NJ$). Here A is a constant of order 1. Now for the original spin $\frac{1}{2}$ Kondo lattice, ρJ had to be of order unity to obtain a Kondo-compensated, non-magnetic state, a physically unrealisable value. However, we see that for large N, ρJ has only to exceed

$$\frac{\text{constant}}{2N \ln N}$$

or that T_k/D must exceed

$$\frac{\text{constant}}{(2N \ln N)^2} \tag{28}$$

to obtain such a state, a much less stringent condition. This argument greatly enhances the theoretical possibility of concentrated Kondo systems having a non-magnetic ground state. The effect of magnetic interactions on such a state could be included by considering fluctuation effects as in the previous chapter.

In concluding this section, let us emphasize that the mean field theory treatment of (4) could be justified using large-N arguments as in the case of a single impurity (Chapter 4). Fluctuations introduce intersite interactions, including the residual effects of the RKKY interaction, as well as on-site corrections. The possibility that these interactions might lead to further phase transitions in the non-magnetic Kondo lattice at finite N provides an impetus for further study.

§2. The $U = \infty$ Hubbard model

a) Introductory remarks

The recent discovery [11] of several anomalous superconducting compounds of uranium, as well as the earlier discovery of superconductivity in the Kondo lattice system $CeCu_2Si_2$, has stimulated interest in the possibilities of phase transitions in metallic systems whose "normal" state shows strongly enhanced electronic masses. Thus in UBe_{13} and UPt_3, large values of X and γ are found above the transition, reminiscent of the intermediate valence compounds, and the specific heat jump at the transition, and entropy at T_c are consistent with the pairing occurring among these "heavy electrons"

themselves. The use of a simple Hubbard model is currently popular as a means of understanding the normal state, with the 5f states assumed to form bands with a fairly strong correlation U on each site. In this situation, with 1 f electron per site, Brinkman and Rice [12] found a mass enhancement which diverged as U approached a critical value U_c from below. This idea has recently been applied to He^3 above its superfluid transition [13]. For the "heavy electron" materials, non-integral occupation of the f bands, and very large U , might be more appropriate [14]. We take up this idea here, with $U = \infty$, applying our previous methods.

b) Mean field theory

The model is an SU(N) invariant, $U = \infty$ Hubbard model which is defined by the Hamiltonian

$$H = t \sum_{\langle ij \rangle} f_{im}^{+} f_{jm} b_j^{+} b_i \tag{29}$$

with constraints

$$Q_i = \sum_m f_{im}^{+} f_{im} + b_i^{+} b_i = 1 \tag{30}$$

on each site i . Here <ij> denotes nearest neighbours and the label m is interpreted as angular momentum, running from -j to j , as in the previous section.

In mean field theory the constraints (30) are introduced merely through a Lagrange multiplier ε_f , taken to be the same on each site, and the b_i's are replaced by their expectation values, which we call b (real) and which are also assumed to be independent of site. Then our self-consistent problem is set by the Hamiltonian

$$H' = b^2 t \sum_{\langle ij \rangle} f_{im}^{+} f_{jm} + \varepsilon_f \sum_i (n_{fi} + b^2 - 1) \tag{31}$$

Varying chemical potential μ yields n_f (= number of f electrons per site) while varying ε_f relates n_f to b^2. The equation is (at T = 0)

$$n_f = -\frac{N}{\pi} \int^{\mu} d\varepsilon \, \mathrm{Im} \sum_{\underline{k}} \frac{1}{\varepsilon - \varepsilon_{\underline{k}} + i\delta} = 1 - b^2 \tag{32}$$

Varying b on each site yields

$$t \sum_{jm} \langle f_{im}^{+} f_{jm} \rangle = -\frac{N}{\pi} \int^{\mu} d\varepsilon \, \mathrm{Im} \sum_{\underline{k}} \sum_{j} \frac{t e^{i\underline{k}.(\underline{R}_j - \underline{R}_i)}}{\varepsilon - \varepsilon_{\underline{k}} + i\delta}$$

$$= -\varepsilon_f \tag{33}$$

where the sum on j is over nearest neighbours of i. Now in a tight binding model,

$$\varepsilon_k = \varepsilon_f + b^2 t \sum_j e^{i\underline{k}.(\underline{R}_j - \underline{R}_i)} \tag{34}$$

and so (33) can be written

$$-\frac{N}{\pi}\int^{M} d\varepsilon \, \mathrm{Im} \sum_{\underline{k}} \frac{(\varepsilon_{\underline{k}} - \varepsilon_f)/b^2}{\varepsilon - \varepsilon_{\underline{k}} + i\delta}$$

$$= N \int^{M} d\varepsilon \sum_{\underline{k}} (\varepsilon_{\underline{k}} - \varepsilon_f)\, \delta(\varepsilon - \varepsilon_{\underline{k}})/b^2$$

$$= N \int^{M} d\varepsilon \, \frac{(\varepsilon - \varepsilon_f)}{b^2} \rho_f(\varepsilon)$$

$$= -\varepsilon_f \qquad (35)$$

on introducing

$$\rho_f(\varepsilon) = -\frac{1}{\pi} \mathrm{Im} \sum_{\underline{k}} \frac{1}{\varepsilon - \varepsilon_{\underline{k}} + i\delta} \qquad (36)$$

So both (32) and (35) depend only on the density of states, not the detailed band structure. Note the similarity of (35) to the self-consistent equation in the Anderson model (e.g. 14); the main difference lies in the form of ρ_f .

So far the expressions are quite general. From a given density of states, ρ_f is obtained by scaling the width by b^2 and shifting the centre by ε_f . Here we will take as a model density of states (without renormalisation)

$$\rho_0(\varepsilon) = \begin{cases} \frac{1}{2D} & , -D < \varepsilon < D \\ 0 & \text{otherwise} \end{cases} \tag{37}$$

Hence

$$\rho_f(\varepsilon) = \frac{1}{b^2}\rho_0\left(\frac{\varepsilon - \varepsilon_f}{b^2}\right)$$

$$= \begin{cases} \frac{1}{2b^2D} & , -b^2D < \varepsilon - \varepsilon_f < b^2D \\ 0 & , \text{otherwise} \end{cases} \tag{38}$$

Then (32), (35) become

$$n_f = \frac{N}{2b^2D}(\mu - \varepsilon_f + b^2D) = 1 - b^2 \tag{39}$$

$$\frac{N}{2b^2D}\left(\frac{1}{2}(\varepsilon_f - \mu)^2 - \frac{1}{2}(b^2D)^2\right) = -\varepsilon_f b^2 \tag{40}$$

We will see that (40) is the ground state energy in this approximation. Note that (40) is analogous to (14), with x^2 replacing $\log x$ on the left hand side, due to the different form of ρ_f. Hence the Hubbard model will not lead to exponential dependence on parameters, as appeared in the Kondo cases.

From (39),

$$\frac{\mu - \varepsilon_f}{b^2 D} = \frac{2n_f}{N} - 1 \tag{41}$$

hence from (40)

$$\varepsilon_f = \frac{ND}{4} - \frac{D}{N}\left(n_f - \frac{N}{2}\right)^2$$

$$= D n_f \left(1 - \frac{n_f}{N}\right) \tag{42}$$

As usual, χ_0 and γ are Fermi liquid properties given by the density of states at μ :

$$\chi_o = \frac{1}{3} j(j+1)(g\mu_B)^2 \frac{N}{2D(1-n_f)}$$

$$\gamma = \frac{\pi^2}{3} k_B^2 \frac{N}{2D(1-n_f)} \tag{43}$$

We now solve for μ . From (41) and (42),

$$\frac{\mu}{D} = n_f\left(1 - \frac{n_f}{N}\right) - (1-n_f) + (1-n_f)\frac{2n_f}{N}$$

$$= -1 + 2n_f + \frac{2n_f}{N} - \frac{3n_f^2}{N} \tag{44}$$

μ is a monotonic function of n_f, whose derivative vanishes only when both $N = 2$ and $n_f = 1$:

$$\frac{1}{D}\frac{d\mu}{dn_f} = 2\left(1+\frac{1}{N}\right) - \frac{6n_f}{N} \tag{45}$$

This gives the compressibility [15]

$$\chi_c = \frac{1}{n_f^2}\frac{dn_f}{d\mu} = \frac{1}{2Dn_f^2\left(1+\frac{1}{N}-\frac{3n_f}{N}\right)} \tag{46}$$

(45) vanishes when $N = 2$ and $n_f = 1$ because of particle hole symmetry in the $N = 2$ model.

The ground state energy of the model is

$$\begin{aligned} E_o &= N\int^{\mu} d\varepsilon\, \varepsilon\, \rho_f(\varepsilon) + \varepsilon_f(b^2-1) \\ &= N\int^{\mu} d\varepsilon(\varepsilon-\varepsilon_f)\rho_f(\varepsilon) \\ &= -b^2\varepsilon_f \\ &= -(1-n_f)n_f\left(1-\frac{n_f}{N}\right)D \end{aligned} \tag{47}$$

using (40), (42). It vanishes when $n_f \to 1$, as in that limit no kinetic energy can be gained by hopping.

c) Discussion

The central result of our mean field theory is the mass enhancement contained in (43), in which the bare density of states is divided by

$$Z_f = 1 - n_f \quad (= b^2) \tag{48}$$

just as in the theory for the Anderson impurity and lattice ((12) and Chapter 2, eq. (66)). This enhancement factor bears a strong resemblance to that of the Brinkman-Rice [12] theory of the metal-insulator transition in the large-U limit [14], where the mass enhancement is the inverse of

$$q \simeq 2\delta = 2(1 - n_f) \tag{49}$$

as $n_f \to 1$. The present theory has the advantage of a straightforward extension to finite temperatures (c.f. [14]).

We have also seen that a smooth large N limit,

$$N \to \infty \quad , \quad n_f \quad , \quad t \ (\text{or } D) \quad \text{fixed}$$

exists for our results. We do not know yet whether the mean field ansatz (31) and (48) are exact in this limit, but we expect in any case a dependence on dimensionality of the lattice to appear in the Hubbard model (unlike the Anderson lattice). In one dimension, the $N = 2$ Hubbard model can be solved exactly for any U and any n_f [16], and in the $U \to \infty$ limit at fixed $n_f < 1$ the susceptibility diverges [17], contrary to (43). We think this is because in one dimension the impenetrable particles cannot pass each other and become trapped

between their neighbours, acting as localised spins rather than a Fermi liquid. In dimensions greater than 1 , the particles can get around one another when $n_f < 1$ and so a Fermi liquid state is possible.

In the Hubbard model for large U , the principal magnetic interaction is an antiferromagnetic nearest neighbour interaction of order

$$t^2/U \tag{50}$$

Accordingly, at finite U additional, magnetic interactions occur and could lead to a magnetic transition (in dimensions greater than 2). Also, as in the case of the Anderson lattice, fluctuation corrections to mean field theory might lead to other transitions away from a Fermi liquid state, perhaps even to (non-phonon-induced) superconductivity. However, for say $N = 2$, it is widely believed that when $n_f = 1$ ("half filling") and U is finite, the ground state is an antiferromagnetic insulator, due to the interaction (50). We are therefore led to propose the following picture for the phase diagram of the Hubbard model at large U and $T = 0$ (Fig. 5.4). At $U = \infty$ we assume that the mean field theory is essentially correct (i.e. we ignore the possibility of transition to a non-Fermi liquid state). The ground state energy is of order (47)

$$E_0 \simeq -(1-n_f)n_f D \tag{51}$$

and we assume this holds also for a mass-enhanced Fermi liquid state at large, finite U (ignoring also magnetic interactions in this phase). At $n_f = 1$ and U finite, the ground state energy is of order (50)

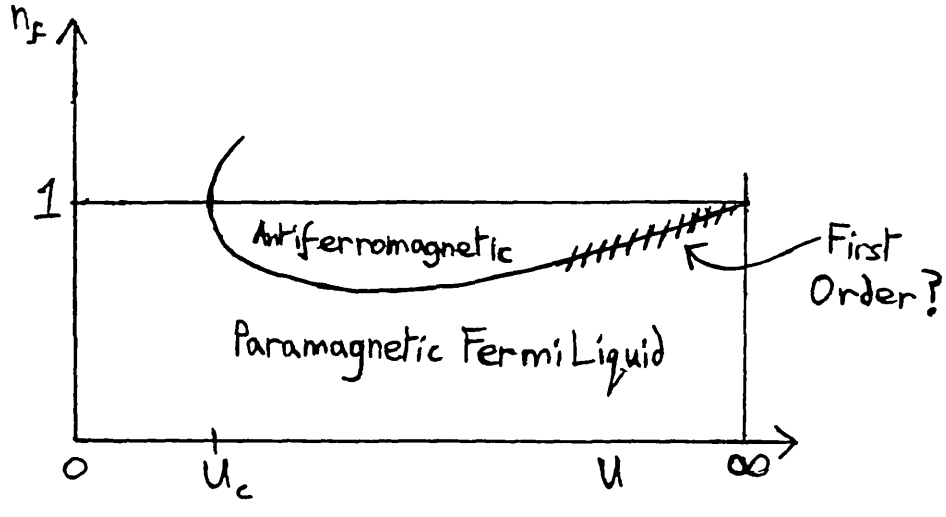


Fig. 5.4. Proposed phase diagram of the Hubbard model

$$E_{mag} \simeq -c D^2/U \tag{52}$$

(as $t \propto D$; c is a constant) and we assume this holds in a magnetic phase near $n_f = 1$. Then comparing (51) and (52) for $n_f \simeq 1$ and $U \simeq \infty$, we find that they are equal when

$$\frac{cD}{U} \simeq 1 - n_f \tag{53}$$

Then the phase diagram of Fig. 5.4 results, which shows also the start of the magnetic phase at a value U_c of order t . The transition at (53) might be first order.

REFERENCES

1. B. Coqblin and J.R. Schrieffer, Phys. Rev. *185* (1969) 847.
2. C. Lacroix and M. Cyrot, Phys. Rev. B *20* (1979) 1969.
3. J.H. Jefferson, J. Phys. C *10* (1977) 3589;
   A.C. Hewson, J. Phys. C *10* (1977) 4973.
4. F.D.M. Haldane, Phys. Rev. B *15* (1977), 281, 2484.
5. D.M. Newns and A.C. Hewson, J. Phys. F *10* (1980) 2429.
6. A. Bringer and H. Lustfeld, Z. Phys. B *28* (1977) 213.
7. A.C. Hewson *et al.*, Proceedings of 4th International Conference on Valence Fluctuations, to be published in J. Magnetism & Magnetic Materials (1985).
8. J.M. Lawrence *et al.*, Rep. Prog. Phys. *44* (1981) 1.
9. N.F. Mott, Phil. Mag. *30* (1973) 403.
10. S. Doniach, Physica *91*B (1977) 231.
11. H.R. Ott *et al.*, Phys. Rev. Lett. *50* (1983) 1595.
    G.R. Stewart *et al.*, Phys. Rev. Lett. *52* (1984) 679.
    G.R. Stewart, Rev. Mod. Phys. *56* (1984) 755.
12. W.F. Brinkman and T.M. Rice, Phys. Rev. B *2* (1970) 4302.
13. D. Vollhardt, Rev. Mod. Phys. *56* (1984) 99.
14. T.M. Rice, K. Ueda, H.R. Ott and H. Rudigier, Phys. Rev. B *31* (1985) 594.
15. P. Nozières, "Theory of Interacting Fermi Systems", Benjamin, 1964.
16. E.H. Lieb and R.Y. Wu, Phys. Rev. Lett. *20* (1968) 1445.
17. H. Shiba, Phys. Rev. B *6* (1972) 930.